

Review of the Neotropical genus *Prasmodon* (Hymenoptera, Braconidae, Microgastrinae), with emphasis on species from Area de Conservación Guanacaste, northwestern Costa Rica

Jose L. Fernandez-Triana^{1,2,†}, James B. Whitfield^{3,‡}, M. Alex Smith^{1,§}, Yves Braet^{4,§}, Winnie Hallwachs^{5,1}, Daniel H. Janzen^{5,¶}

1 Department of Integrative Biology and the Biodiversity Institute of Ontario, University of Guelph, Guelph, ON N1G 2W1 Canada **2** Canadian National Collection of Insects, 960 Carling Ave., Ottawa, ON K1A 0C6 Canada **3** Department of Entomology, University of Illinois, Urbana, IL 61801 USA **4** Unité d'Entomologie fonctionnelle et évolutive, Gembloux Agro-Bio Tech, Université de Liège, B-1030 Gembloux, Belgique; and Département d'entomologie, IRSNB, Rue Vautier 29, 1000 Bruxelles, Belgique **5** Department of Biology, University of Pennsylvania, Philadelphia, PA 19104-6018 USA

† <http://zoobank.org/4469D91F-BBC1-4CBF-8263-EBFE2A95E4BF>

‡ <http://zoobank.org/7A98AB5F-552D-4437-8F5D-C593CA713506>

§ <http://zoobank.org/E46EE6EB-E096-4FCD-BF5A-F91D4A8294EE>

¶ <http://zoobank.org/C1A1006D-C170-430D-9D9F-27AB0878DDDD>

¶ <http://zoobank.org/B2F86601-DF32-469C-942F-11116282C467>

<http://zoobank.org/4491369A-CFA6-4614-AC09-1137CCD06F9A>

Corresponding author: Jose Fernandez-Triana (jftriana@uoguelph.ca)

Academic editor: G. Broad | Received 4 December 2013 | Accepted 14 March 2014 | Published 28 March 2014

<http://zoobank.org/6F9DA9D1-5000-45DB-AB0E-5212EF158781>

Citation: Fernández-Triana JL, Whitfield JB, Smith MA, Braet Y, Hallwachs W, Janzen DH (2014) Review of the Neotropical genus *Prasmodon* (Hymenoptera, Braconidae, Microgastrinae), with emphasis on species from Area de Conservación Guanacaste, northwestern Costa Rica. Journal of Hymenoptera Research 37: 1–52. doi: 10.3897/JHR.37.6748

Abstract

The Microgastrinae genus *Prasmodon* is revised and the following 16 new species are described: *erenadupontae* and *verhoogenokus* (authored by Braet and Fernández-Triana), and *almasolisae*, *aureus*, *bobpoolei*, *bobrobinsi*, *dondavisi*, *johnbrowni*, *masoni*, *mikepoguei*, *nixonii*, *paulgoldsteini*, *scottmilleri*, *silvatlanticus*, *subfuscus*, and *tijucaensis* (authored by Fernández-Triana and Whitfield). The greatest species richness is found in the Amazon basin, but the genus extends throughout the rain forests of Central and South America. Leaf-rolling and webbing caterpillars of Crambidae and Elachistidae are the only known hosts for these parasitoids.

Keywords

Microgastrinae, *Prasmodon*, parasitoid biology, Neotropics, Area de Conservación Guanacaste, Costa Rica, species descriptions, caterpillars

Introduction

The subfamily Microgastrinae (Hymenoptera: Braconidae) is a species-rich and taxonomically difficult lineage of parasitoid wasps that attack caterpillars (Lepidoptera), and also one of the main taxa used in the biological control of caterpillar pests in forestry and agriculture (Whitfield 1995, 1997). Close to 2,500 species have been described worldwide, although the total species richness may be as high as 40,000+ (Rodríguez et al. 2013).

The last two decades have seen an increase in the study of microgastrine wasps in the Neotropics – as a result of the publication of a key to New World genera (Whitfield 1997) and numerous biodiversity inventories carried out in the Neotropics. Among the sites more comprehensively studied, Area de Conservación Guanacaste (ACG), in north-western Costa Rica, is an important and iconic effort to inventory all species of caterpillars, their food plants, and their parasitoids (Janzen et al. 2009). The fauna of ACG parasitoids has been the focus of many taxonomic revisions since the 1980's, and those of microgastrines in the past decade (Deans et al. 2003, Janzen et al. 2003, Janzen and Hallwachs 2011, Valerio et al. 2005, 2009, Grinter et al. 2009, Whitfield et al. 2012, Smith et al. 2007, 2008, Fernández-Triana et al. 2013, Fernández-Triana et al. 2014).

This paper, a continuation of those studies, deals with *Prasmodon*. This genus was described by Nixon (1965) as monotypic, based on a striking species from Peru, *Prasmodon eminens* Nixon. Forty years later, a second species, *Prasmodon zlotnicki* Valerio & Rodríguez, was discovered and described from ACG (Valerio et al. 2005). Our study has found many additional undescribed Neotropical species in ACG and South America. Here we describe 16 of them, along with new host information when available. There are more species yet to describe, but we do not have sufficient specimens for that task at present.

Since Nixon's original description of *Prasmodon*, little progress has been made in determining its relationships with other microgastrine genera. Mason (1981) suggested a "*Prasmodon* group" based on his intuitive view of their phylogeny, without clarifying which genera might be included. Based on characters he mentions in his reclassification, however, it appears that the genera *Clarkinella* Mason, 1981 and *Beyarslania* Koçak & Kemal, 2009 (the latter a recent replacement name for the preoccupied name *Xenogaster* Mason) might be candidates for inclusion in this group, possibly along with the more recently described genus *Neoclarkinella* Rema & Narendran, 1996. Morphological study of many specimens of *Pseudapanteles* Ashmead, 1898 indicates some possibility of a close relationship with *Prasmodon* as well (although Mason treated it as a distinct lineage). Early molecular analyses with three genes (Mardulyn and Whitfield 1999; Whitfield et al. 2002) were inconclusive in resolving this possible relationship, but occasionally showed some possible

relationship of *Prasmodon* to *Pseudapanteles*; when morphological data were added to the mix (Whitfield et al. 2002), a closer relationship with *Clarkinella* and *Beyarslania* (the latter named as *Xenogaster* in that paper) is suggested, but with low support. A more recent phylogenetic study incorporating seven genes and comparative morphology (Banks and Whitfield 2006) did not sample *Clarkinella* and *Beyarslania*, but again found *Prasmodon* to be related to *Pseudapanteles* with reasonably strong support. The matter still requires the analysis of both multiple genes and broader taxon sampling.

Methods

Most of the specimens used in this study came from ACG. They were reared (usually, see <http://janzen.sas.upenn.edu> for details for any particular specimen) or Malaise-trapped, and host caterpillars and other ecological information are considered along with DNA barcodes (COI gene) when available (Fig. 105). Additionally, a collection of *Prasmodon* specimens from French Guiana was available (personal collection of YB, collected during several field expeditions and also obtained through collaborations with various people living there). We also studied the South American specimens of *Prasmodon* in the Canadian National Collection of Insects (CNC) in Ottawa, Canada. The non-ACG material did not have associated host or molecular data, with the exception of a few, mostly short DNA barcodes (usually 160 bp) from some CNC specimens. Altogether 140+ specimens were studied.

The specimens of the new species are deposited in the CNC, Natural History Museum, London, United Kingdom (BMNH), the Illinois Natural History Survey, Champaign, Illinois, United States (INHS), the Instituto Nacional de Biodiversidad, Santo Domingo, Costa Rica (INBio), the National Museum of Natural History, the Smithsonian Institution, Washington DC, United States (NMNH), Naturalis Biodiversity Center Leiden, the Netherlands, (RMNH), Institut Royal des Sciences Naturelles de Belgique Brussels, Belgium (IRSNB), and Museum National d'Histoire Naturelle, Paris, France (MNHN).

Morphological terms and measurements of structures are mostly as used by Mason (1981), Huber and Sharkey (1993), Whitfield (1997), Karlsson and Ronquist (2012), and Fernández-Triana et al. (2014). Non-morphological characters are also provided in the key whenever available (e.g., geographical distribution, hosts). Those features are included in brackets at the end of the corresponding couplet and are intended as supplementary information to aid identification.

The new species descriptions are based on the holotype female, with other specimens studied (when available) for intraspecific variation.

Lucid 3.5.4 (<http://www.lucidcentral.com/>) software was used to generate automatic descriptions of the species and to prepare Lucid identification keys. A dataset of 22 characters and 90 character-states was used to provide uniform descriptions for all species treated. The description format includes one sentence per character, with the character mentioned first and the character-state following after a colon, e.g., "Scape

color: entirely yellow”. Whenever a species scored more than one character-state, the description included all of the pertaining character-states separated by “or”, e.g., “Scape color: entirely yellow or partially brown to black”. Whenever a character-state was coded as uncertain due to poor condition of the specimen(s), the description includes the details of the character-state as best assessed, followed by a question mark, e.g., “Scape color: entirely yellow (?)”. Sometimes a character could not be coded due to missing body parts in the available specimens; in such instances the feature was left out of the description for that particular species.

In most cases we used a simplified convention to code color, considering it as either pale (white, light yellow, orange-yellow, light brown-yellow) or dark (dark brown, black). For details on the exact color patterns on the body, we provide extensive illustrations for every species.

Photos were taken with a Keyence VHX-1000 Digital Microscope, using a lens with a range of 13–130 \times . Multiple images through the focal plane were taken of a structure and these were combined to produce a single in-focus image, using the software associated with the Keyence System.

A map with the distribution of all species was generated using SimpleMapp (Shorthouse 2010).

DNA barcodes for all ACG inventory Microgastrinae were obtained using DNA extracts prepared from single legs using a glass fibre protocol (Ivanova et al. 2006). Extracts were re-suspended in 30 μ l of dH₂O, and a 658-bp region near the 5' terminus of the COI gene was amplified using standard primers (LepF1–LepR1) following established protocols (Smith et al. 2006, 2007, 2008). If the initial 658 bp amplification was not successful composite sequences were generated using internal primers. Primer information for individual sequences can be retrieved from the Barcode of Life Data System (BOLD) (Ratnasingham and Hebert 2007), but primers are as detailed in Smith et al. (2008). DNA barcoding data and related information for all specimens studied in this paper can be accessed at: dx.doi.org/10.5883/DS-ASPRAS.

In the taxonomic treatment of species, “Specimens Examined” presents the specimen’s information in the following format: “Number of females/males examined, acronym of the storing institution between parenthesis, COUNTRY: State/Province, Region, city, other locality details, latitude/longitude coordinates (in decimal degrees), collection date, collector name, biological information on host (starting with “ex”), ACG database codes (in the format “yy-SRNP-xxxxxx” for the host caterpillar or parasitoid lot reared from it, or “DHJPARxxxxxx” for an individual parasitoid specimen).

Results

We describe here 16 new species from seven countries (Brazil, Colombia, Costa Rica, Ecuador, French Guiana, Peru and Suriname); increasing the number of *Prasmodon*

species from two to 18. There are at least three additional species (one each from Brazil, Costa Rica and Ecuador) in the CNC collection, only represented by 1-2 males each, with no molecular or biological data associated. Those species will remain undescribed until more specimens, especially females, become available. Males that cannot be associated with females have usually proven to be almost useless in Microgastrinae taxonomy (e.g., Austin 1990; Whitfield 1997).

The distribution of species by country and by major bioregion shows some interesting patterns (Fig. 104). We found 10 species of *Prasmodon* in Costa Rica, out of roughly 140 rearings and 8 Malaise-trapped specimens from ACG. Seven species were recorded from Brazil, out of some 30 Malaise-trapped specimens. Ecuador (6 specimens), French Guiana (20 specimens), and Peru (3 specimens) had three species each. Colombia (3 specimens) and Suriname (1 specimen) had one species each.

Altogether, Central America (only known specimens are from ACG) had 10 of the total species found (55.6%), while South America had nine species (50%). *Prasmodon eminens* was the only species shared between Central and South America (Fig. 104), but even that might be an artifact because that species is thought to actually comprise a complex of morphologically cryptic species (e.g. Valerio et al. 2005). The South American fauna has been much more poorly sampled than has been that of ACG, and many fewer South American specimens were available for us to study; it is very likely that more collecting will reveal a substantial number of new species.

As for major bioregions, ACG had 10 species, sharing one of them with the Amazonia bioregion (for simplicity, we consider here ACG as one region altogether, even though it is a mosaic of ecosystems, just as the other so-called “bioregions”). Amazonia had six species, one shared with ACG, and three shared with the Guyana lowland rainforests (which has no endemic species on its own). The Atlantic Forest of Brazil had three species, all endemic to that region (Fig. 104).

The ACG *Prasmodon* specimens have been collected in relatively low-elevation areas (95–980 m), in intact rain forest or secondary vegetation where there used to be intact rain forest 0–100 years earlier, except for *Prasmodon paulgoldsteini*, which has been found (6 Malaise-trapped specimens) only in ACG dry forest at about 300 m elevation. Based on the data currently available, *Prasmodon* is largely a genus of Neotropical rain forests. Although the most species-rich area at present is Central America (ACG), we speculate that further collecting will reveal the highest diversity to be actually found in South America.

In a first analysis of the biology of the genus, Valerio et al. (2005) reported that species of *Prasmodon* in ACG are solitary parasitoids of leaf-rolling or leaf-webbing Spilomelinae (Crambidae), feeding on shrubs, treelets and tree saplings across a wide range of plant families (Cyathaceae, Araliaceae, Euphorbiaceae, Fabaceae). Successive sampling and improved taxonomy of the hosts in ACG has revealed that the only hosts are Crambidae and Elachistidae (see host records associated with each species below). Hosts are only known for the ACG specimens.

Diagnosis of the genus *Prasmodon*

This is one of the most recognizable genera of Microgastrinae (Mason 1981, Whitfield 1997, Valerio et al. 2005). The body size (3.3–5.8 mm, with most species 4.0 mm or more) and the fore wing length (3.8–6.2 mm, with most species 4.2 mm or more) are among the largest within microgastrine wasps. The body coloration is mostly yellow-orange, with the wings usually infumate (e.g. Figs 1, 2, 7, 8, 13, 14). The notauli are deeply impressed (Figs 5, 11, 17, 22, 27, 32, 38, 44, 50, 56, 62, 68, 73, 80, 86, 92, 94, 95). The fore wing has a closed areolet (second submarginal cell), and the vannal lobe in the hind wing is reduced (e.g., Figs 17, 22, 63, 75, 95). The propodeum has a clearly defined transverse carina crossing the median longitudinal carina (e.g. Figs 5, 17, 39, 45). The hypopygium is inflexible (e.g., Figs 43, 55, 70). The combination of body size and color, notauli, transverse carina on propodeum, and inflexible hypopygium are particularly useful to distinguish *Prasmodon*.

Key to species of *Prasmodon*

[Throughout the key the acronyms T1, T2, etc., are used for morphological terms mediotergite 1, 2, etc.; and F refers to flagellomere number, e.g. F12]

- 1 Mesosoma and metasoma entirely yellow-orange dorsally (Figs 5, 6, 11, 12, 17, 18, 27, 28, 32, 34, 38, 39, 44, 45, 56, 58, 92, 93), except for very small black spot on axillar complex (as in Fig. 5) **2**
- Mesosoma and/or metasoma with some brown coloration dorsally (Figs 23, 50, 51, 63, 69, 75, 80, 81, 86, 87, 94, 95), in addition to very small black spot on axillar complex **10**
- 2(1) Apical flagellomeres yellow or yellowish-white, contrasting with rest brown to black (Figs 3, 13, 30, 54, 90) **3**
- All flagellomeres brown to black (as in Figs 11, 12, 24, 40) **7**
- 3(2) Antenna mostly dark brown to black; with small, apical area (F15–16, and occasionally apical half of F14) which is yellow-brown, lighter in colour than remaining flagellomeres (Figs 3, 13) **4**
- Antenna with yellow area much larger (at least including F12–15, and usually apical half of F11 and basal half of F16), much lighter compared to remaining flagellomeres (Figs 30, 54) **5**
- 4(3) Metatarsus almost entirely yellow-white (Fig. 13); posterior 0.1–0.2 of mesotibia dark brown to black; body length 4.2–4.3 mm (X=4.3 mm), rarely 4.5 mm; fore wing length 4.5–4.6 mm (X=4.6 mm), rarely 4.8 mm; T1 5.6 × as long as width at posterior margin [Hosts: Elachistidae, mostly *Anteotricha* feeding on Bignoniaceae] ***Prasmodon bobpoolei* Fernández-Triana & Whitfield, sp. n.**
- Metatarsus dark brown to black (except for anterior 0.7 of first metatarsomere) (Fig. 1); mesotibia entirely yellow; body length 4.5–4.9 mm (X=4.8

- mm); fore wing length 5.0–5.3 mm (X=5.1 mm); T1 4.0 × as long as width at posterior margin [Hosts: Elachistidae, mostly *Antaeotricha* feeding on Meliaceae].....***Prasmodon almasolisae* Fernández-Triana & Whitfield, sp. n.**
- 5(3) Fore wing with a pale area centrally (Figs 30, 33) which gives the wing a banded appearance; anterior 0.4–0.5 of vein 3M (and usually part or all of veins 2M and r-m) yellow-orange, contrasting with all other veins which are dark brown (Fig. 33); scutoscuteellar sulcus with 4 impressions (Fig. 32); T1 distinctly narrowing at around 0.5 its length, with both anterior and posterior margins clearly wider than its median width (Fig. 34).....
-***Prasmodon erenadupontae* Braet & Fernández-Triana, sp. n.**
- Fore wing either mostly hyaline, or entirely infumate (except for small hyaline area near veins (RS+M)b and 2M); all veins dark brown (Figs 53, 89); scutoscuteellar sulcus usually with more than 5 impressions (Figs 56, 92); T1 distinctly narrowing posteriorly, width at posterior margin clearly less than width at anterior margin and median width (Figs 58, 89, 93)..... **6**
- 6(5) Hypostomal carina not raised (e.g. Figs 16, 57); hind wing subbasal cell mostly setose (Fig. 44); T1 less than 5.0 × as long as width at posterior margin; T2 5.0 × as wide at posterior margin as median length
-***Prasmodon nixonii* Fernández-Triana & Whitfield, sp. n.**
- Hypostomal carina highly raised (Figs 9, 25, 31); hind wing subbasal cell mostly without setae (Fig. 39); T1 6.0 × as long as width at posterior margin; T2 less than 3.0 × as wide at posterior margin as median length
-***Prasmodon verhoogdenokus* Braet & Fernández-Triana, sp. n.**
- 7(2) Ovipositor sheaths relatively short, 0.3 × as long as metatibia length (Fig. 43); all legs entirely yellow (Fig. 40).....
-***Prasmodon masonii* Fernández-Triana & Whitfield, sp. n.**
- Ovipositor much longer, 0.5–0.6 × as long as metatibia length (Figs 7, 24, 35); at least posterior 0.1–0.2 of metatibia and most of metatarsus (and sometimes parts of middle leg) dark brown to black (Figs 7, 26, 35, 37)..... **8**
- 8(7) Scape entirely yellow (Fig. 9); fore wing with most veins golden yellow, pterostigma mostly yellow, with central part brown (Figs 8, 10) [Ecuador].....
-***Prasmodon aureus* Fernández-Triana & Whitfield, sp. n.**
- Scape partially dark brown to black (Figs 25, 35, 38); fore wing with most veins and pterostigma entirely dark brown (Figs 24, 36) [Costa Rica, ACG]..... **9**
- 9(8) Posterior 0.1–0.2 of mesotibia, apical segment of mesotarsus, posterior 0.2–0.3 of metatibia, and metatibia spurs, dark brown to black (Figs 35, 37); scutoscuteellar sulcus with 5–6 impressions (Fig. 38); hind wing with subbasal cell mostly without setae (Fig. 39); T1 evenly narrowing towards posterior margin, its length 6.3 × as width at posterior margin (Fig. 39) [Hosts: Crambidae, *Asturodes fimbriauralis*DHJ02, *Eulepte alialis*, *Piletosoma thialis*, *Phostria* Janzen05, feeding on many plant families]..***Prasmodon jobnbrownii* Fernández-Triana & Whitfield, sp. n.**
- Mesotibia, mesotarsus, and metatibia spurs entirely yellow-orange (Figs 24, 26); posterior 0.1–0.2 of metatibia dark brown to black; scutoscuteellar sulcus

- with 4 impressions (Fig. 27); hind wing with subbasal cell mostly setose (although it may be a small area without setae near lower margin of wing, as in Fig. 28); T1 more or less parallel-side until half its length, then slightly narrowing towards posterior margin (Figs 27, 28), its length 3.3–3.7 × as width at posterior margin [Hosts: Crambidae, *Preneſta* feeding on Apocynaceae: *Preneſta* Janzen196, *Preneſta* Janzen195, *Preneſta scyllalis*DHJ03].....
-***Prasmodon dondavisi* Fernández-Triana & Whitfield, sp. n.**
- 10(1) Only metasoma with some brown coloration on mediotergites; mesosoma completely yellow-orange (Figs 22, 23, 62, 63, 68, 69, 73, 75, 95)..... **11**
- Both mesosoma and metasoma with brown to black areas (Figs 50, 51, 80, 81, 86, 87, 94)..... **15**
- 11(10) Metasoma almost completely yellow-orange (Fig. 95), with only small brown areas centrally on mediotergites 4–7 (usually only on mediotergites 5–6); larger species, body length 5.0–5.3 mm and fore wing length 5.2–5.6 mm... ..
-***Prasmodon eminens* Nixon, 1965**
- Metasoma with brown to black areas covering most of mediotergites 4–7, and also part of mediotergites 3 and 8 (Figs 23, 63, 69, 75); smaller species, body length 3.8–4.0 mm and fore wing length 4.0–4.6 mm..... **12**
- 12(11) All coxae, pronotum, mesopleuron, metapleuron, and propodeum white to very light yellow, contrasting with rest of mesosoma yellow to orange-yellow (Figs 64, 68, 69); T1 3.7 × as long as width at posterior margin. [Hosts: Crambidae, *Omiodes*, *Triuncidia*, feeding on many plant families].....
-***Prasmodon scottmilleri* Fernández-Triana & Whitfield, sp. n.**
- Metacoxa, pronotum, most of mesopleuron, metapleuron and at least anterior 0.5 of propodeum yellow-orange, same color than most of mesosoma (Figs 19, 22, 23, 59, 61–63, 70, 72, 75); T1 5.0–6.0 × as long as width at posterior margin **13**
- 13(12) Humeral complex, part of axillar complex, and scutoscutellar sulcus dark brown to black; notauli very deeply impressed and with darker coloration than rest of anteromesoscutum (Fig. 73); hind wing subbasal cell mostly without setae (Figs 71, 75) [Brazil]
-***Prasmodon silvatlanticus* Fernández-Triana & Whitfield, sp. n.**
- Humeral complex, axillar complex, and scutoscutellar sulcus orange-yellow, same colour than rest of mesosoma (Figs 22, 62); notauli not as strongly impressed as above, and same coloration than rest of anteromesoscutum; hind wing subbasal cell usually mostly setose (as in Fig. 63) [Costa Rica, ACG]..... **14**
- 14(13) Propodeum with median longitudinal and transverse carinae clearly marked, without additional carination pattern (Fig. 23); T3–T7 mostly brown (Figs 19, 23) [Host: Crambidae, *Palpita jairusalis* DHJ01 feeding on Apocynaceae].....
-***Prasmodon bobrobbinsi* Fernández-Triana & Whitfield, sp. n.**
- Propodeum with irregular carinae in addition to median longitudinal and transverse carinae (Fig. 63); T3 yellow-orange; T4–T7 mostly orange with brown coloration restricted to central part of tergites (Fig. 63) [Host: un-

- known, Malaise-trapped]
 ***Prasmodon paulgoldsteini* Fernández-Triana & Whitfield, sp. n.**
 15(10) Mesosoma with extensive brown coloration: anteromesoscutum mid-frontal and lateral areas, lateral face of scutellum, axillar complex, and metascutellum (Figs 76, 77, 80, 81); T1 with posterior 0.2–0.3 brown (Figs 77, 81); metacoxa with small brown spot on posterior 0.1 (Fig. 76); metatrochanter and metatrochantellus brown.....
 ***Prasmodon subfuscus* Fernández-Triana & Whitfield, sp. n.**
 – Mesosoma at most with anteromesoscutum mid-frontal and lateral areas brown (Figs 46, 50, 82, 86, 94); T1, metacoxa, metatrochanter and metatrochantellus fully yellow-white or yellow-orange (Figs 51, 82, 87, 94) **16**
 16(15) Metatibia and metatarsus entirely yellow (Figs 82, 85); wings hyaline, at most with very faint infumation on anterior 0.5 (Fig. 83); anteromesoscutum with only lateral areas brown, rest orange-yellow (Fig. 86) [Brazil]
 ***Prasmodon tijucaensis* Fernández-Triana & Whitfield, sp. n.**
 – Posterior 0.1–0.2 of metatibia and most of metatarsus dark brown to black (Figs 46, 49, 94); wings infumate (Fig. 47); anteromesoscutum usually with mid-frontal and lateral areas brown, rest orange-yellow (Fig. 50) [Costa Rica, ACG] **17**
 17(16) Metasoma with only thin brown areas centrally on T4–T8 (Fig. 94); hind wing subbasal cell mostly without setae (Fig. 94) [Hosts: Crambidae, Ategu-mia, *Desmia*, *Diacme*, *Herpetogramma*, *Phostria* feeding on five plant families] ***Prasmodon zlotnicki* Valerio & Rodríguez, 2005**
 – Metasoma with most of T3–T8 dark brown (Figs 46, 51); hind wing subbasal cell mostly setose (Figs 48, 50) [Hosts: Elachistidae feeding on three plant families] ***Prasmodon mikepoguei* Fernández-Triana & Whitfield, sp. n.**

Taxonomic treatment of species, in alphabetical order

***Prasmodon almasolisae* Fernández-Triana & Whitfield, sp. n.**

<http://zoobank.org/3C6F2705-DC55-4192-89E1-66FF9BC2F570>

http://species-id.net/wiki/Prasmodon_almasolisae

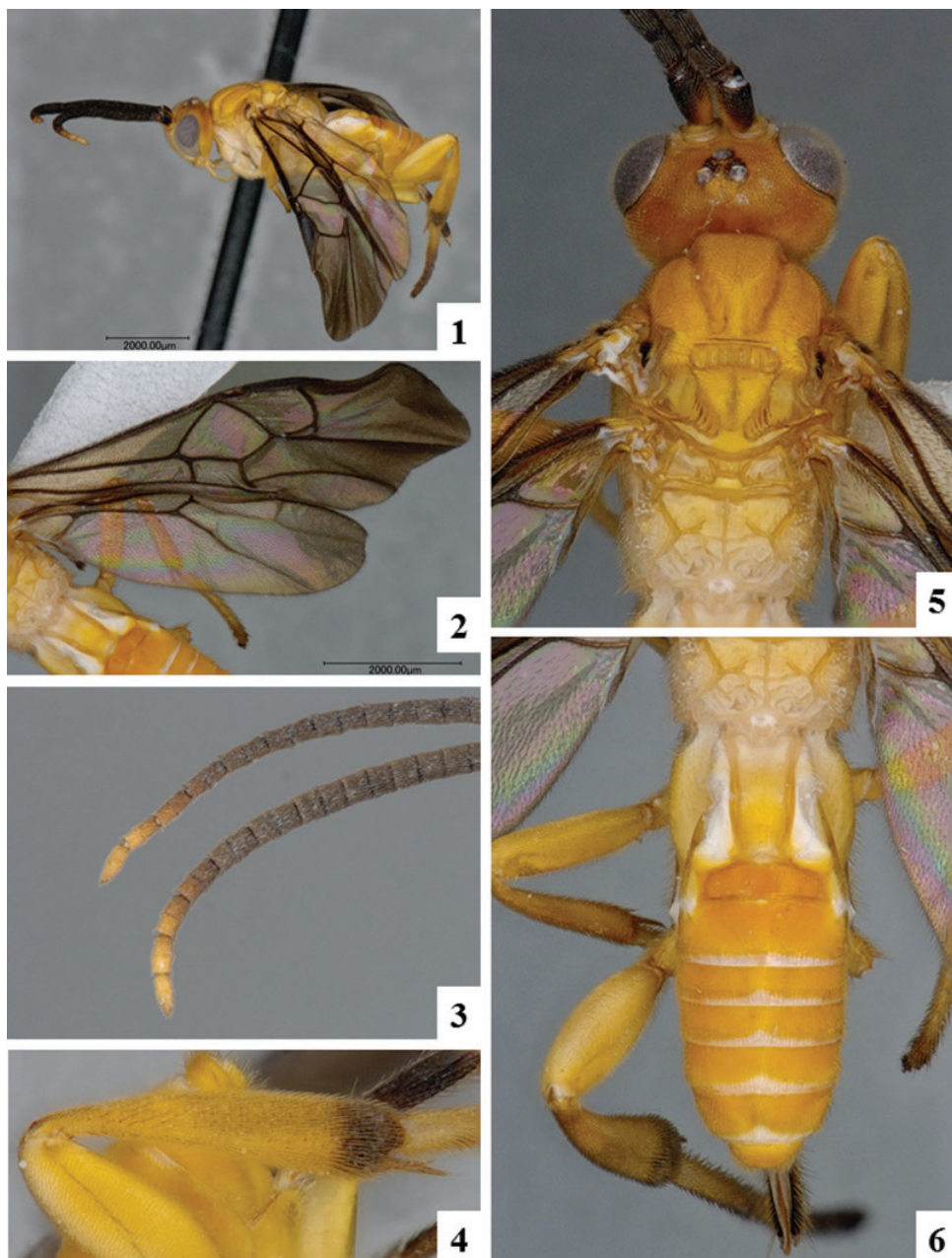
Figs 1–6, 101

Type locality. COSTA RICA, ACG, Alajuela Province, Sector Rincon Rain Forest, Sendero Anonas, 405m, 10.90528, -85.27882.

Holotype. ♀ in CNC. Specimen labels: 1. DHJPAR0038908. 2. Voucher: D.H.Janzen & W.Hallwachs, DB: <http://janzen.sas.upenn.edu>, Area de Conservación Guanacaste, COSTA RICA, 10-SRNP-40859.

Paratypes. 2 ♀, 2 ♂ (CNC, NMNH). COSTA RICA, ACG database codes: DHJPAR0038170, DHJPAR0038913, DHJPAR0040001, DHJPAR0040518.

Description. Female. Body length 4.9–5.0 mm, rarely 4.5–4.6 mm. Fore wing length 4.9–5.0 mm, 5.1–5.2 mm, rarely 5.3–5.4 mm. Body color: meso- and meta-



Figures 1–6. *Prasmodon almasolisae* **1** Habitus **2** Fore wing **3** Antenna (partially) **4** Metatibia **5** Head and mesosoma, dorsal view **6** Propodeum and metasoma, dorsal view.

soma entirely yellow-orange (with the exception of a very small black spot on axillar complex) (Figs 5, 6). Scape color: partially dark brown to black (Fig. 5). Flagellomeres color: most flagellomeres brown to black, except for small apical area (F15–16, and occasionally apical half of F14) which is yellow-brown (Fig. 3). Tegula and humeral

complex color: tegula pale, humeral complex partially dark/partially pale. Mesotibia color: entirely yellow. Metatibia color: posterior 0.1–0.3 dark brown to black (Fig. 4). Metatibia spurs color: yellow-orange. Metatarsus color: dark brown to black (except for anterior 0.7 or less of first metatarsomere) (Fig. 1). Fore wing color pattern: hyaline. Fore wing veins color: all veins dark brown (Fig. 2). Pterostigma color: entirely dark brown. Hypostomal carina: not raised. Scutoscutellar sulcus: with 6 impressions (Fig. 5). Areolet height÷vein r length (fore wing): 0.2 ×. Hind wing subbasal cell: mostly without setae (Fig. 5). Hind tarsal claws: with pectination uniform, teeth thick and relatively evenly spaced. Shape of mediotergite 1: distinctly narrowing posteriorly, width at posterior margin clearly less than width at anterior margin and median width (Fig. 6). Mediotergite 1 length÷width at posterior margin 3.6–4.0 ×. Mediotergite 2 width at posterior margin÷length: 3.1–3.5 ×. Ovipositor sheaths length: 0.6 × as long as metatibia, rarely 0.5 × as long as metatibia.

Male. As female but with flagellomeres fully dark brown to black.

Molecular data. Sequences in BOLD: 11, barcode compliant sequences: 11 (Fig. 105).

Biology and ecology. Hosts: Elachistidae, *Antaeotricha radicalis*, *Antaeotricha ribbei*, *Antaeotricha* Janzen07, *Antaeotricha thapsinopa*, elachJanzen01 Janzen131, *Gonionota* Janzen116, *Stenoma* Janzen129.

Distribution. Costa Rica, ACG rain forest.

Etymology. This species is named in honour of Alma Solis of the SEL/USDA laboratory in the National Museum of Natural History, Smithsonian Institution, Washington, D.C, in recognition of her decades of taxonomic knowledge and support contributing to understanding the species-level and higher taxonomy of the Crambidae, Pyralidae and Thyrididae of ACG, INBio and Costa Rica, as well as other parts of the world.

***Prasmodon aureus* Fernández-Triana & Whitfield, sp. n.**

<http://zoobank.org/306A4FAB-DCD8-42C0-981F-C6B8D97EDC64>

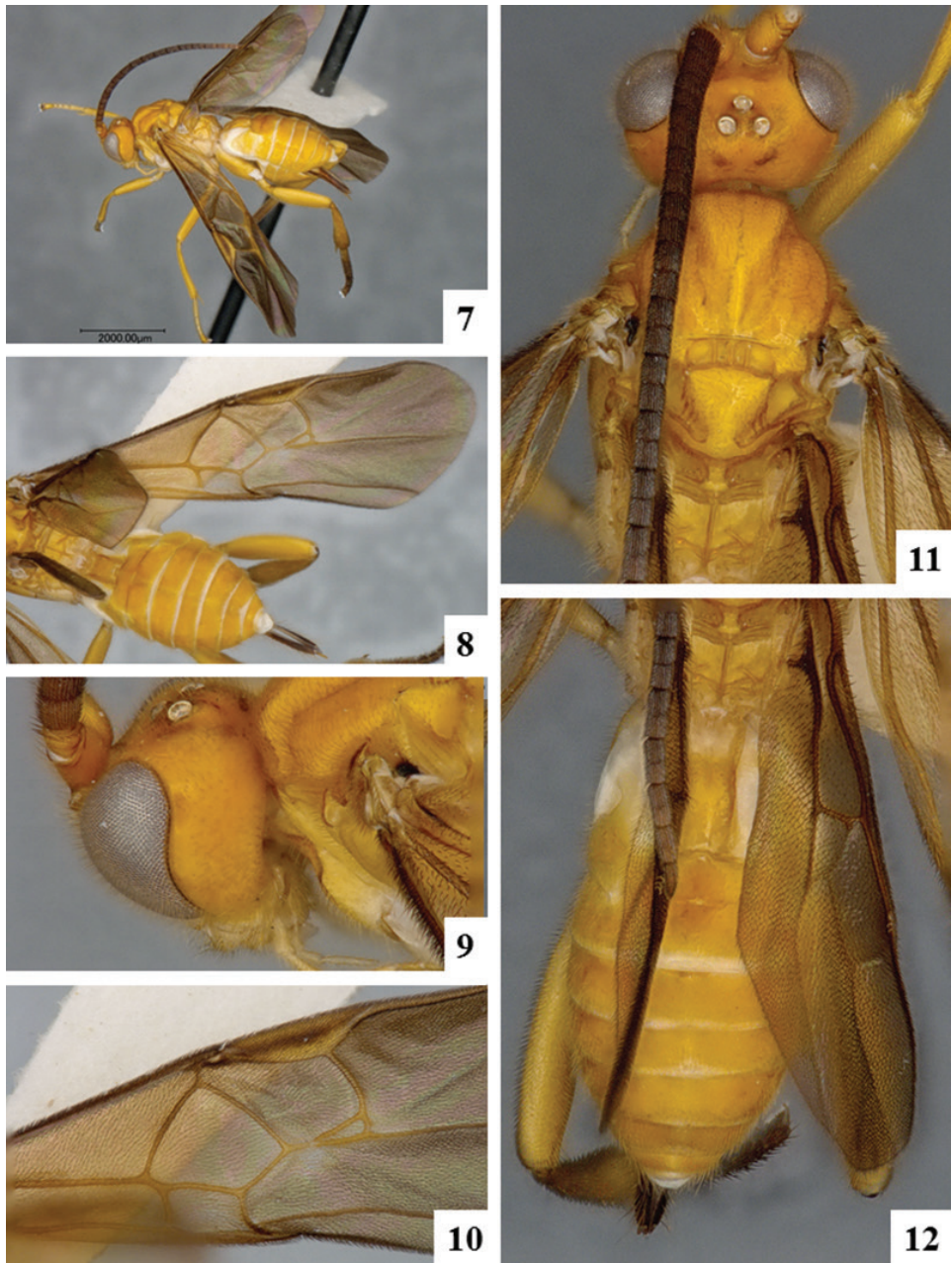
http://species-id.net/wiki/Prasmodon_aureus

Figs 7–12

Type locality. ECUADOR, Napo, Limoncocha, 250m.

Holotype. ♀ in CNC. Specimen labels: 1. ECUADOR, Napo, Limoncocha, 250m, 15–28.VI.1976, S. & J. Peck. 2. DNA Voucher, CNCHYM 01955.

Description. Female. Body length 5.5–5.6 mm. Fore wing length 5.9–6.0 mm. Body color: meso- and metasoma entirely yellow-orange (with the exception of a very small black spot on axillar complex) (Figs 7, 11, 12). Scape color: entirely yellow (Fig. 11). Flagellomeres color: all flagellomeres brown to black (Figs 11, 12). Tegula and humeral complex color: both pale. Mesotibia color: entirely yellow. Metatibia color: posterior 0.1–0.3 dark brown to black. Metatibia spurs color: yellow-orange. Metatarsus color: dark brown to black (except for anterior 0.7 or less of first metatarsomere). Fore wing color pattern: uniformly and entirely infumate (except for small hyaline area



Figures 7–12. *Prasmodon aureus*. **7** Habitus **8** Fore wing **9** Head and mesosoma (partially), lateral view **10** Detail of fore wing **11** Head and mesosoma, dorsal view **12** Propodeum and metasoma, dorsal view.

near veins (RS+M)b and 2M). Fore wing veins color: most veins golden yellow (Figs 8, 10). Pterostigma color: mostly yellow, with central part brown (Fig. 10). Hypostomal carina: highly raised (Fig. 9). Scutoscutellar sulcus: with 4 impressions (Fig. 11).

Areolet height÷vein r length (fore wing): 0.2 ×. Hind wing subbasal cell: mostly with setae. Hind tarsal claws: with pectination uniform, teeth thick and relatively evenly spaced. Shape of mediotergite 1: distinctly narrowing posteriorly, width at posterior margin clearly less than width at anterior margin and median width. Mediotergite 1 length÷width at posterior margin 6.1–6.5 ×. Mediotergite 2 width at posterior margin÷length: 3.1–3.5 ×. Ovipositor sheaths length: 0.5 × as long as metatibia.

Male. Unknown.

Molecular data. Sequences in BOLD: 1, barcode compliant sequences: 0.

Biology and ecology. Unknown.

Distribution. Ecuador, Napo.

Etymology. From Latin “aureus” = golden, referring to the yellow coloration of the fore wing veins, a unique feature among all known species of *Prasmodon*.

***Prasmodon bobpoolei* Fernández-Triana & Whitfield, sp. n.**

<http://zoobank.org/00CA5006-4B13-4D9C-A7A7-58A6841F7192>

http://species-id.net/wiki/Prasmodon_bobpoolei

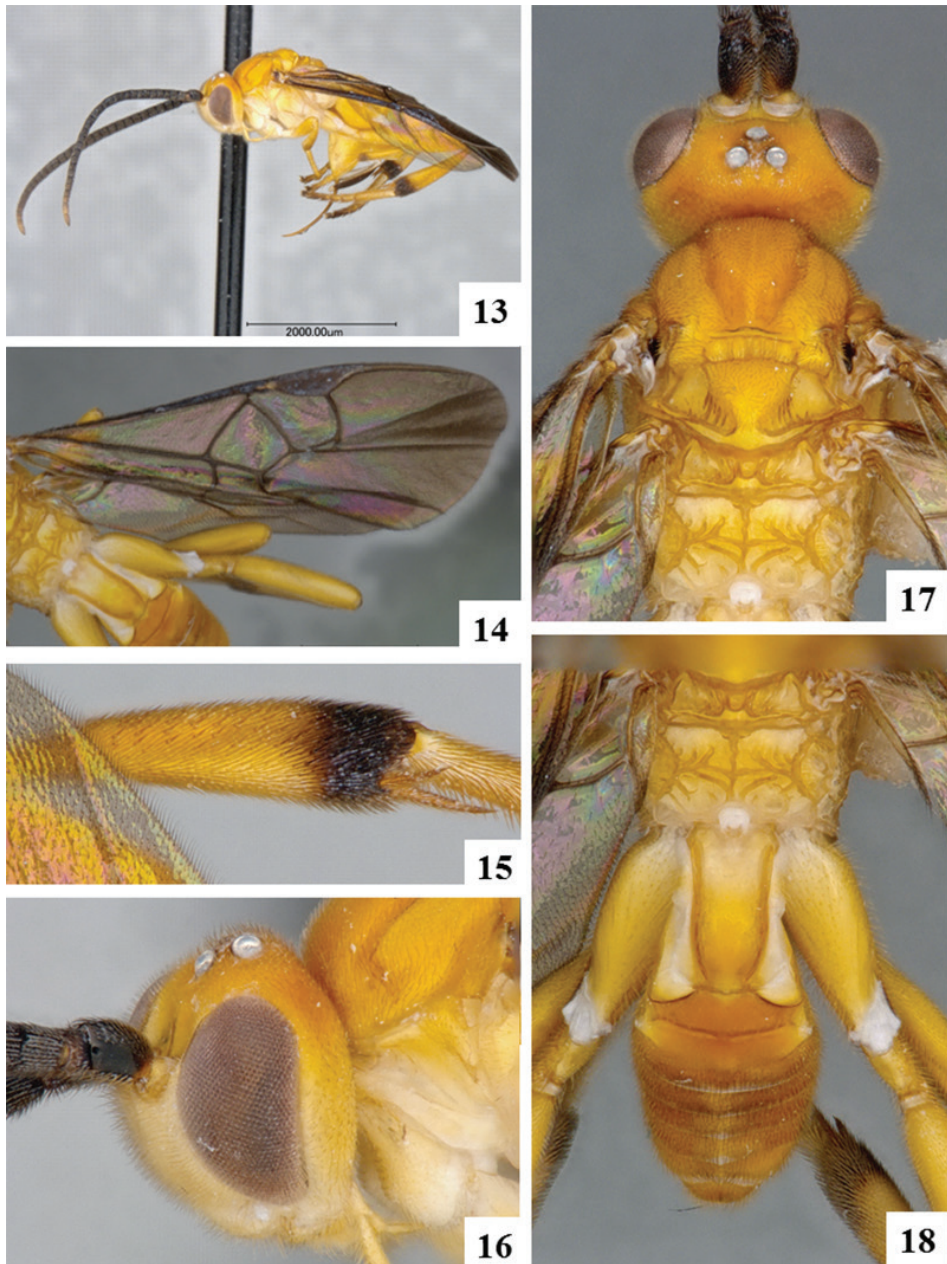
Figs 13–18, 99

Type locality. COSTA RICA, ACG, Alajuela, Province, Sector Rincon Rain Forest, Montanya Figueres, 460m, 10.88367, -85.29081.

Holotype. ♀ in CNC. Specimen labels: 1. DHJPAR0045302. 2. Voucher: D.H.Janzen & W.Hallwachs, DB: <http://janzen.sas.upenn.edu>, Area de Conservación Guanacaste, COSTA RICA, 11-SRNP-42719.

Paratype. 4 ♀, 2 ♂ (CNC, NMNH). COSTA RICA, ACG database codes: DHJPAR0038211, DHJPAR0038246, DHJPAR0039997, DHJPAR0040003, DHJPAR0040005, DHJPAR0045165.

Description. Female. Body length 4.1–4.2 mm, 4.3–4.4 mm, rarely 4.5–4.6 mm. Fore wing length 4.5–4.6 mm, rarely 4.7–4.8 mm. Body color: meso- and metasoma entirely yellow-orange (with the exception of a very small black spot on axillar complex). Scape color: partially dark brown to black (Figs 17, 18). Flagellomeres color: most flagellomeres brown to black, except for small apical area (F15–16, and occasionally apical half of F14) which is yellow-brown (Fig. 13). Tegula and humeral complex color: tegula pale, humeral complex partially dark/partially pale. Mesotibia color: posterior 0.1–0.2 dark brown to black. Metatibia color: posterior 0.1–0.3 dark brown to black (Fig. 15). Metatibia spurs color: yellow-orange (Fig. 15). Metatarsus color: entirely yellow-white. Fore wing color pattern: uniformly and entirely infumate (except for small hyaline area near veins (RS+M)b and 2M). Fore wing veins color: all veins dark brown (Fig. 14). Pterostigma color: entirely dark brown. Hypostomal carina: not raised (Fig. 16). Scutoscutellar sulcus: with 5 impressions (Fig. 17). Areolet height÷vein r length (fore wing): 0.2 ×. Hind wing subbasal cell: mostly without setae. Hind tarsal claws: with pectination uniform, teeth thick and relatively evenly spaced. Shape of mediotergite 1: distinctly narrowing posteriorly, width at posterior margin clearly less than



Figures 13–18. *Prasmodon bobpoolei*. **13** Habitus **14** Fore wing **15** Metatibia **16** Head and mesosoma (partially), lateral view **17** Head and mesosoma, dorsal view **18** Propodeum and metasoma, dorsal view.

width at anterior margin and median width (Fig. 18). Mediotergite 1 length+width at posterior margin 5.6–6.0 ×. Mediotergite 2 width at posterior margin+length: 2.6–3.0 ×. Ovipositor sheaths length: 0.6 × as long as metatibia, rarely 0.5 × as long as metatibia.

Male. As female but with flagellomeres fully dark brown to black.

Molecular data. Sequences in BOLD: 15, barcode compliant sequences: 15 (Fig. 105).

Biology and ecology. Host: Elachistidae, *Antaeotricha* BioLep38, *Antaeotricha* Janzen110, *Antaeotricha* Janzen126, *Gonioterma* Janzen212, *Stenomoma* Janzen129.

Distribution. Costa Rica, ACG rain forest.

Etymology. This species is named in honour of Bob Poole of the National Museum of Natural History, Smithsonian Institution, Washington, D.C, in recognition of his decades of taxonomic knowledge and support contributing to understanding the species-level and higher taxonomy of the Noctuoidea and Geometroidea of ACG, INBio and Costa Rica, as well as other parts of the world.

***Prasmodon bobrobbinsi* Fernández-Triana & Whitfield, sp. n.**

<http://zoobank.org/4C754CF8-825E-42AE-99C0-D59F17DC178A>

http://species-id.net/wiki/Prasmodon_bobrobbinsi

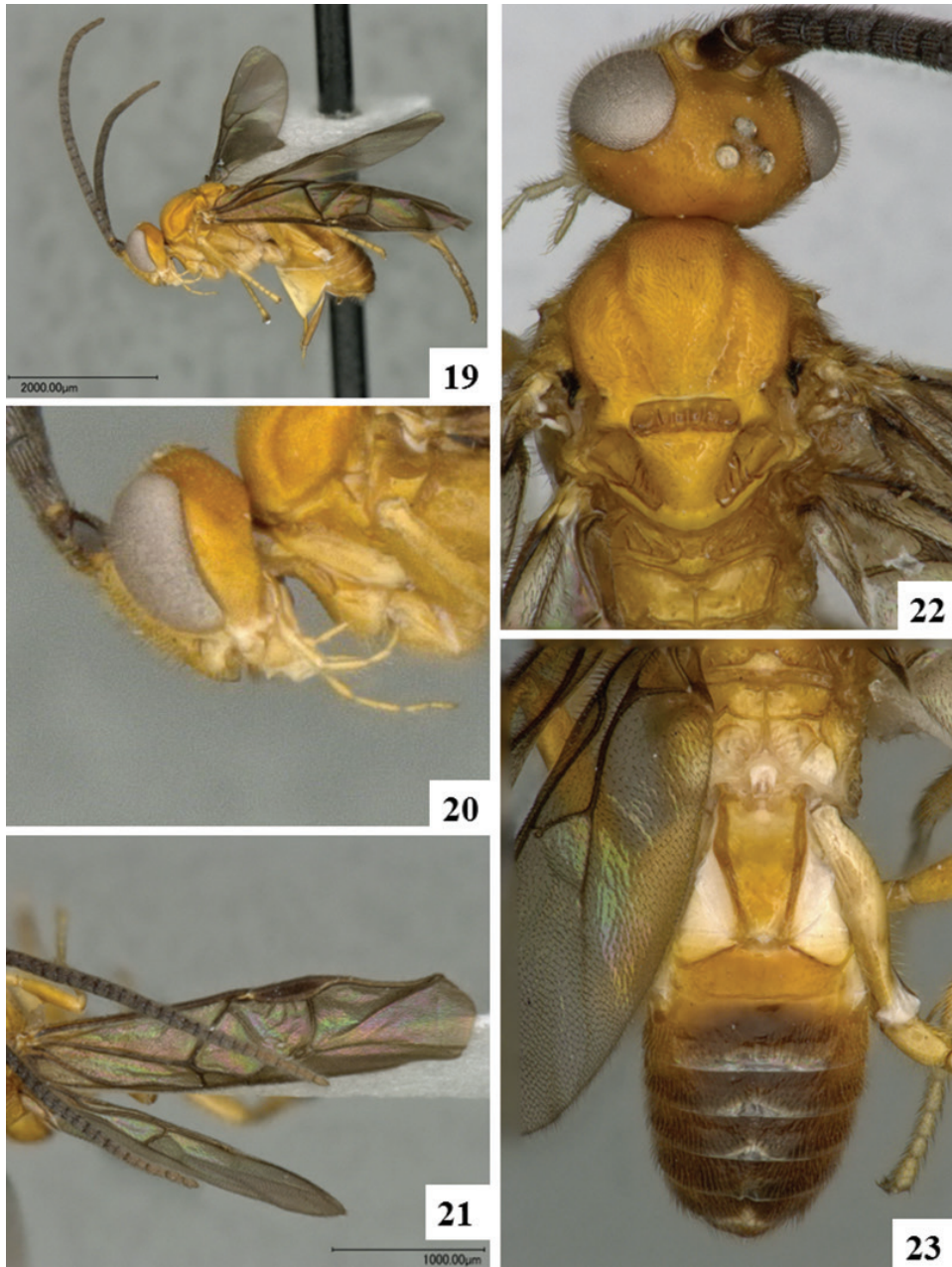
Figs 19–23, 100

Type locality. COSTA RICA, ACG, Alajuela Province, Sector Rincon Rain Forest, San Lucas, 320m, 10.91847, -85.30338.

Holotype. ♀ in CNC. Specimen labels: 1. DHJPAR0038915. 2. Voucher: D.H.Janzen & W.Hallwachs, DB: <http://janzen.sas.upenn.edu>, Area de Conservación Guanacaste, COSTA RICA, 10-SRNP-40484.

Paratype. 1 ♀, 1 ♂ (CNC). COSTA RICA, ACG database codes: DHJPAR0040012, 09-SRNP-3496.

Description. Female. Body length 3.7–3.8 mm or 3.9–4.0 mm. Fore wing length 3.9–4.0 mm or 4.1–4.2 mm. Body color: mesosoma entirely yellow-orange (with the exception of a very small black spot on axillar complex), metasoma with brown to black areas covering most of mediotergites 4–7 (and also part of mediotergites 3 and 8) (Figs 19, 22, 23). Scape color: partially dark brown to black. Flagellomeres color: all flagellomeres brown to black (Figs 19, 21). Tegula and humeral complex color: tegula pale, humeral complex partially dark/partially pale. Mesotibia color: entirely yellow. Metatibia color: posterior 0.1–0.3 dark brown to black. Metatibia spurs color: yellow-orange. Metatarsus color: dark brown to black (except for anterior 0.7 or less of first metatarsomere). Fore wing color pattern: uniformly and entirely infumate (except for small hyaline area near veins (RS+M)b and 2M). Fore wing veins color: all veins dark brown (Fig. 21). Pterostigma color: entirely dark brown. Hypostomal carina: highly raised (Fig. 20). Scutoscutellar sulcus: with 6 impressions (Fig. 22). Areolet height+vein r length (fore wing): 0.2 ×. Hind wing subbasal cell: mostly with setae. Hind tarsal claws: with pectination uniform, teeth thick and relatively evenly spaced. Shape of mediotergite 1: distinctly narrowing posteriorly, width at posterior margin clearly less than width at anterior margin and median width (Fig. 23). Mediotergite 1 length+width at posterior margin 4.1–4.5 × or 4.6–5.0 ×. Mediotergite 2 width at posterior margin+length: 2.6–3.0 ×. Ovipositor sheaths length: 0.5 × as long as metatibia.



Figures 19–23. *Prasmodon bobrobbinsi*. **19** Habitus **20** Head and mesosoma (partially), lateral view **21** Fore wing and antenna (partially) **22** Head and mesosoma, dorsal view **23** Propodeum and metasoma, dorsal view.

Male. Morphologically similar to females.

Molecular data. Sequences in BOLD: 2, barcode compliant sequences: 2 (Fig. 105).

Biology and ecology. Host: Crambidae, *Palpita jairusalis*DHJ01.

Distribution. Costa Rica, ACG rain forest.

Etymology. This species is named in honour of Bob Robbins of the National Museum of Natural History, Smithsonian Institution, Washington, D.C, in recognition of his decades of taxonomic knowledge and support, contributing to understanding the species-level and higher taxonomy of the Lycaenidae of ACG, INBio and Costa Rica, as well as other parts of the world.

***Prasmodon dondavis* Fernández-Triana & Whitfield, sp. n.**

<http://zoobank.org/31AF25BD-0151-46EF-A980-1B9BF3BB339E>

http://species-id.net/wiki/Prasmodon_dondavis

Figs 24–28

Type locality. COSTA RICA, ACG, Alajuela Province, Sector Rincón Rain Forest, Jacobo, 461m, 10.94076, -85.3177.

Holotype. ♀ in CNC. Specimen labels: 1. DHJPAR0040002. 2. Voucher: D.H.Janzen & W.Hallwachs, DB: <http://janzen.sas.upenn.edu>, Area de Conservación Guanacaste, COSTA RICA, 09-SRNP-69586.

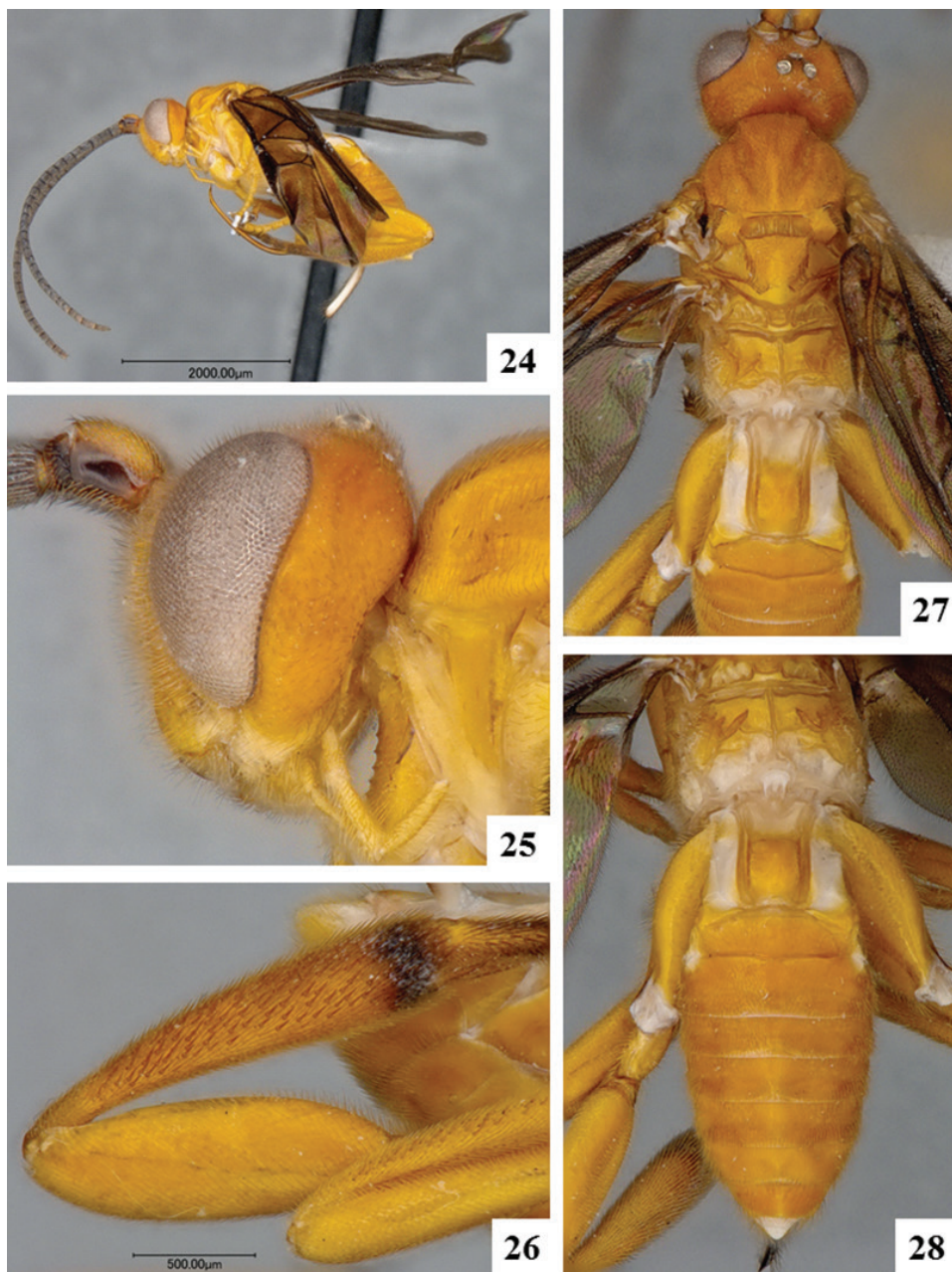
Paratype. 1 ♀, 9 ♂ (CNC, INHS, NMNH,). COSTA RICA, ACG database code: DHJPAR003990, DHJPAR0039992, DHJPAR0039994, DHJPAR0039995, DHJPAR0039998, DHJPAR004000, DHJPAR0040004, DHJPAR0040006, DHJPAR0040007, DHJPAR0040010.

Description. Female. Body length 5.3–5.4 mm or 5.5–5.6 mm. Fore wing length 5.5–5.6 mm or 5.7–5.8 mm. Body color: meso- and metasoma entirely yellow-orange (with the exception of a very small black spot on axillar complex) (Figs 24, 27, 28). Scape color: partially dark brown to black. Flagellomeres color: all flagellomeres brown to black (Fig. 24). Tegula and humeral complex color: both pale. Mesotibia color: entirely yellow. Metatibia color: posterior 0.1–0.3 dark brown to black (Fig. 26). Metatibia spurs color: yellow-orange. Metatarsus color: dark brown to black (except for anterior 0.7 or less of first metatarsomere). Fore wing color pattern: uniformly and entirely infumate (except for small hyaline area near veins (RS+M)b and 2M). Fore wing veins color: all veins dark brown. Pterostigma color: entirely dark brown. Hypostomal carina: not raised (Fig. 25). Scutoscutellar sulcus: with 4 impressions (Fig. 27). Areolet height÷vein r length (fore wing): 0.3 ×. Hind wing subbasal cell: mostly with setae. Hind tarsal claws: with pectination uniform, teeth thick and relatively evenly spaced. Shape of mediotergite 1: distinctly narrowing at around 0.5 its length, with both anterior and posterior margins clearly wider than its median width (Fig. 28). Mediotergite 1 length÷width at posterior margin 3.1–3.5 × or 3.6–4.0 ×. Mediotergite 2 width at posterior margin÷length: 3.1–3.5 ×. Ovipositor sheaths length: 0.5 × as long as metatibia.

Male. Morphologically similar to females.

Molecular data. Sequences in BOLD: 17, barcode compliant sequences: 15 (Fig. 105).

Biology and ecology. Hosts: Crambidae feeding on Apocynaceae: *Prenesta* Janzen196, *Prenesta* Janzen195, *Prenesta scyllalis*DHJ03.



Figures 24–28. *Prasmodon dondavisi*. **24** Habitus **25** Head and mesosoma (partially), lateral view **26** Metatibia **27** Head and mesosoma, dorsal view **28** Propodeum and metasoma, dorsal view.

Distribution. Costa Rica, ACG rain forest.

Etymology. This species is named in honour of Don Davis of the National Museum of Natural History, Smithsonian Institution, Washington, D.C, in recognition

of his decades of taxonomic knowledge and support, contributing to understanding the species-level and higher taxonomy of the Tineoidea and other small impossible moths of ACG, INBio and Costa Rica, as well as other parts of the world.

***Prasmodon eminens* Nixon, 1965**

http://species-id.net/wiki/Prasmodon_eminens

Figs 95, 97

Prasmodon eminens Nixon, 1965: 206.

Type locality. PERU: Chanchamayo.

Holotype. ♂, NHM (not examined).

Material examined. 8 ♀, 18 ♂ (BMNH, CNC, INBio, INHS, NMNH), Costa Rica, ACG; 2 ♂ (CNC), Ecuador, Pichincha, Rio Palenque, 160–200m.

Description. Female. Body length 4.9–5.0 mm, 5.1–5.2 mm, rarely 5.3–5.4 mm. Fore wing length 5.1–5.2 mm, 5.3–5.4 mm, rarely 5.5–5.6 mm. Body color: mesosoma entirely yellow-orange (with the exception of a very small black spot on axillar complex), metasoma with only small brown areas centrally on mediotergites 4–7 (usually only on mediotergites 5–6) (Fig. 95). Scape color: partially dark brown to black. Flagellomeres color: most flagellomeres brown to black, except for small apical area (F15–16, and occasionally apical half of F14) which is yellow-brown. Tegula and humeral complex color: both pale. Mesotibia color: posterior 0.1–0.2 dark brown to black. Metatibia color: posterior 0.1–0.3 dark brown to black (Fig. 95). Metatibia spurs color: dark brown to black. Metatarsus color: dark brown to black (except for anterior 0.7 or less of first metatarsomere) (Fig. 95). Fore wing color pattern: uniformly and entirely infumate (except for small hyaline area near veins (RS+M)b and 2M). Fore wing veins color: all veins dark brown (Fig. 95). Pterostigma color: entirely dark brown. Hypostomal carina: not raised. Scutoscutellar sulcus: with 5 impressions or with 6 impressions. Areolet height÷vein r length (fore wing): 0.2 ×. Hind wing subbasal cell: mostly without setae. Hind tarsal claws: with pectination uniform, teeth thick and relatively evenly spaced. Shape of mediotergite 1: distinctly narrowing posteriorly, width at posterior margin clearly less than width at anterior margin and median width (Fig. 95). Mediotergite 1 length÷width at posterior margin 4.1–4.5 ×. Mediotergite 2 width at posterior margin÷length: 3.1–3.5 ×, rarely 2.6–3.0 ×. Ovipositor sheaths length: 0.5 × as long as metatibia or 0.6 × as long as metatibia.

Male. As female but with flagellomeres fully dark brown to black.

Molecular data. Sequences in BOLD: 67, barcode compliant sequences: 61 (Fig. 105).

Biology and ecology. Hosts: Crambidae, *Anarmodia nebulosalis*, *Asturodes fimbriauralis*DHJ02, *Bocchoris marucalis*, *Ceratocilia sixolalis*, *Desmia* Janzen07, *Desmia* Solis19, *Eulepte concordalis*, *Eulepte* Janzen12, *Eulepte* Solis15, *Mimophobetron pyropsalis*, *Omiodes fulvicauda*, *Omiodes humeralis*, *Pantographa suffusalis*, *Parastenia retractalis*, *Phostria mapetalis*, *Piletosoma thialis*, *Portentomorpha xanthialis*, and *Syllepte amando*DHJ02.

Distribution. Widely distributed in rain forest in northern South America and Central America, including Brazil (Mardulyn and Whitfield 1999), Costa Rica, ACG rain forest (Valerio et al. 2005), Ecuador (this paper), and Peru (Nixon 1965).

Comments. This species was described by Nixon (1965) based on one male specimen. Valerio et al. (2005) extensively illustrated the species, including the cocoon and adults, but until now no detailed description of the female was available. DNA barcodes were made available recently by Smith et al. (2013). Host records are considerably expanded here, based on new data from the ongoing inventory of ACG parasitoids. Valerio et al. (2005) mentioned that this species shows some regional morphological variation and might well represent a complex of sibling species. Since we were not able to examine the holotype, or DNA barcode it, we infer from its morphological description that the ACG *Prasmodon eminens* is the same species.

***Prasmodon erenadupontae* Braet & Fernández-Triana, sp. n.**

<http://zoobank.org/D163BA78-BDE4-4F8E-B549-909751C9785A>

http://species-id.net/wiki/Prasmodon_erenadupontae

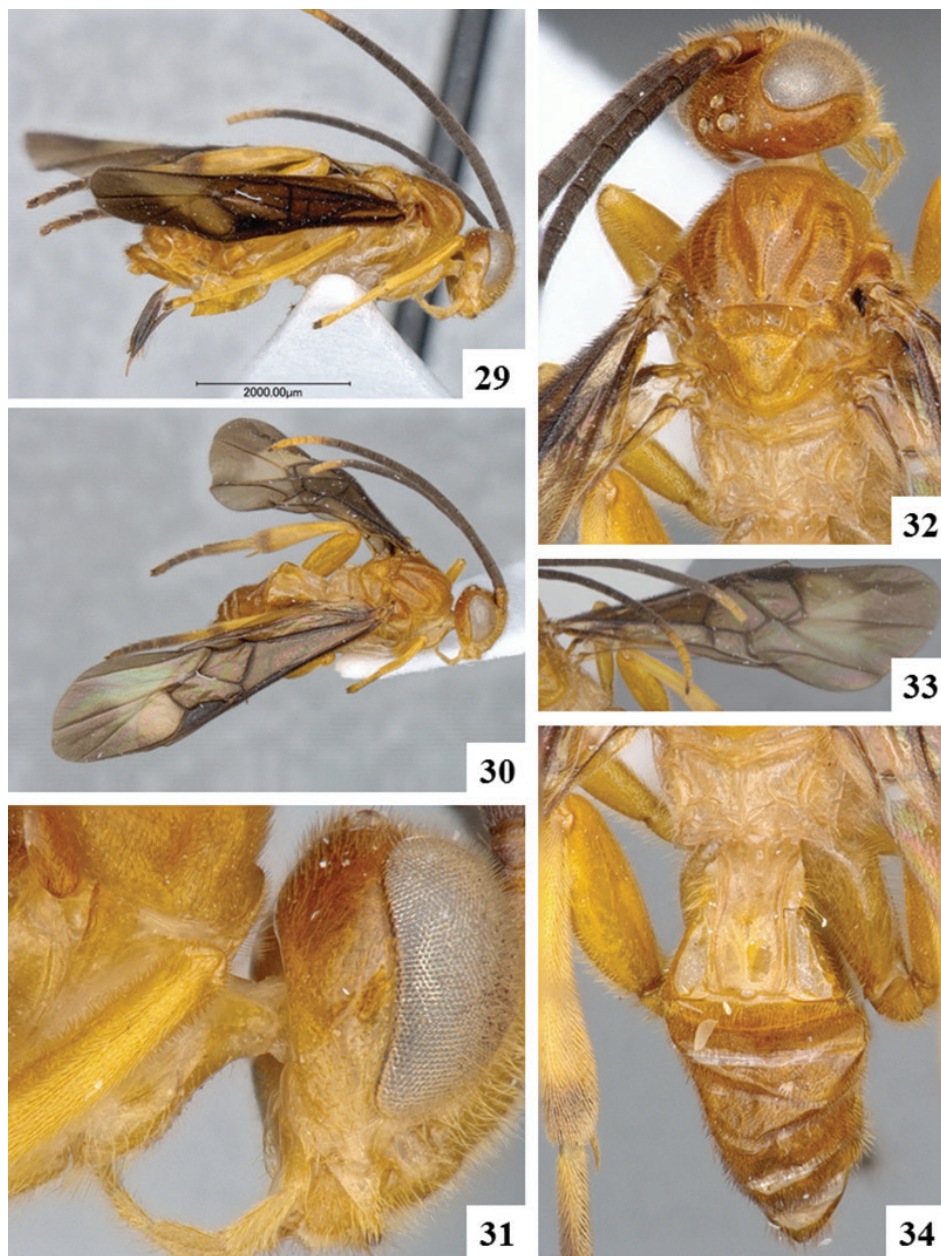
Figs 29–34

Type locality. FRENCH GUIANA, Saul.

Holotype. ♀ in MNHN. Specimen labels: 1. Guyane Francaise, Saul, 29.IX.2010, SEAG rec 2010.

Paratype. 2 ♀, 3 ♂ (CNC, IRSNB). French Guiana, same locality than holotype, 17–26.ix.2010 (1 ♀, 1 ♂); Montagne de Kaw, Relais Patawa, ix.1999 (1 ♀); Nouragues Reserve, Inselberg, 16.x.2010 (1 ♂); Brazil, Mato Grosso, Sinop, xi.1975 (1 ♂).

Description. Female. Body length 5.3–5.4 mm, 5.5–5.6 mm or 5.7–5.8 mm. Fore wing length 5.9–6.0 mm or 6.1–6.2 mm. Body color: meso- and metasoma entirely yellow-orange (with the exception of a very small black spot on axillar complex) (Figs 29, 32, 34). Scape color: partially dark brown to black. Flagellomeres color: with relatively extense yellow area (at least including F13–15, and usually apical half of F11 and basal half of F16) (Fig. 30). Tegula and humeral complex color: both pale. Mesotibia color: entirely yellow. Metatibia color: posterior 0.1–0.3 dark brown to black. Metatibia spurs color: yellow-orange. Metatarsus color: dark brown to black (except for anterior 0.7 or less of first metatarsomere) (Fig. 30). Fore wing color pattern: mostly infumate, but with pale area centrally which gives the wing a banded appearance (Figs 30, 33). Fore wing veins color: anterior 0.4–0.5 of vein 3M (and usually part or all of veins 2M and r-m) yellow-orange, contrasting with all other veins which are dark brown (Fig. 33). Pterostigma color: entirely dark brown (Fig. 30). Hypostomal carina: highly raised (Fig. 31). Scutoscuteellar sulcus: with 4 impressions (Fig. 32). Areolet height÷vein r length (fore wing): 0.2 ×. Hind wing subbasal cell: mostly without setae. Hind tarsal claws: with pectination uniform, teeth thick and relatively evenly spaced. Shape of mediotergite 1: distinctly narrowing at around 0.5 its length, with both anterior and posterior margins clearly wider than its median



Figures 29–34. *Prasmodon arenadupontae*. **29** Habitus **30** Body, dorso-lateral view **31** Head and mesosoma (partially), lateral view **32** Head and mesosoma, dorsal view **33** Fore wing **34** Propodeum and metasoma, dorsal view.

width (Fig. 34). Mediotergite 1 length+width at posterior margin 2.9–3.0 ×. Mediotergite 2 width at posterior margin+length: 3.6–4.0 ×. Ovipositor sheaths length: 0.5 × as long as metatibia.

Male. Morphologically similar to females, but with antenna only yellow on flagellomeres 15–16 (females with flagellomeres 12–16 yellow).

Molecular data. Sequences in BOLD: 1, barcode compliant sequences: 1.

Biology and ecology. Malaise trapped.

Distribution. Brazil, French Guiana.

Etymology. Named after Erena Dupont (the partner of YB) who shares his passion in entomology and for her strong support.

Comments. The only specimen with associated molecular data is the male paratype from Brazil.

***Prasmodon johnbrowni* Fernández-Triana & Whitfield, sp. n.**

<http://zoobank.org/F131E6A1-F5FF-414D-803F-7719C0E2A533>

http://species-id.net/wiki/Prasmodon_johnbrowni

Figs 35–39, 103

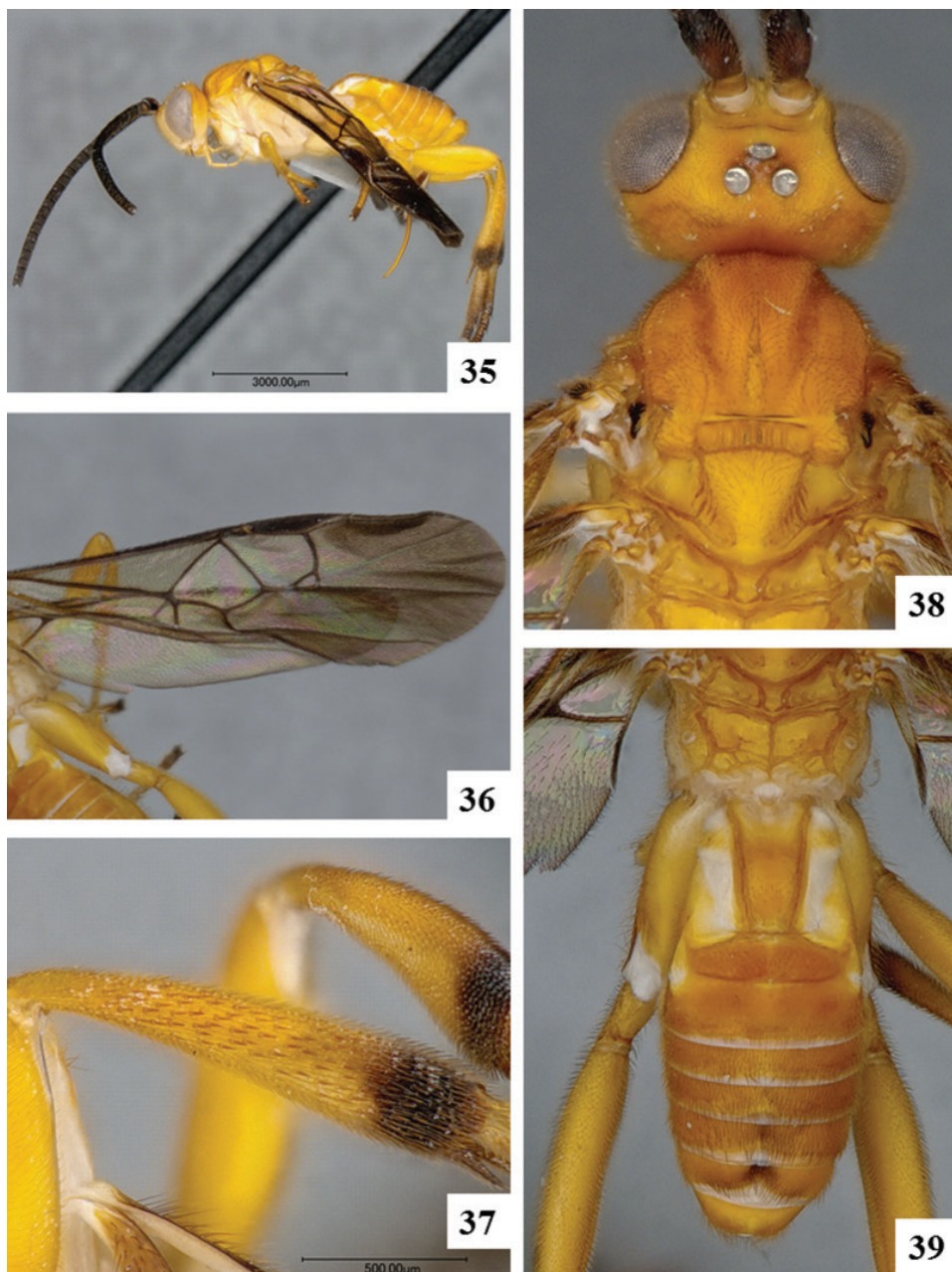
Type locality. COSTA RICA, ACG, Alajuela Province, Sector Rincon Rain Forest, Estación Llanura, 135m, 10.93332, -85.25331.

Holotype. ♀ in CNC. Specimen labels: 1. DHJPAR0035300. 2. Voucher: D.H.Janzen & W.Hallwachs, DB: <http://janzen.sas.upenn.edu>, Area de Conservación Guanacaste, COSTA RICA, 09-SRNP-44366.

Paratype. 5 ♀, 2 ♂ (CNC, NMNH). COSTA RICA, ACG database code: DHJPAR0038172, DHJPAR0038174, DHJPAR0038175, DHJPAR0038177, DHJPAR0038922, DHJPAR0039993.

Description. Female. Body length 4.5–4.6 mm, 4.7–4.8 mm, 4.9–5.0 mm, rarely 5.1–5.2 mm. Fore wing length 4.9–5.0 mm, 5.1–5.2 mm, rarely 5.3–5.4 mm. Body color: meso- and metasoma entirely yellow-orange (with the exception of a very small black spot on axillar complex) (Figs 35, 38, 39). Scape color: partially dark brown to black. Flagellomeres color: all flagellomeres brown to black (Fig. 35). Tegula and humeral complex color: tegula pale, humeral complex dark. Mesotibia color: posterior 0.1–0.2 dark brown to black. Metatibia color: posterior 0.1–0.3 dark brown to black (Fig. 37). Metatibia spurs color: dark brown to black (Figs 35, 37). Metatarsus color: dark brown to black (except for anterior 0.7 or less of first metatarsomere). Fore wing color pattern: uniformly and entirely infumate (except for small hyaline area near veins (RS+M)b and 2M). Fore wing veins color: all veins dark brown (Fig. 36). Pterostigma color: entirely dark brown (Fig. 38). Hypostomal carina: not raised. Scutoscuteellar sulcus: with 6 impressions, rarely with 5 impressions. Areolet height+vein r length (fore wing): 0.3 ×. Hind wing subbasal cell: mostly without setae. Hind tarsal claws: with pectination uniform, teeth thick and relatively evenly spaced. Shape of mediotergite 1: distinctly narrowing posteriorly, width at posterior margin clearly less than width at anterior margin and median width (Fig. 39). Mediotergite 1 length+width at posterior margin 6.1–6.5 ×. Mediotergite 2 width at posterior margin+length: 2.6–3.0 ×. Ovipositor sheaths length: 0.5 × as long as metatibia or 0.6 × as long as metatibia.

Male. Morphologically similar to females.



Figures 35–39. *Prasmodon johnbrowni*. **35** Habitus **36** Fore wing **37** Metatibia **38** Head and mesosoma, dorsal view **39** Propodeum and metasoma, dorsal view.

Molecular data. Sequences in BOLD: 12, barcode compliant sequences: 12 (Fig. 105).

Biology and ecology. Hosts: Crambidae, *Asturodes fimbriauralis*DHJ02, *Asturodes fimbriauralis*, *Eulepte alialis*, *Piletosoma thialis*, *Phostria* Janzen05.

Distribution. Costa Rica, ACG rain forest.

Etymology. This species is named in honour of John Brown of the SEL/USDA laboratory in the National Museum of Natural History, Smithsonian Institution, Washington, D.C, in recognition of his decades of taxonomic knowledge and support contributing to understanding the species-level and higher taxonomy of the Tortricoidea of ACG, INBio and Costa Rica, as well as other parts of the world.

***Prasmodon masoni* Fernández-Triana & Whitfield, sp. n.**

<http://zoobank.org/39CD8542-C231-4CDB-A67B-57782406696B>

http://species-id.net/wiki/Prasmodon_masoni

Figs 40–45

Type locality. BRAZIL, Mato Grosso, Sinop.

Holotype. ♀ in CNC. Specimen labels: 1. BRAZIL, Mato Grosso, Sinop, X.1974., M. Alvarenga, Mal. Trap. 2. DNA Voucher, CNCHYM 01962.

Paratype. 1 ♀, 6 # M (CNC), Brazil, same locality than holotype, collecting dates: x.1974, x.1975, ii.1976.

Other material examined. 1 ♀ (CNC) from Brazil, Amazonas, Estirar de Ecuador, Rio Javari, ix.1979.

Description. Female. Body length 3.5–3.6 mm, rarely 3.9–4.0 mm. Fore wing length 3.7–3.8 mm, rarely 4.1–4.2 mm. Body color: meso- and metasoma entirely yellow-orange (with the exception of a very small black spot on axillar complex) (Figs 40, 44, 45). Scape color: partially dark brown to black (Fig. 44). Flagellomeres color: all flagellomeres brown to black (Figs 40–42). Tegula and humeral complex color: both pale. Mesotibia color: entirely yellow. Metatibia color: entirely yellow (Fig. 43). Metatibia spurs color: yellow-orange. Metatarsus color: entirely yellow-white (Fig. 43). Fore wing color pattern: hyaline. Fore wing veins color: all veins dark brown. Pterostigma color: entirely dark brown. Hypostomal carina: not raised (Fig. 42). Scutoscutellar sulcus: with 4 impressions (Fig. 44). Areolet height÷vein r length (fore wing): 0.2 x, rarely 0.3 x. Hind wing subbasal cell: mostly with setae (Figs 44, 45). Hind tarsal claws: with pectination (teeth) very irregular in spacing and length. Shape of mediotergite 1: distinctly narrowing posteriorly, width at posterior margin clearly less than width at anterior margin and median width (Fig. 45). Mediotergite 1 length÷width at posterior margin 4.1–4.5 x or 4.6–5.0 x. Mediotergite 2 width at posterior margin÷length: 2.6–3.0 x. Ovipositor sheath length: 0.3 x as long as metatibia.

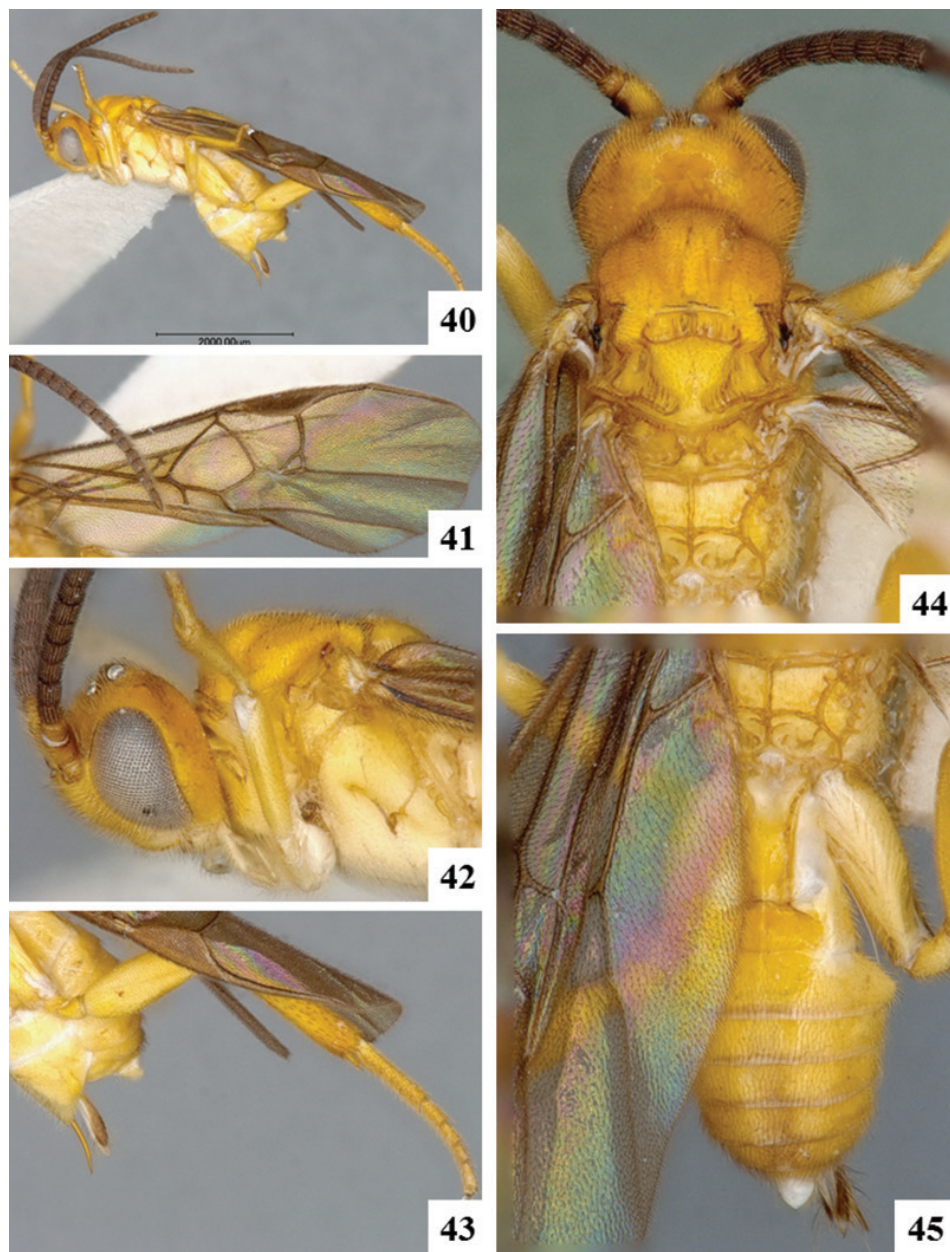
Male. Morphologically similar to female.

Molecular data. No DNA barcodes were obtained for this species.

Biology and ecology. Malaise-trapped.

Distribution. Brazil, Mato Grosso.

Etymology. Named after William R. M. Mason, the greatest Canadian expert on Microgastrinae. The holotype and paratype specimen had a label written by Mason, who considered them to represent a new species (Mason, 1981), which remained undescribed until now.



Figures 40–45. *Prasmodon masoni*. **40** Habitus **41** Fore wing **42** Head and mesosoma (partially), lateral view **43** Hypopygium, ovipositor, ovipositor sheaths, and hind leg (partially), lateral view **44** Head and mesosoma, dorsal view **45** Propodeum and metasoma, dorsal view.

Comments. We have included here one female from a locality (Rio Javari, Brazil) far from the type locality (Sinop, where all other specimens of the species were collected). The female from Rio Javari resembles the female holotype and another female

paratype, but was not included as part of the paratype series in case it is eventually found to represent a different species. We also studied another 15 CNC male specimens of *Prasmodon* that were collected in Mato Grosso. They seem to represent 2–3 additional species. However, no molecular or host information is available for those specimens, and the morphological data are inadequate to properly describe them at present.

***Prasmodon mikepoguei* Fernández-Triana & Whitfield, sp. n.**

<http://zoobank.org/A2BBA863-E45D-4A6C-AAFD-217CE7FABBC2>

http://species-id.net/wiki/Prasmodon_mikepoguei

Figs 46–51, 96

Type locality. COSTA RICA, ACG, Guanacaste Province, Sector Pitilla, Leonel, 510m, 10.99637, -85.40195.

Holotype. ♂ in CNC. Specimen labels: 1. DHJPAR0038222. 2. Voucher: D.H.Janzen & W.Hallwachs, DB: <http://janzen.sas.upenn.edu>, Area de Conservación Guanacaste, COSTA RICA, 09-SRNP-72161.

Description. Male. Body length 3.7–3.8 mm. Fore wing length 4.1–4.2 mm. Body color: meso- and metasoma with brown to black areas, metasoma with most of tergites 2–8 dark brown (Figs 46, 50, 51). Scape color: partially dark brown to black. Flagellomeres color: all flagellomeres brown to black (Fig. 47). Tegula and humeral complex color: tegula pale, humeral complex dark. Mesotibia color: entirely yellow. Metatibia color: posterior 0.1–0.3 dark brown to black (Fig. 49). Metatibia spurs color: yellow-orange. Metatarsus color: dark brown to black (except for anterior 0.7 or less of first metatarsomere). Fore wing color pattern: uniformly and entirely infumate (except for small hyaline area near veins (RS+M)b and 2M). Fore wing veins color: all veins dark brown. Pterostigma color: entirely dark brown. Hypostomal carina: not raised. Scutoscutellar sulcus: with 4 impressions (Fig. 50). Hind wing subbasal cell: mostly with setae (Figs 48, 50, 51). Hind tarsal claws: with pectination uniform, teeth thick and relatively evenly spaced. Shape of mediotergite 1: distinctly narrowing posteriorly, width at posterior margin clearly less than width at anterior margin and median width (Fig. 51).

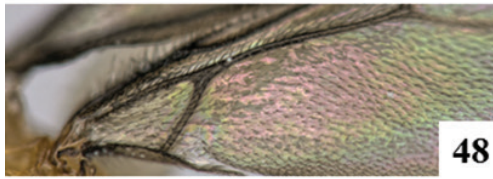
Female. Unknown.

Molecular data. Sequences in BOLD: 4, barcode compliant sequences: 4 (Fig. 105).

Biology and ecology. Hosts: Elachistidae, *Chlamydastis tryphon*, *Antaeotricha* BioLep42, *Antaeotricha* Janzen07.

Distribution. Costa Rica, ACG rain forest.

Etymology. This species is named in honour of Mike Pogue of the SEL/USDA laboratory in the National Museum of Natural History, Smithsonian Institution, Washington, D.C, in recognition of his decades of taxonomic knowledge and support contributing to understanding the species-level and higher taxonomy of the Notodontidae and Noctuidae of ACG, INBio and Costa Rica, as well as other parts of the world.



Figures 46–51. *Prasmodon mikepoguei*. **46** Habitus **47** Fore wing **48** Detail of the hind wing **49** Metatibia **50** Head and mesosoma, dorsal view **51** Propodeum and metasoma, dorsal view.

***Prasmodon nixon* Fernández-Triana & Whitfield, sp. n.**

<http://zoobank.org/989FD927-8A4A-4582-A69D-DE20AFA9841D>

http://species-id.net/wiki/Prasmodon_nixon

Figs 52–58

Type locality. PERU, Loreto, Iquitos, Barillal.

Holotype. ♀ in CNC. Specimen labels: 1. PERU: Loreto, Iquitos, Barillal, 10.ii.1984, L. Huggert. 2. DNA Voucher, CNCHYM 01957.

Paratype. 1 ♀ (IRSNB). French Guiana, Montagne de Kaw, Relais Patawa, v.2001.

Description. Female. Body length 4.3–4.4 mm or 4.5–4.6 mm. Fore wing length 4.5–4.6 mm or 4.7–4.8 mm. Body color: meso- and metasoma entirely yellow-orange (with the exception of a very small black spot on axillar complex) (Figs 52, 56, 58). Scape color: partially dark brown to black. Flagellomeres color: with relatively extensive yellow area (at least including F13–15, and usually apical half of F11 and basal half of F16) (Figs 52–54). Tegula and humeral complex color: both pale. Mesotibia color: entirely yellow. Metatibia color: entirely yellow (Fig. 55). Metatibia spurs color: yellow-orange. Metatarsus color: dark brown to black (except for anterior 0.7 or less of first metatarsomere). Fore wing color pattern: hyaline. Fore wing veins color: all veins dark brown (Fig. 53). Pterostigma color: entirely dark brown. Hypostomal carina: not raised (Fig. 57). Scutoscutellar sulcus: with 6 impressions (Fig. 56). Areolet height÷vein r length (fore wing): 0.2 ×. Hind wing subbasal cell: mostly with setae. Hind tarsal claws: with 1 or 2 teeth on anterior 0.3 of claw. Shape of mediotergite 1: distinctly narrowing posteriorly, width at posterior margin clearly less than width at anterior margin and median width (Fig. 58). Mediotergite 1 length÷width at posterior margin 4.6–5.0 ×. Mediotergite 2 width at posterior margin÷length: 3.6–4.0 ×. Ovipositor sheaths length: 0.5 × as long as metatibia.

Male. Unknown.

Molecular data. Sequences in BOLD: 1, barcode compliant sequences: 0.

Biology and ecology. Malaise-trapped.

Distribution. French Guiana, Peru.

Etymology. Named to honour Gilbert E. J. Nixon, one of the great British experts on Microgastrinae and the first person to describe a species of *Prasmodon*.

***Prasmodon paulgoldsteini* Fernández-Triana & Whitfield, sp. n.**

<http://zoobank.org/3AD73865-F1F1-415F-9DDB-41BFAA5D0E1A>

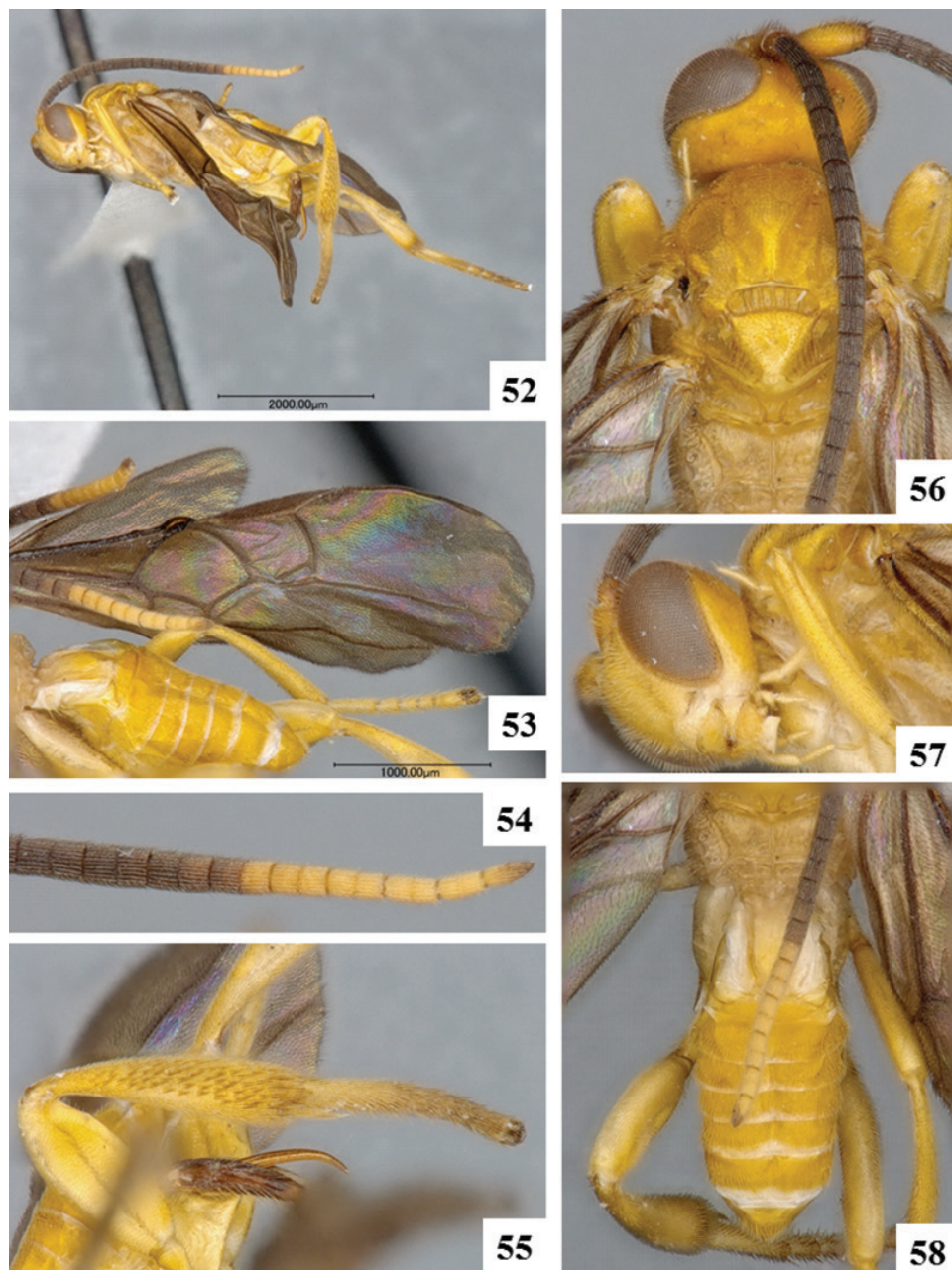
http://species-id.net/wiki/Prasmodon_paulgoldsteini

Figs 59–63

Type locality. COSTA RICA, Guanacaste, ACG, Sector Santa Rosa, Bosque San Emilio, 300m, 10.84389, -85.61384.

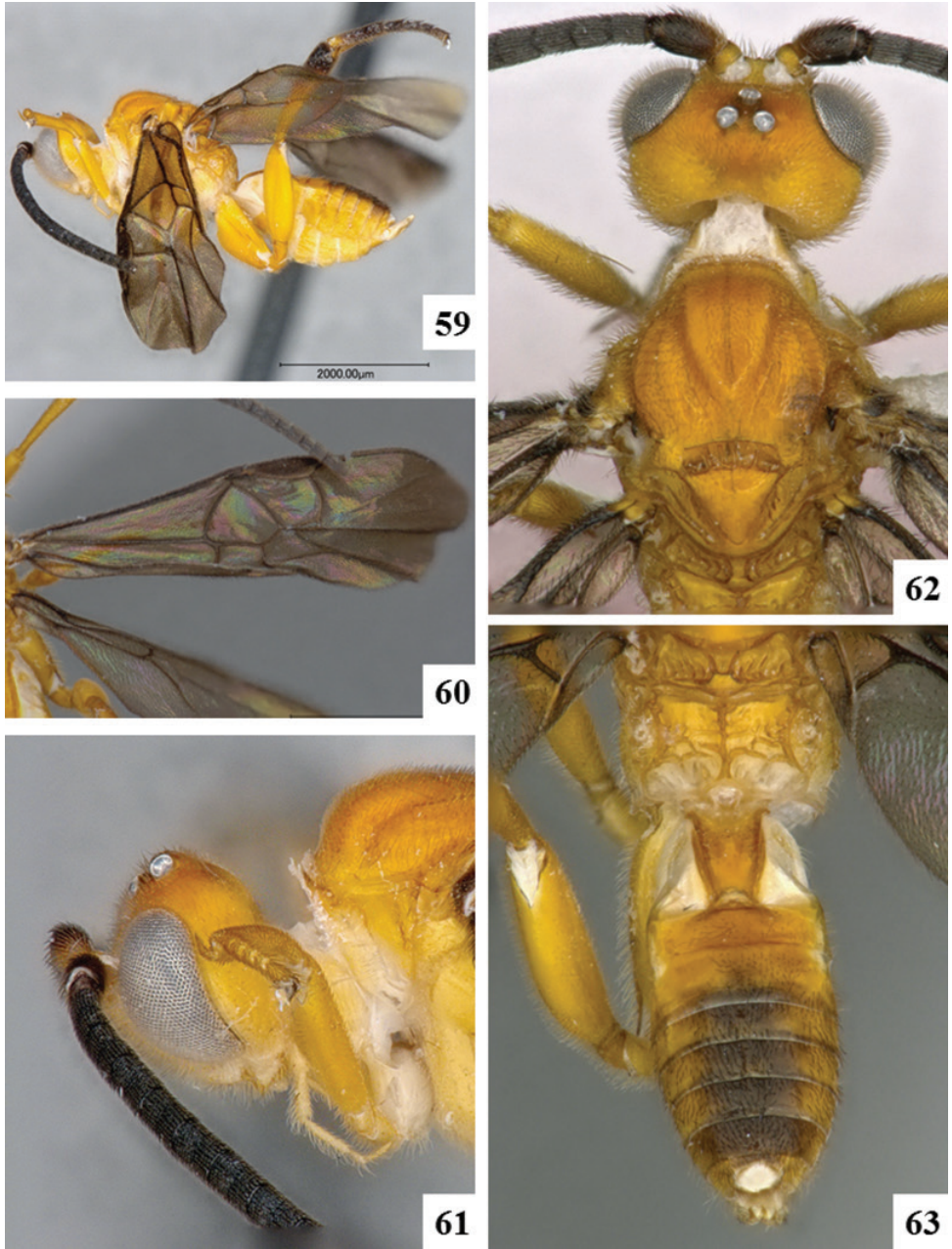
Holotype. ♂ in CNC. Specimen labels: 1. DHJPAR0013126.

Paratypes. 4 ♂ (CNC, NMNH). COSTA RICA, ACG database codes: DHJPAR0013131, DHJPAR0013124, DHJPAR0013125, DHJPAR0013132.



Figures 52–58. *Prasmodon nixonii*. **52** Habitus **53** Fore wing **54** Antenna (partially) **55** Metatibia **56** Head and mesosoma, dorsal view **57** Head and mesosoma (partially), lateral view **58** Propodeum and metasoma, dorsal view.

Description. Male. Body length 4.1–4.2 mm. Fore wing length 4.3–4.4 mm. Body color: mesosoma entirely yellow-orange (with the exception of a very small black spot on axillar complex), metasoma with only small brown areas centrally on medioter-



Figures 59–63. *Prasmodon paulgoldsteini*. **59** Habitus **60** Fore wing **61** Head and mesosoma (partially), lateral view **62** Head and mesosoma, dorsal view **63** Propodeum and metasoma, dorsal view.

gites 4–7 (usually only on mediotergites 5–6) (Figs 62, 63). Scape color: partially dark brown to black. Flagellomeres color: all flagellomeres brown to black (Fig. 59). Tegula and humeral complex color: tegula pale, humeral complex partially dark/partially pale.

Mesotibia color: entirely yellow. Metatibia color: posterior 0.1–0.3 dark brown to black (Fig. 59). Metatibia spurs color: yellow-orange. Metatarsus color: dark brown to black (except for anterior 0.7 or less of first metatarsomere). Fore wing color pattern: uniformly and entirely infumate (except for small hyaline area near veins (RS+M)b and 2M). Fore wing veins color: all veins dark brown (Fig. 60). Pterostigma color: entirely dark brown. Hypostomal carina: highly raised. Scutoscutellar sulcus: with 5 impressions or with 6 impressions. Hind wing subbasal cell: mostly with setae. Hind tarsal claws: with pectination (teeth) very irregular in spacing and length. Shape of mediotergite 1: distinctly narrowing posteriorly, width at posterior margin clearly less than width at anterior margin and median width (Fig. 63).

Female. Unknown.

Molecular data. Sequences in BOLD: 6, barcode compliant sequences: 6 (Fig. 105).

Biology and ecology. Malaise trapped.

Distribution. Costa Rica, ACG.

Comments. At present this species is only known from males, but it was described because of clear morphological and molecular differences with the other species within the genus.

Etymology. This species is named in honour of Paul Goldstein working in the SEL/USDA laboratory in the National Museum of Natural History, Smithsonian Institution, Washington, D.C, and with the Department of Entomology of the University of Maryland, in recognition of his intense effort to solve the *Desmia* (Crambidae, Spilomelinae) many-species taxonomic puzzle for ACG.

***Prasmodon scottmilleri* Fernández-Triana & Whitfield, sp. n.**

<http://zoobank.org/8BCFA3EE-53D0-4582-AE6B-A31D544DE9B1>

http://species-id.net/wiki/Prasmodon_scottmilleri

Figs 64–69, 98

Type locality. COSTA RICA, ACG, Alajuela Province, Sector Rincon Rain Forest, Camino Albergue Oscar, 560m, 10.87741, -85.32363.

Holotype. ♀ in CNC. Specimen labels: 1. DHJPAR0043031. 2. Voucher: D.H.Janzen & W.Hallwachs, DB: <http://janzen.sas.upenn.edu>, Area de Conservación Guanacaste, COSTA RICA, 11-SRNP-610.

Paratype. 1 ♂ (CNC). COSTA RICA, ACG database code: DHJPAR0038914.

Description. Female. Body length 3.9–4.0 mm. Fore wing length 4.5–4.6 mm. Body color: mesosoma entirely yellow-orange (with the exception of a very small black spot on axillar complex), metasoma with brown to black areas covering most of mediotergites 4–7 (and also part of mediotergites 3 and 8). Scape color: partially dark brown to black. Flagellomeres color: most flagellomeres brown to black, except for small subapical area (F14–15) which is yellow-brown (Figs 64, 67). Tegula and humeral complex color: tegula pale, humeral complex partially dark/partially pale. Mesotibia color: posterior 0.1–0.2 dark brown to black. Metatibia color: posterior 0.1–0.3



Figures 64–69. *Prasmodon scottmilleri*. **64** Habitus **65** Fore wing **66** Detail of the hind wing **67** Antenna (partially) **68** Head and mesosoma, dorsal view **69** Propodeum and metasoma, dorsal view.

dark brown to black (Fig. 64). Metatibia spurs color: yellow-orange. Metatarsus color: dark brown to black (except for anterior 0.7 or less of first metatarsomere) (Fig. 64). Fore wing color pattern: uniformly and entirely infumate (except for small hyaline area

near veins (RS+M)b and 2M). Fore wing veins color: all veins dark brown (Fig. 65). Pterostigma color: entirely dark brown. Hypostomal carina: highly raised. Scutoscutellar sulcus: with 4 impressions. Areolet height+vein r length (fore wing): $0.15 \times$ or less. Hind wing subbasal cell: mostly without setae (Figs 65, 69). Hind tarsal claws: with pectination (teeth) very irregular in spacing and length. Shape of mediotergite 1: distinctly narrowing posteriorly, width at posterior margin clearly less than width at anterior margin and median width (Fig. 69). Mediotergite 1 length+width at posterior margin $3.6\text{--}4.0 \times$. Mediotergite 2 width at posterior margin+length: $3.6\text{--}4.0 \times$. Ovipositor sheaths length: $0.6 \times$ as long as metatibia.

Male. As female but with flagellomeres fully dark brown to black.

Molecular data. Sequences in BOLD: 6, barcode compliant sequences: 5 (Fig. 105).

Biology and ecology. Hosts: Crambidae, four species of *Omiodes* and *Triuncidia eupalusalis*DHJ02.

Distribution. Costa Rica, ACG rain forest.

Etymology. This species is named in honour of Scott Miller of the National Museum of Natural History, Smithsonian Institution, Washington, D.C, in recognition of his decades of taxonomic knowledge and support contributing to understanding the species-level and higher taxonomy of the Dalceridae, Lasiocampidae, and other fat fuzzy moths of ACG, INBio and Costa Rica, as well as other parts of the world, and administrating Lepidoptera biodiversity development at the Smithsonian Institution.

***Prasmodon silvatlanticus* Fernández-Triana & Whitfield, sp. n.**

<http://zoobank.org/A9F2150A-1D0C-402E-9945-FC21A1663857>

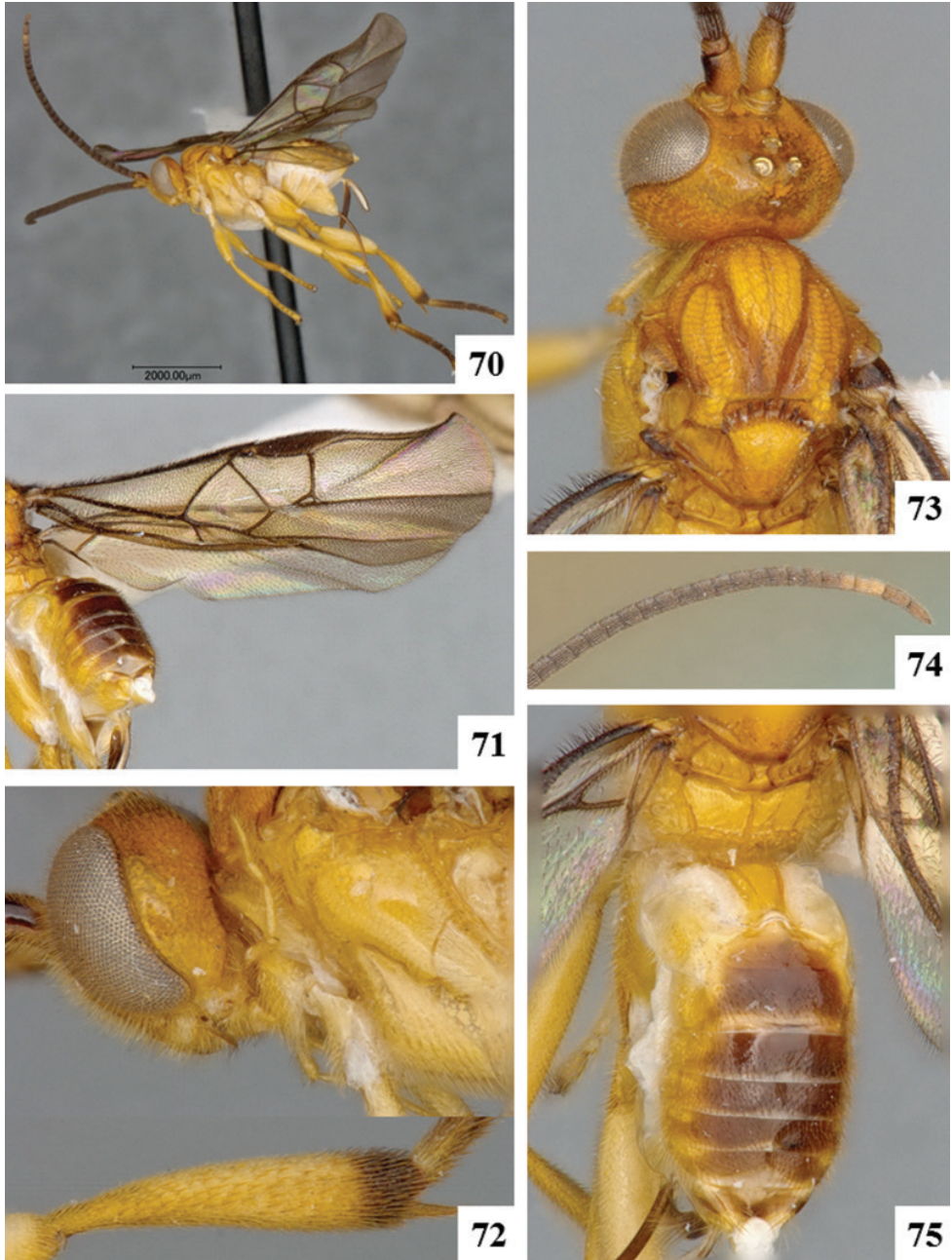
http://species-id.net/wiki/Prasmodon_silvatlanticus

Figs 70–75

Type locality. BRAZIL, Est. Rio de Janeiro, Silva Jardim.

Holotype. ♀ in CNC. Specimen labels: 1. BRAZIL, Est. Rio de Janeiro, Silva Jardim, viii.1974, F. M. Oliveira. 2. DNA Voucher CNCHYM 01960.

Description. Female. Body length 4.1–4.2 mm. Fore wing length 4.5–4.6 mm. Body color: mesosoma entirely yellow-orange (with the exception of a very small black spot on axillar complex), metasoma with brown to black areas covering most of mediotergites 4–7 (and also part of mediotergites 3 and 8). Scape color: partially dark brown to black. Flagellomeres color: most flagellomeres brown to black, except for small subapical area (F14 and apical half of F13) which is yellow-brown (Figs 70, 74). Tegula and humeral complex color: tegula pale, humeral complex dark. Mesotibia color: entirely yellow. Metatibia color: posterior 0.1–0.3 dark brown to black (Figs 70, 72). Metatibia spurs color: yellow-orange. Metatarsus color: dark brown to black (except for anterior 0.7 or less of first metatarsomere) (Fig. 70). Fore wing color pattern: hyaline. Fore wing veins color: all veins dark brown (Fig. 71). Pterostigma color: entirely dark brown. Hypostomal carina: highly raised (Fig. 72). Scutoscutellar sulcus: with 6 impressions. Areolet height+vein r length (fore wing): $0.15 \times$ or less. Hind



Figures 70–75. *Prasmodon silvatlanticus*. **70** Habitus **71** Fore wing **72** Head and mesosoma (partially), lateral view **73** Head and mesosoma, dorsal view **74** Antenna **75** Propodeum and metasoma, dorsal view.

wing subbasal cell: mostly without setae. Hind tarsal claws: with pectination uniform, teeth thick and relatively evenly spaced. Shape of mediotergite 1: distinctly narrowing posteriorly, width at posterior margin clearly less than width at anterior margin and

median width (Fig. 75). Mediotergite 1 length÷width at posterior margin 5.6–6.0 ×. Mediotergite 2 width at posterior margin÷length: 2.6–3.0 ×. Ovipositor sheaths length: 0.6 × as long as metatibia.

Male. Unknown.

Molecular data. Sequences in BOLD: 1, barcode compliant sequences: 0.

Biology and ecology. Unknown.

Distribution. Brazil, Rio de Janeiro.

Etymology. From Latin “silva”=“forest” and “atlanticus”=Atlantic, referring to the Atlantic Forest biome, where this and other species of *Prasmodon* have been found. The first part of the name also refers to the type locality (Silva Jardim).

Comments. The only known specimen was considered by Mason (1981) to be a new species, which remained undescribed until now.

***Prasmodon subfuscus* Fernández-Triana & Whitfield, sp. n.**

<http://zoobank.org/8BD6E416-FF8F-4FDC-8581-9C97B061BA2A>

http://species-id.net/wiki/Prasmodon_subfuscus

Figs 76–81

Type locality. BRAZIL, Rio de Janeiro, Silva Jardim.

Holotype. #1 in CNC. Specimen labels: 1. BRAZIL, Est. Rio de Janeiro, Silva Jardim, viii.1974, F. M. Oliveira. 2. DNA Voucher CNCHYM 01961.

Description. Male. Body length 4.5–4.6 mm. Fore wing length 5.1–5.2 mm. Body color: meso- and metasoma with brown to black areas, metasoma with most of tergites 2–8 dark brown (Figs 77, 80, 81). Scape color: partially dark brown to black (Fig. 79). Flagellomeres color: all flagellomeres brown to black (Fig. 76). Tegula and humeral complex color: tegula pale, humeral complex dark. Metatibia color: posterior 0.1–0.3 dark brown to black (Fig. 78). Metatibia spurs color: yellow-orange (Fig. 78). Fore wing color pattern: uniformly and entirely infumate (except for small hyaline area near veins (RS+M)_b and 2M). Fore wing veins color: all veins dark brown (Fig. 77). Pterostigma color: entirely dark brown. Hypostomal carina: highly raised (Fig. 79). Scutoscutellar sulcus: with 5 impressions. Hind wing subbasal cell: mostly without setae. Hind tarsal claws: with pectination (teeth) very irregular in spacing and length. Shape of mediotergite 1: distinctly narrowing posteriorly, width at posterior margin clearly less than width at anterior margin and median width (Fig. 81).

Female. Unknown.

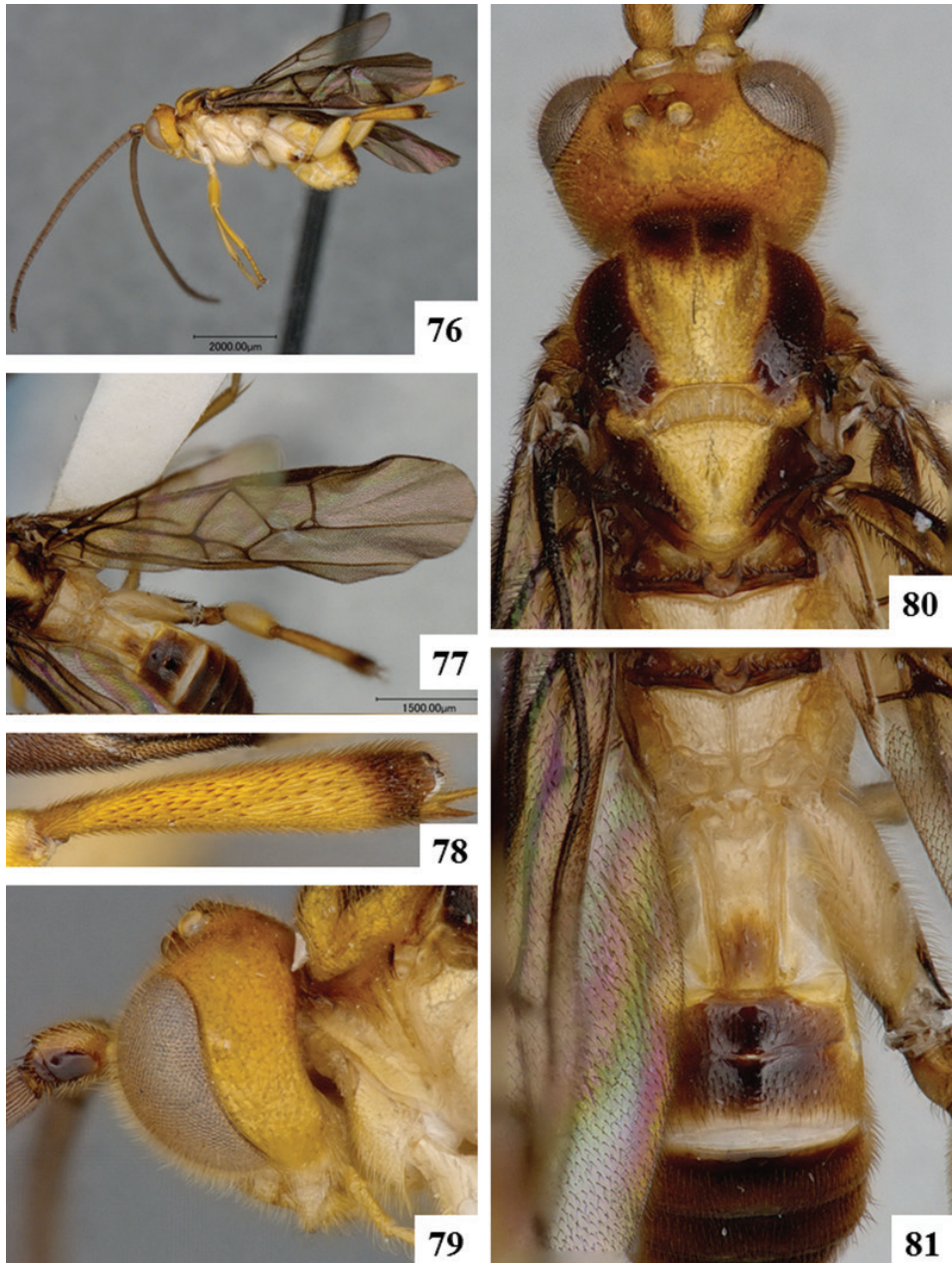
Molecular data. Sequences in BOLD: 1, barcode compliant sequences: 0.

Biology and ecology. Unknown.

Distribution. Brazil, Rio de Janeiro.

Etymology. From Latin “subfuscus”=brownish, referring to the extensive brown coloration of the species, by far the least yellow of all known species of *Prasmodon*.

Comments. This species, only known from a single male, was collected in the same locality and on the same date as *Prasmodon silvatlanticus*, which is known only



Figures 76–81. *Prasmodon subfuscus*. **76** Habitus **77** Fore wing **78** Metatibia **79** Head and mesosoma (partially), lateral view **80** Head and mesosoma, dorsal view **81** Propodeum and metasoma, dorsal view.

from a single female. Both specimens are morphologically distinct, with different coloration of mesosoma, mediotergite 1, metacoxa, and trochanter (Figs 70, 73, 75 vs Figs 76, 80, 81), as well as shape of mediotergite 2. We have not found sexual di-

morphism among any of the known species of *Prasmodon* (other than slight variations in the color of apical flagellomeres), and thus we do not think that the differences observed represent sexual dimorphism within a single species. Further evidence to consider those two specimens as separate species is provided by DNA barcoding; even though only short sequences (164 bp) could be recovered from both of them, they differed by 15 bp (9.5%).

The exact collection locality of *Prasmodon subfuscus* is not clear from the original labels. “Silva Jardim” is a municipality of 938 km² in the Brazilian state of Rio de Janeiro. Within the municipality is located the “Reserva Biologica de Poço das Antas”, the largest lowland Atlantic Forest reserve in the state of Rio de Janeiro, containing 50 km² of mostly secondary, evergreen forest. The area is very diverse (e.g., it contains at least 365 plant and 77 mammal species, Brito et al. 2004). This Atlantic Forest is one of the planet’s biodiversity hotspots, with an extremely diverse and unique mix of forest types (http://www.conservation.org/where/priority_areas/hotspots/Pages/hotspots_main.aspx). Thus, it is no surprise that two species of *Prasmodon* species occur in that region, just as multiple species do in the ACG rain forest in Costa Rica.

***Prasmodon tijucaensis* Fernández-Triana & Whitfield, sp. n.**

<http://zoobank.org/0E2B527E-FEDB-478C-B739-08AE323E559D>

http://species-id.net/wiki/Prasmodon_tijucaensis

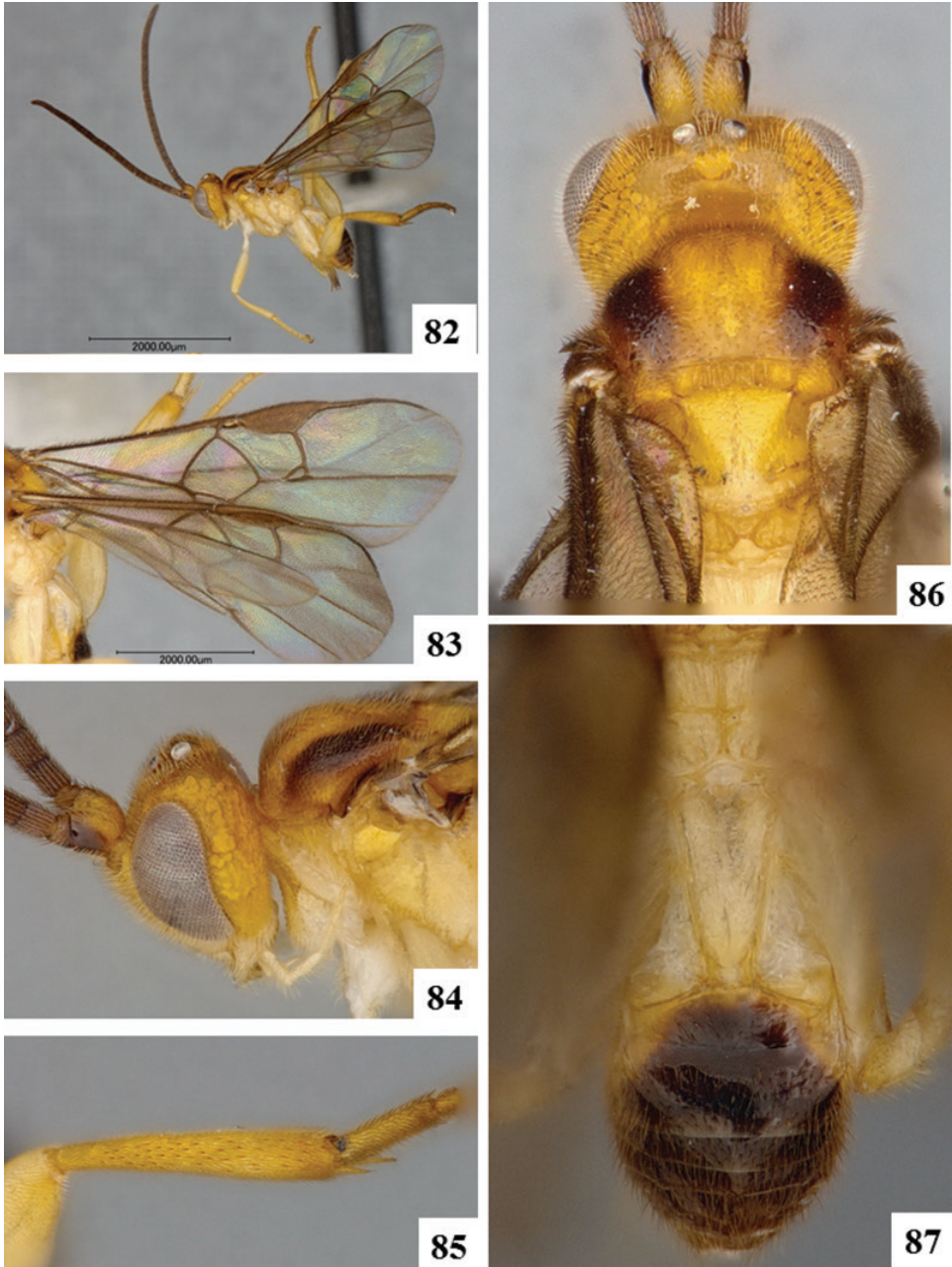
Figs 82–87

Type locality. BRAZIL, Rio de Janeiro, Guanabara, Floresta da Tijuca (Tijuca Forest).

Holotype. ♀ in CNC. Specimen labels: 1. BRAZIL, Guanabara, Floresta da Tijuca, ii.1974, M. Alvarenga. 2. DNA Voucher CNCHYM 01959.

Description. Female. Body length 3.3–3.4 mm. Fore wing length 3.7–3.8 mm. Body color: meso- and metasoma with brown to black areas, metasoma with most of tergites 2–8 dark brown (Fig 86, 87). Scape color: partially dark brown to black (Fig. 86). Flagellomeres color: all flagellomeres brown to black (Fig. 82). Tegula and humeral complex color: both dark. Mesotibia color: entirely yellow. Metatibia color: entirely yellow (Fig. 85). Metatibia spurs color: yellow-orange. Metatarsus color: entirely yellow-white. Fore wing color pattern: hyaline (Fig. 83). Fore wing veins color: all veins dark brown (Fig. 83). Pterostigma color: entirely dark brown. Hypostomal carina: not raised (Fig. 84). Scutoscutellar sulcus: with 7 impressions (Fig. 86). Areolet height+vein r length (fore wing): 0.3 ×. Hind wing subbasal cell: mostly with setae. Hind tarsal claws: with 1 or 2 teeth on anterior 0.3 of claw. Shape of mediotergite 1: distinctly narrowing posteriorly, width at posterior margin clearly less than width at anterior margin and median width (Fig. 87). Mediotergite 1 length+width at posterior margin 6.1–6.5 ×. Mediotergite 2 width at posterior margin+length: 2.1–2.5 ×. Ovipositor sheaths length: 0.4 × as long as metatibia.

Male. Unknown.



Figures 82–87. *Prasmodon tijucaensis*. **82** Habitus **83** Fore wing **84** Head and mesosoma (partially), lateral view **85** Metatibia **86** Head and mesosoma, dorsal view **87** Propodeum and metasoma, dorsal view.

Molecular data. Sequences in BOLD: 1, barcode compliant sequences: 0.

Biology and ecology. Unknown.

Distribution. Brazil, Rio de Janeiro.

Etymology. The name honours the type locality, Floresta da Tijuca, which is among the world's largest urban forests.

Comments. The only known specimen was considered by Mason (1981) to be a new species, which remained undescribed until now.

***Prasmodon verhoogdenokus* Braet & Fernández-Triana, sp. n.**

<http://zoobank.org/7456681F-AAEC-4B62-ABC3-B1C9EB3387F2>

http://species-id.net/wiki/Prasmodon_verhoogdenokus

Figs 88–93

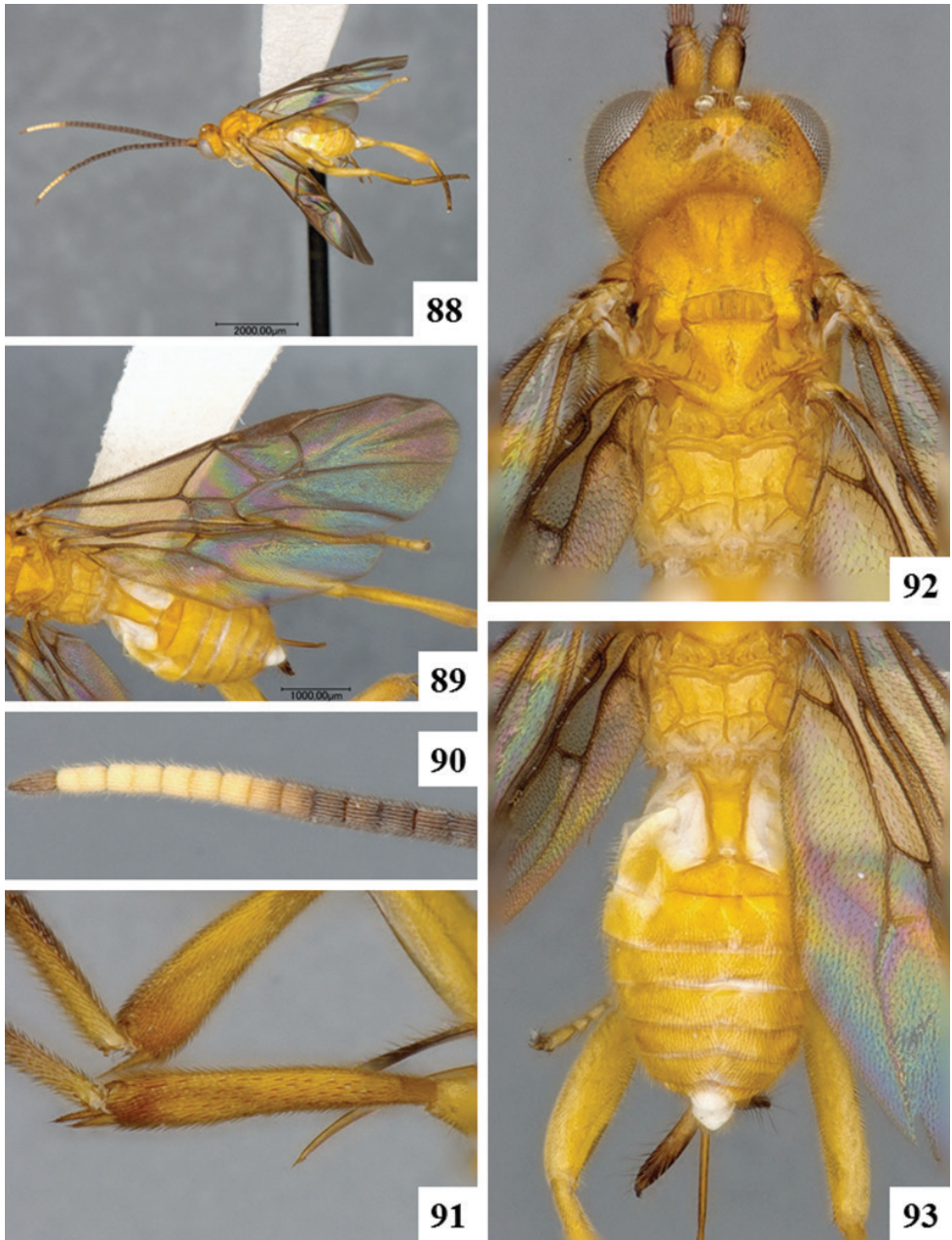
Type locality. BRAZIL, Mato Grosso, Vila Vera, 500m, -12.7667, -55.5.

Holotype. ♀ in CNC. Specimen labels: 1. BRAZIL, Vila Vera, M. Grosso, 500m, 12°46'S, 55°30'W, X.1973, M. Alvarenga. 2. DNA Voucher, CNCHYM 01971.

Paratype. 6 ♀ (CNC, RMNH, IRSNB, MNHN). Ecuador, Napo, Tena, 400m, 16–17.ii.1987 (1 ♀); French Guiana, Saul, collecting dates: 2.ix.2010, 17.ix.2010, 26.x.2010 (3 ♀), Saul, Crique popote, Mont Belvédère, xii.2000 (1 ♀), Kourou, Piste Soumourou, 13.vi–20.vii.2002 (1 ♀).

Other material examined. 3 ♂ from Colombia, Amazonas, PNN Amacayacu, San Martin, 150m (INHS); 2 ♂ from Ecuador, Napo, P. Misahualli, 350m (CNC); 98 ♂ from French Guiana, Sinamary, Barrage de Petit-Saut; Inselberg Itoupé; RNR Trinité, Zone Aya; Nourages Reserve; Montagne de Kaw, Relais Patawa; and Saul (CNC and IRSNB); 2 ♂ from Peru, Madre de Dios, Rio Tampobata, Sachavacayoc center; and Loreto, Matse's Reserved Zone, site Jenaro Herrera, Rio Ucayali (CNC); 1 ♂ from Suriname, Paramaribo Zoo (RMNH).

Description. Female. Body length 4.1–4.2 mm, 4.3–4.4 mm, 4.5–4.6 mm, rarely 3.9–4.0 mm or 4.7–4.8 mm. Fore wing length 4.3–4.4 mm, 4.5–4.6 mm, rarely 4.9–5.0 mm. Body color: meso- and metasoma entirely yellow-orange (with the exception of a very small black spot on axillar complex) (Figs 92, 93). Scape color: partially dark brown to black (Fig. 92). Flagellomeres color: with relatively extense yellow area (at least including F13–15, and usually apical half of F11 and basal half of F16) (Fig. 88, 91). Tegula and humeral complex color: tegula pale, humeral complex partially dark/partially pale. Mesotibia color: entirely yellow. Metatibia color: posterior 0.1–0.3 dark brown to black. Metatibia spurs color: yellow-orange. Metatarsus color: dark brown to black (except for anterior 0.7 or less of first metatarsomere). Fore wing color pattern: mostly infumate, but with pale area centrally which gives the wing a banded appearance. Fore wing veins color: all veins dark brown (Fig. 89). Pterostigma color: entirely dark brown. Hypostomal carina: highly raised. Scutoscutellar sulcus: with 6 impressions, rarely with 5 impressions. Areolet height÷vein r length (fore wing): 0.15 × or less. Hind wing subbasal cell: mostly without setae. Hind tarsal claws: with pectination (teeth) very irregular in spacing and length. Shape of mediotergite 1: distinctly narrowing posteriorly, width at posterior margin clearly less than width at anterior margin and median width (Fig. 93). Mediotergite 1 length÷width at posterior margin



Figures 88–93. *Prasmodon verhoogdenokus*. **88** Habitus **89** Fore wing **90** Antenna (partially) **91** Metatibia **92** Head and mesosoma, dorsal view **93** Propodeum and metasoma, dorsal view.

5.6–6.0 ×. Mediotergite 2 width at posterior margin+length: 2.6–3.0 ×. Ovipositor sheaths length: 0.6 × as long as metatibia, rarely 0.5 × as long as metatibia.

Male. Morphologically similar to females, except for antenna.

Molecular data. Sequences in BOLD: 1, barcode compliant sequences: 0. Two additional short sequences are available from two male specimens, but they were not included in the paratype series (see Comments below).

Biology and ecology. Light trapped and Malaise trapped.

Distribution. Brazil, Colombia, Ecuador, French Guiana, Peru, Suriname.

Etymology. From Dutch “verhoogde nok”= raised ridge, referring to the raised hypostomal carina.

Comments. The wide distribution of *Prasmodon verhoogdenokus* throughout South America, suggests it may represent a complex of morphologically cryptic species. At present there is no host known for the species, and the molecular data are meagre. Two male specimens from Ecuador that appear to be of this species rendered partial DNA sequences that differed by approximately 5% bp from the partial barcode of the female holotype (but the COI sequences for those three specimens only overlap for 240 bp). Although males included under this species look morphologically similar to the female holotype and the paratypes, they have been left out of the paratype series.

***Prasmodon zlotnicki* Valerio & Rodriguez, 2005**

http://species-id.net/wiki/Prasmodon_zlotnicki

Fig. 94, 102

Prasmodon zlotnicki Valerio & Rodriguez, 2005: 31.

Type locality. COSTA RICA: ACG, Alajuela Province, Sector San Cristobal, Sendero Corredor, 620 m, 10.87868, -85.38963. In the holotype description, the province was erroneously given as Guanacaste Province.

Holotype. ♀, INBio (examined).

Material examined. 8 ♀, 1 ♂ (CNC, INBio, NMNH).

Description. Female. Body length 4.5–4.6 mm. Fore wing length 5.1–5.2 mm or 5.3–5.4 mm. Body color: meso- and metasoma with brown to black areas, those on metasoma only thin brown areas centrally on tergites 4–8 (Fig. 94). Scape color: partially dark brown to black. Flagellomeres color: most flagellomeres brown to black, except for small apical area (F15–16, and occasionally apical half of F14) which is yellow-brown (Fig. 94). Tegula and humeral complex color: tegula pale, humeral complex partially dark/partially pale. Mesotibia color: posterior 0.1–0.2 dark brown to black. Metatibia color: posterior 0.1–0.3 dark brown to black (Fig. 94). Metatibia spurs color: dark brown to black (Fig. 94). Metatarsus color: dark brown to black (except for anterior 0.7 or less of first metatarsomere). Fore wing color pattern: uniformly and entirely infumate (except for small hyaline area near veins (RS+M)b and 2M). Fore wing veins color: all veins dark brown. Pterostigma color: entirely dark brown. Hypostomal carina: highly raised. Scutoscuteellar sulcus: with 6 impressions. Areolet height+vein r length (fore wing): 0.2 ×. Hind wing subbasal cell: mostly without setae. Hind tarsal claws: with pectination (teeth) very irregular in spacing and length. Shape of mediotergite 1: distinctly narrow-

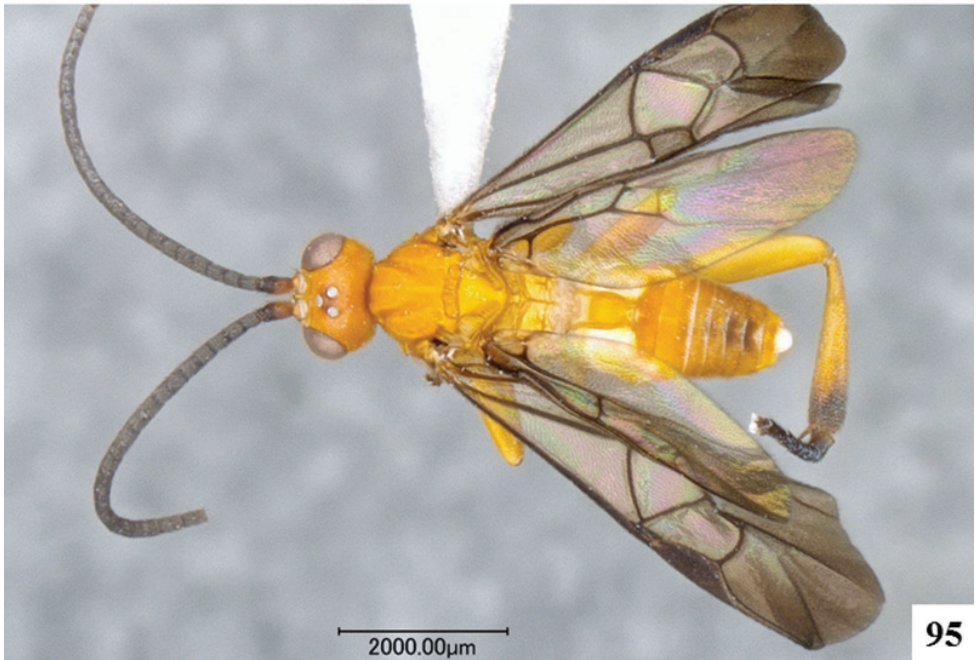


Figure 94–95. **94** *Prasmodon zlotnicki*. Body, dorsal view **95** *Prasmodon eminens*. Body, dorsal view.



Figure 96–97. 96 Cocoon of *Prasmodon mikepoguei* 97 Cocoon of *Prasmodon eminens*.



Figure 98–99. 98 Cocoon of *Prasmodon scottmilleri* 99 Cocoon of *Prasmodon bobpoolei*.



Figure 100–101. 100 Cocoon of *Prasmodon bobrobbinsi* 101 Cocoon of *Prasmodon almasolisae*.



102



103

Figure 102–103. 102 Cocoon of *Prasmodon zlotnicki* 103 Cocoon of *Prasmodon johnbrowni*.

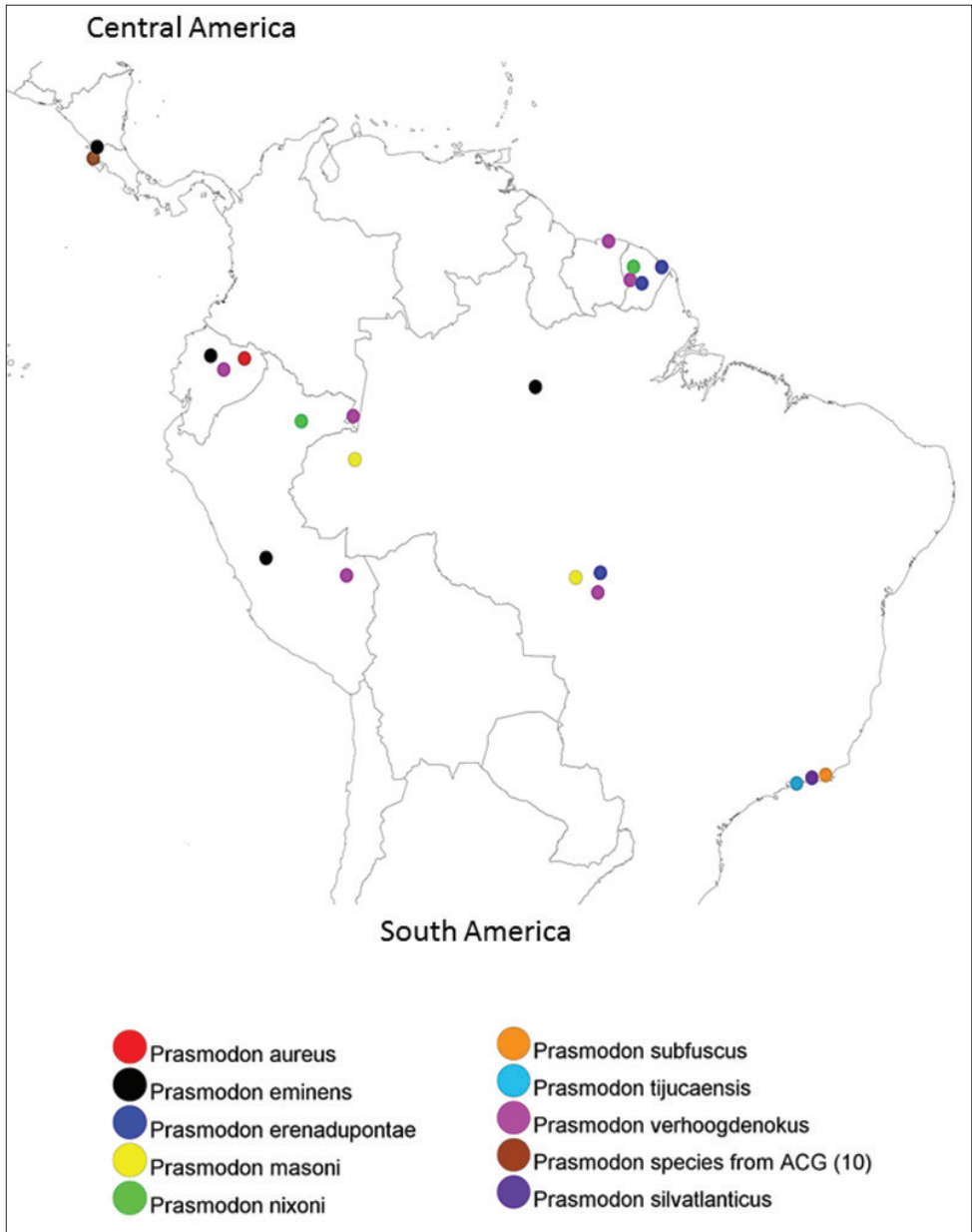


Figure 104. Distribution map of *Prasmodon* species in Central and South America.

ing posteriorly, width at posterior margin clearly less than width at anterior margin and median width (Fig. 94). Mediotergite 1 length÷width at posterior margin 4.6–5.0 x, 5.1–5.5 x, rarely 3.6–4.0 x. Mediotergite 2 width at posterior margin÷length: 3.1–3.5 x or 3.6–4.0 x. Ovipositor sheaths length: 0.5 x as long as metatibia.

Male. One male, the first found for the species. It is morphologically similar to females.

Molecular data. Sequences in BOLD: 11, barcode compliant sequences: 11 (Fig. 105).

Biology and ecology. Hosts: Crambidae, *Ategumia lotanalis*DHJ07, *Desmia ploralis*DHJ01, *Desmia* Janzen07, *Desmia* Solis19 *Diacme* biolep02, *Herpetogramma* Solis10, *Herpetogramma* Solis11, *Phostria* Janzen05.

Distribution. Costa Rica, ACG rain forest (Valerio et al. 2005).

Acknowledgements

JFT is greatly indebted to John Huber and Caroline Boudreault (CNC) for helping with the preparation of many specimens used in this study. Thanks also go to Odette Morvan and Jean Cerda for their help for their long term collections in the “Montagne de Kaw”, the members of the “Société Entomologique Antilles Guyane” for their support in logistic and their collecting in several stations in French Guiana, and all other people who have kindly housed or supported the work of YB. The study has been supported by U.S. National Science Foundation grants BSR 9024770 and DEB 9306296, 9400829, 9705072, 0072730, 0515699 to DHJ, and grants from the Wege Foundation, International Conservation Fund of Canada, Jessie B. Cox Charitable Trust, Blue Moon Fund, Guanacaste Dry Forest Conservation Fund (GDFCF), Area de Conservación Guanacaste, Permian Global, and University of Pennsylvania (DHJ), and by the intense efforts of the ACG/GDFCF parataxonomist team that found and reared the parasitoids described here, to say nothing of the international taxasphere that labors to obtain and develop the caterpillar and parasitoid taxonomy essential to this effort in science and conservation. The reviews of Gavin Broad and two anonymous reviewers greatly improved the manuscript.

References

- Austin AD (1990) Revision of the enigmatic Australasian genus *Miropotes* Nixon (Hymenoptera: Braconidae: Microgastrinae), with comments on the phylogenetic importance of the female ovipositor system. *Systematic Entomology* 15: 43–68. doi: 10.1111/j.1365-3113.1990.tb00302.x
- Banks JC, Whitfield JB (2006) Dissecting the ancient rapid radiation of microgastrine wasp genera using additional nuclear genes. *Molecular Phylogenetics and Evolution* 41: 690–703. doi: 10.1016/j.ympev.2006.06.001
- Brito D, Oliveira LC, Mello MAR (2004) An overview of mammalian conservation at Poço das Antas Biological Reserve, southeastern Brazil. *Journal for Nature Conservation* 12(4): 219–228. doi: 10.1016/j.jnc.2004.09.001

- Deans AR, Whitfield JB, Janzen DH (2003) Taxonomy and natural history of the Microgastrinae genus *Alphomelon* Mason (Hymenoptera: Braconidae). *Journal of Hymenoptera Research* 12(1): 1–41.
- Fernández-Triana J, Cardinal S, Whitfield JB, Hallwachs W, Smith MA, Janzen DH (2013) A review of the New World species of the parasitoid wasp *Iconella* (Hymenoptera: Braconidae, Microgastrinae). *ZooKeys* 321: 65–87. doi: 10.3897/zookeys.321.5160
- Fernández-Triana J, Whitfield JB, Rodriguez JJ, Smith MA, Janzen DH, Hallwachs W, Hajibabaei M, Burns JM, Solis MA, Brown J, Cardinal S, Goulet H, Hebert PDN (2014) Review of *Apanteles* (Hymenoptera: Braconidae, Microgastrinae) from Area de Conservación Guanacaste, northwestern Costa Rica, with keys to all described species from Mesoamerica. *ZooKeys* 383: 1–565. doi: 10.3897/zookeys.383.6418
- Grinter CC, Whitfield JB, Connahs H, Dyer LA, Hallwachs W, Janzen DH (2009) A key to New World *Distatrix* Mason (Hymenoptera: Braconidae), with descriptions of six new reared Neotropical species. *Journal of Insect Science (Tucson)* 9(29): 1–17. doi: 10.1673/031.009.2901
- Huber JT, Sharkey MJ (1993) Structure. In: Goulet H, Huber JT (Eds) *Hymenoptera of the world: an identification guide to families*. Agriculture Canada Research Branch, Monograph No. 1894E, Ottawa, Canada, 13–59.
- Ivanova NV, deWaard JR, Hebert PDN (2006) An inexpensive, automation-friendly protocol for recovering high-quality DNA. *Molecular Ecology Notes* 6: 998–1002. doi: 10.1111/j.1471-8286.2006.01428.x
- Janzen DH, Walker AK, Whitfield JB, Delvare G, Gauld ID (2003) Host specificity and hyperparasitoids of three new Costa Rican species of *Microplitis* Foerster (Hymenoptera: Braconidae: Microgastrinae), parasitoids of sphingid caterpillars. *Journal of Hymenoptera Research* 12(1): 42–76.
- Janzen DH, Hallwachs W, Blandin P, Burns JM, Cadiou J, Chacon I, Dapkey T, Deans AR, Epstein ME, Espinoza B, Franclemont JG, Haber WA, Hajibabaei M, Hall JPW, Hebert PDN, Gauld ID, Harvey DJ, Hausmann A, Kitching I, Lafontaine D, Landry J, Lemaire C, Miller JY, Miller JS, Miller L, Miller SE, Montero J, Munroe E, Rab Green S, Ratnasingham S, Rawlins JE, Robbins RK, Rodriguez JJ, Rougerie R, Sharkey MJ, Smith MA, Solis MA, Sullivan JB, Thiaucourt P, Wahl DB, Weller SJ, Whitfield JB, Willmott KR, Wood DM, Woodley NE, Wilson JJ (2009) Integration of DNA barcoding into an ongoing inventory of complex tropical biodiversity. *Molecular Ecology Resources* 9 (Supplement 1): 1–26. doi: 10.1111/j.1755-0998.2009.02628.x
- Janzen DH, Hallwachs W (2011) Joining inventory by parataxonomists with DNA barcoding of a large complex tropical conserved wildland in northwestern Costa Rica. *PLoS ONE* 6(8): e18123. doi: 10.1371/journal.pone.0018123
- Karlsson D, Ronquist F (2012) Skeletal morphology of *Opius dissitus* and *Biosteres carbonarius* (Hymenoptera: Braconidae), with a discussion of terminology. *PLoS ONE* 7(4): e32573. doi: 10.1371/journal.pone.0032573
- Kimura M (1980). A simple method for estimating evolutionary rate of base substitutions through comparative studies of nucleotide sequences. *Journal of Molecular Evolution* 16: 111–120. doi: 10.1007/BF01731581

- Mardulyn P, Whitfield JB (1999) Phylogenetic signal in the COI, 16S and 28S genes for inferring relationships among genera of Microgastrinae (Hymenoptera: Braconidae); evidence of a high diversification rate in this group of parasitoids. *Molecular Phylogenetics and Evolution* 12: 282–294. doi: 10.1006/mpev.1999.0618
- Mason WRM (1981) The polyphyletic nature of *Apanteles* Foerster (Hymenoptera: Braconidae): A phylogeny and reclassification of Microgastrinae. *Memoirs of the Entomological Society of Canada*, Ottawa, Canada, 147 pp.
- Nixon G (1965) A reclassification of the tribe Microgasterini (Hymenoptera: Braconidae). *Bulletin of the British Museum (Natural History), Entomology series, Supplement 2*: 1–284.
- Ratnasingham S, Hebert PDN (2007) BOLD: The Barcode of Life Data System (www.barcodinglife.org). *Molecular Ecology Notes* 7: 355–364. doi: 10.1111/j.1471-8286.2007.01678.x
- Rodriguez JJ, Fernández-Triana J, Smith MA, Janzen DH, Hallwachs W, Erwin TL, Whitfield JB (2013) Extrapolations from field studies and known faunas converge on dramatically increased estimates of global microgastrine parasitoid wasp species richness (Hymenoptera: Braconidae). *Insect Conservation and Diversity* 6: 530–536. doi: 10.1111/icad.12003
- Shorthouse DP (2010) SimpleMapp, an online tool to produce publication-quality point maps. <http://www.simplemapp.net> [accessed 3 December, 2013]
- Saitou N, Nei M (1987). The neighbor-joining method: A new method for reconstructing phylogenetic trees. *Molecular Biology and Evolution* 4: 406–425.
- Smith MA, Woodley NE, Janzen DH, Hallwachs W, Hebert PDN (2006) DNA barcodes reveal cryptic host-specificity within the presumed polyphagous members of a genus of parasitoid flies (Diptera: Tachinidae). *Proceedings of the National Academy of Sciences* 103: 3657–3662. doi: 10.1073/pnas.0511318103
- Smith MA, Wood DM, Janzen DH, Hallwachs W, Hebert PDN (2007) DNA barcodes affirm that 16 species of apparently generalist tropical parasitoid flies (Diptera, Tachinidae) are not all generalists. *Proceedings of the National Academy of Sciences* 104: 4967–4972. doi: 10.1073/pnas.0700050104
- Smith MA, Rodriguez JJ, Whitfield JB, Deans AR, Janzen DH, Hallwachs W, Hebert PDN (2008) Extreme diversity of tropical parasitoid wasps exposed by iterative integration of natural history, DNA barcoding, morphology, and collections. *Proceedings of the National Academy of Sciences* 105: 12359–12364. doi: 10.1073/pnas.0805319105
- Smith MA, Fernández-Triana JL, Eveleigh E, Gómez J, Guclu C, Hallwachs W, Hebert PDN, Hrcek J, Huber JT, Janzen DH, Mason PG, Miller SE, Quicke DLJ, Rodriguez JJ, Rougerie R, Shaw MR, Varkonyi G, Ward D, Whitfield JB, Zaldívar-Riverón A (2013) DNA barcoding and the taxonomy of Microgastrinae wasps (Hymenoptera, Braconidae): impacts after 8 years and nearly 20 000 sequences. *Molecular Ecology Resources* 13: 168–176. doi: 10.1111/1755-0998.12038
- Valerio AA, Rodriguez JJ, Whitfield JB, Janzen DH (2005) *Prasmodon zlotnicki*, a new Neotropical species of the genus *Prasmodon* Nixon (Braconidae: Microgastrinae) from Costa Rica, with the first host records for the genus. *Zootaxa* 1016: 29–38.
- Valerio AA, Whitfield JB, Janzen DH (2009) Review of world *Parapanteles* Ashmead (Hymenoptera: Braconidae: Microgastrinae), with description of fourteen new Neotropical species and the first description of the final instar larvae. *Zootaxa* 2084: 1–49.

- Whitfield JB (1995) Checklist of the Microgastrinae (Hymenoptera: Braconidae) in America north of Mexico. *Journal of the Kansas Entomological Society* 68: 245–262.
- Whitfield JB (1997) Subfamily Microgastrinae. In: Wharton RA, Marsh PM, Sharkey MJ (Eds) *Manual of the New World genera of the family Braconidae (Hymenoptera)*. Special Publication No. 1, International Society of Hymenopterists, Washington, D.C., 333–364.
- Whitfield JB, Mardulyn P, Austin AD, Downton M (2002) Phylogenetic relationships among microgastrine braconid wasp genera based on data from the 16S, COI and 28S genes and morphology. *Systematic Entomology* 27: 337–359. doi: 10.1046/j.1365-3113.2002.00183.x
- Whitfield JB, Fernández-Triana J, Janzen DH, Hallwachs W, Smith A, Cardinal S (2012) *Mariapanteles* (Hymenoptera, Braconidae), a new genus of Neotropical microgastrine parasitoid wasp discovered through biodiversity inventory. *ZooKeys* 208: 61–80. doi: 10.3897/zookeys.208.3326

Supplementary material I

Supplementary information for studied specimens of *Prasmodon* (Hymenoptera: Braconidae, Microgastrinae) from ACG, Costa Rica

Authors: Jose L. Fernandez-Triana, James B. Whitfield, Alex M. Smith, Winnie Hallwachs, Daniel H. Janzen

Data type: Collection details, taxonomic information, DNA sequence, accession numbers

Copyright notice: This dataset is made available under the Open Database License (<http://opendatacommons.org/licenses/odbl/1.0/>). The Open Database License (ODbL) is a license agreement intended to allow users to freely share, modify, and use this Dataset while maintaining this same freedom for others, provided that the original source and author(s) are credited.

Link: doi: 10.3897/JHR.37.6784.app1

A new species of *Horismenus* Walker (Hymenoptera, Eulophidae) from ootheca of *Liturgusa* Saussure (Mantodea, Liturgusidae) from Central Amazonas, Brazil

Christer Hansson^{1†}, Diego G. Pádua^{2‡}, Karine Schoeninger^{2§},
Antonio A. Agudelo^{2,¶}, Márcio L. Oliveira^{2,¶¶}

1 *Scientific Associate of the Natural History Museum, Cromwell Road, London SW7 5BD, United Kingdom*

2 *Programa de Pós-Graduação em Entomologia, Instituto Nacional de Pesquisas da Amazônia, André Araújo, 2936, CEP 96060, Manaus, Amazonas, Brasil*

† <http://zoobank.org/EC91EABD-7115-4B05-BC80-9195C86FA55D>

‡ <http://zoobank.org/62984359-999A-41DB-AF0E-6722EAD52DB9>

§ <http://zoobank.org/3B37E557-99CD-49BC-944F-8032B655216F>

¶ <http://zoobank.org/F7A9367B-9FE5-4198-8726-B067999B551A>

¶¶ <http://zoobank.org/32031B61-1FD0-416F-9AC1-8F7E5BC49072>

Corresponding author: *Christer Hansson* (christerdennis@gmail.com)

Academic editor: *S. Schmidt* | Received 30 November 2013 | Accepted 2 February 2014 | Published 28 March 2014

<http://zoobank.org/DACB1E82-CCBB-4839-B261-66B3EED290EF>

Citation: Hansson C, Pádua DG, Schoeninger K, Agudelo AA, Oliveira ML (2014) A new species of *Horismenus* Walker (Hymenoptera, Eulophidae) from ootheca of *Liturgusa* Saussure (Mantodea, Liturgusidae) from Central Amazonas, Brazil. *Journal of Hymenoptera Research* 37: 53–60. doi: 10.3897/JHR.37.6729

Abstract

A new species of *Horismenus* Walker, *H. liturgusae* Hansson & Schoeninger (Hymenoptera: Eulophidae), is described from material reared from an ootheca of an unidentified mantid species of genus *Liturgusa* Saussure (Mantodea: Liturgusidae). The new species is compared to *H. argus* Hansson, a species it is very similar to. *Horismenus liturgusae* **sp. n.** is gregarious and 49 adult specimens developed in the ootheca. This is the first record of a *Horismenus* species parasitizing mantids, and the first record of a *Horismenus* species from an ootheca.

Keywords

Chalcidoidea, Entedoninae, parasitic wasp, gregarious parasitoid

Introduction

Genus *Horismenus* Walker is one of the largest genera of the Eulophidae, Hansson (2009) included 400 species, which included all species known at that time. The genus has its main distribution in tropical America, but several species are also known from temperate North America. In addition two species have been recorded outside of the Americas, one from Europe (Bouček 1965) and one from India (Narendran et al. 2011). The species are parasitoids, developing either as primary or secondary parasitoids on a wide range of hosts. Hosts are known for 25% of the species and include immature insects from seven insect orders and several families, but also eggs (egg sacks) of four different families of spiders (Hansson 2009).

In Brazil species of *Horismenus* have been observed emerging from leafminer larvae (*Phyllocnistis citrella* Stainton) in citrus culture in the state of Acre (Thomazini and Albuquerque 2005), and as secondary parasitoids of the braconid *Cotesia alius* (Muesebeck) (Neto and Di Mare 2010). The record reported here, from ootheca of an unidentified species of *Liturgusa* Saussure, is the first record from the order Mantodea and also the first record from an ootheca.

The mantid genus *Liturgusa* (Fig. 13) is represented by 13 species in the Neotropics, of which eight are known from Brazil (Agudelo et al. 2007). It is the most common and widely distributed genus of the Liturgusidae. The species of this genus possess great agility and dexterity when moving, and also have an excellent camouflage, similar to lichens growing on tree trunks. Previously an unidentified Hymenoptera has been reared from oothecae of *Liturgusa maya* (Saussure & Zehntner) (Ehrmann 2002).

Material and methods

Photos

The colour photos were made with Nikon SMZ1500 and Leica M165C stereomicroscopes and 5MP Nikon DS-L1 and DFC420 cameras respectively. Photos were taken at different focus levels, and Helicon Focus Pro version 4.75 and Leica Application Suite v3.4.1 (2009 version) were used to merge them into a single image. The SEM photos were made from uncoated specimens on their original cardboard mounting. These photos were taken in low vacuum mode on a Hitachi SU3500 scanning electron microscope.

Abbreviations of morphological terms

DE, distance between eyes, measured across the narrowest part on frons/vertex; **DO**, diameter of anterior ocellus; **HE**, height of eye in frontal view; **HW**, height of the forewing, measured across the widest part of the wing; **LC**, length of median carina on propodeum, measured from anterior margin of carina to posterior margin of propodeum; **LG**, length of the gaster; **LM**, length of the marginal vein; **LP**, length of the petiole; **LS**, length of

hind tibial spur; **LT**, length of hind tarsus; **LW**, length of the forewing, measured from the base of the marginal vein to the apical margin of the wing; **MM**, length of the mesosoma, measured along the median mesosoma, from the pronotal collar carina to posterior margin of the propodeum; **MS**, malar space; **OOL**, the distance between eye and posterior ocellus; **PM**, length of the postmarginal vein; **POL**, the distance between posterior ocelli; **POO**, the distance between posterior ocelli and occipital margin; **ST**, length of the stigmal vein; **WC**, width of the median carina on the propodeum, measured at equal distance from the anterior and posterior margins of the carina; **WG**, width of the submedian groove, measured at equal distance from the anterior and posterior margins of median propodeum; **WH**, width of the head, measured at widest part; **WM**, width of mouth opening; **WP**, width of the petiole, measured at the attachment point of the gaster; **WT**, width of the thorax, measured across the widest part which is usually just in front of the attachment point of the forewing, the “shoulders”. For illustrations of the terms see Hansson (2009). Ratios given in the description are from female holotype and one male paratype.

Acronyms

BMNH the Natural History Museum, London, United Kingdom.

INPA Instituto Nacional de Pesquisas da Amazônia, Amazonas, Brazil.

Rearing

The conical-shaped ootheca (Fig. 14) was collected from a trunk of a *Lecythis prance* S.A. Mori (Lecythidaceae) at mid level, located in the grove Campus I of the Instituto Nacional de Pesquisas da Amazônia (INPA) and brought to the Laboratory of Hymenoptera, where the ootheca was stored in a glass container capped with fabric. After approximately three weeks 27 nymphs of *Liturgusa* emerged from the ootheca, and after one additional week 49 specimens of *Horismenus liturgusae* sp. n. emerged from the same ootheca. Furthermore, we found seven unhatched pupae of *H. liturgusae* within the ootheca. The mantid nymphs and the wasps emerged through the same single opening at the apex of the ootheca.

Species description

***Horismenus liturgusae* Hansson & Schoeninger, sp. n.**

<http://zoobank.org/73E0A73A-AADD-4660-B70C-1EAFB61FF4DA>

http://species-id.net/wiki/Horismenus_liturgusae

Figures 1–12

Diagnosis. Antennal scrobes joining below frontal suture (Figs 2, 3); mesoscutum with engraved reticulation (Fig. 5); scutellum smooth and shiny (Fig. 5); mesoscutum and scutellum metallic dark purple (Fig. 9); propodeal callus with three setae (Fig. 5);



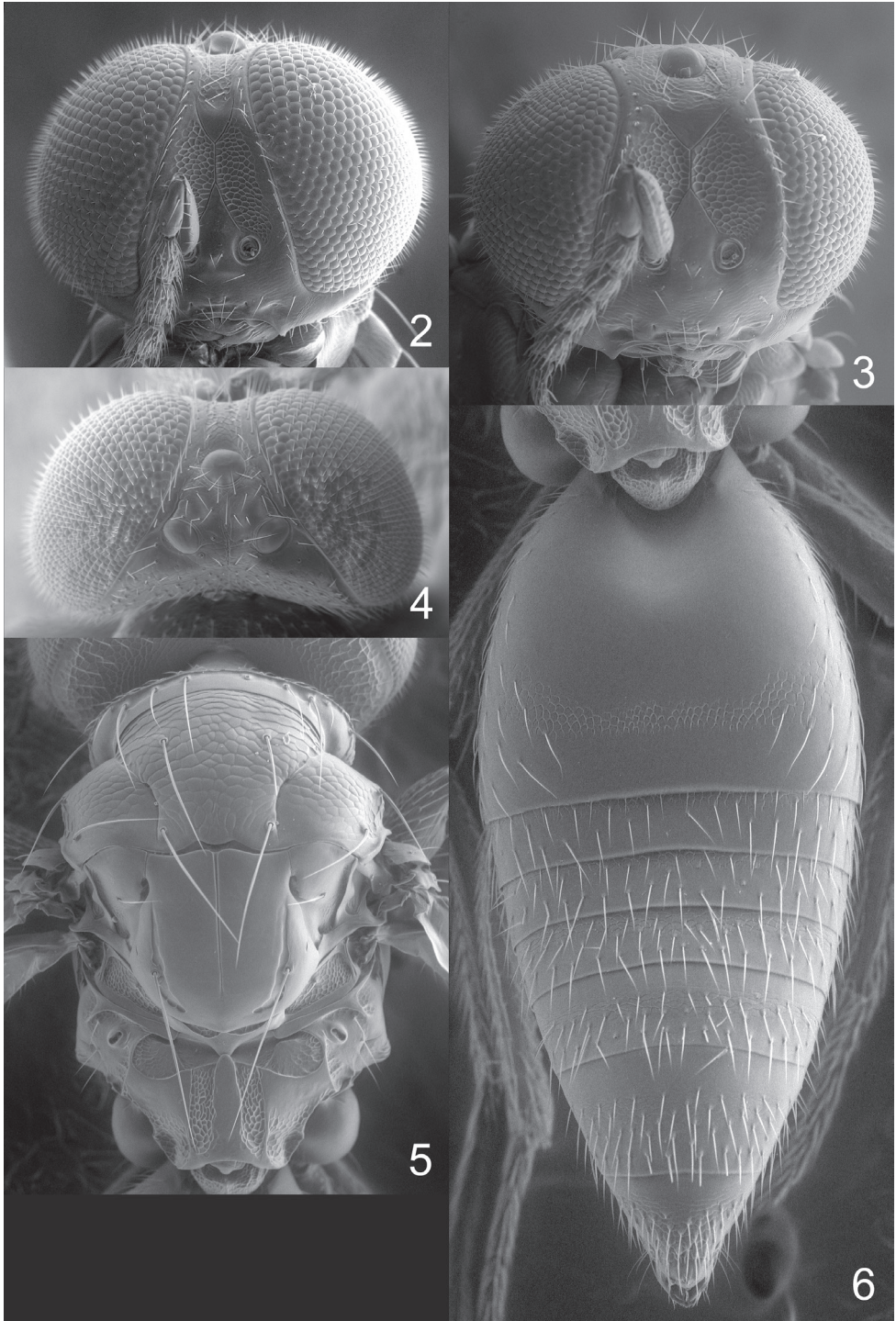
Figure 1. *Horismenus liturgusae* sp. n. female, habitus, length of specimen 2.1 mm.

femora and tibiae pale; eyes very large and frons very narrow (Figs 2–4, 7, 8), DE/DO = 1.4 in female, 2.9 in male; gaster conspicuously hairy (Figs 6, 12). Similar to *H. argus* Hansson but with larger eyes in both sexes (DE/DO = 2.5 in female, and = 3.3 in male of *H. argus*), entire mesoscutum metallic dark purple (metallic bluish-green in *H. argus*) and with engraved reticulation throughout (sidelobes and anterior 1/2 of midlobe with raised and strong reticulation in *H. argus*), propodeal callus with three setae (two setae in *H. argus*), forewing costal cell with 2–5 setae on ventral side close to submarginal vein (costal cell bare in *H. argus*).

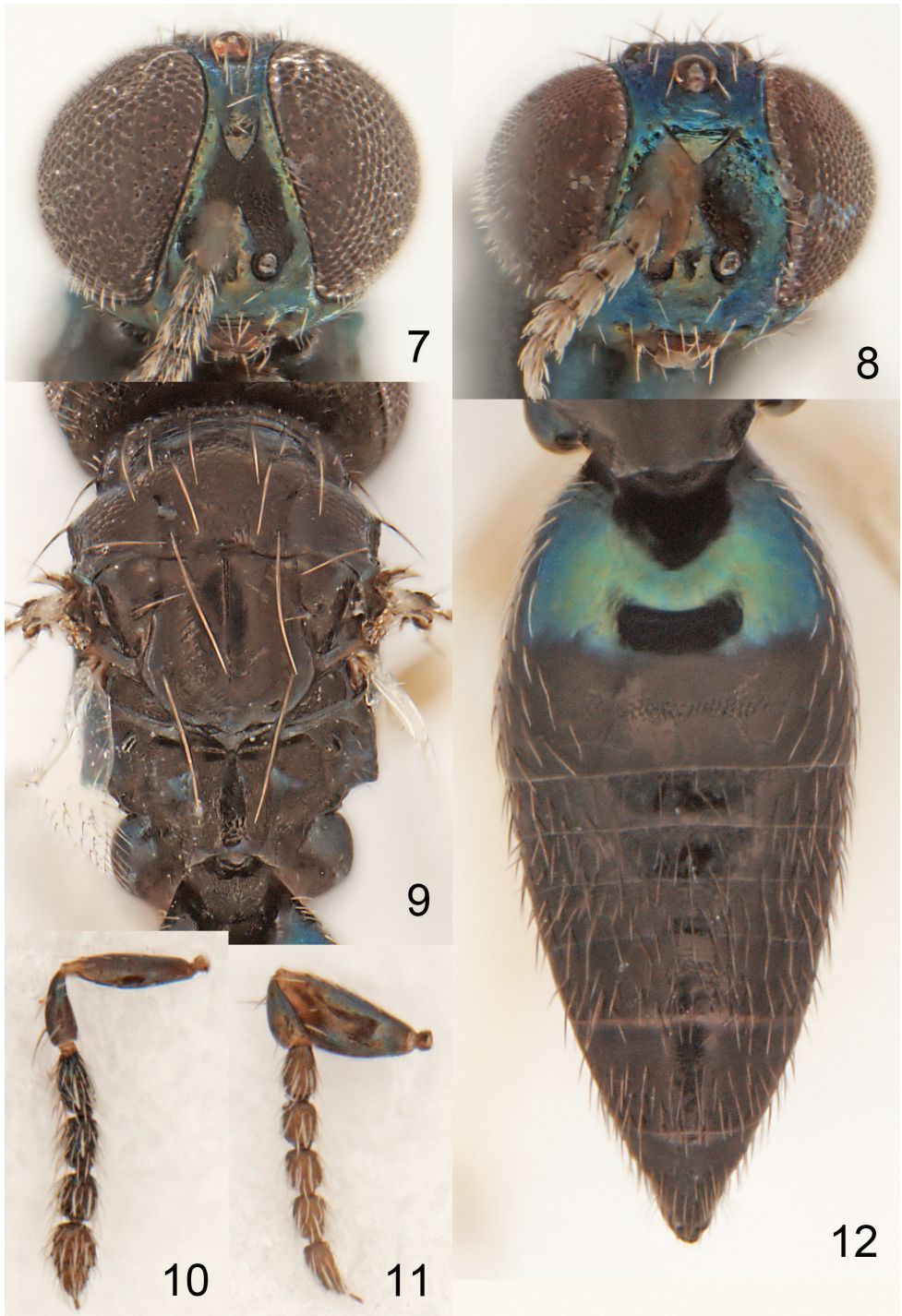
Description. FEMALE. Length 2.1–2.2 mm.

Entire antenna dark brown with metallic green tinges (Fig. 10). Frons metallic dark purple with parts close to eyes, part below level of toruli and part above frontal suture metallic bluish-green (Fig. 7). Vertex with anterior 1/2 metallic bluish-green, posterior 1/2 metallic dark purple. Mesoscutum, scutellum and propodeum metallic dark purple, mesoscutum with anterior margin metallic bluish-green (Fig. 9). Coxae metallic bluish-green; remaining parts of legs yellowish-white, mid and hind femora slightly infusate (Fig. 1). Wings hyaline (Fig. 1). Petiole metallic dark purple. Gaster with first tergite with anterior 2/3 metallic bluish-green, posterior 1/3 metallic dark purple; remaining tergites metallic dark purple (Fig. 12).

Antenna as in Fig. 10. Frons below level of toruli, interscrobial area, areas along inner margin of eyes, and part just above frontal suture smooth and shiny, remaining parts with raised reticulation; frontal suture V-shaped, incomplete, does not reach eyes;



Figures 2–6. *Horismenus liturgusae* sp. n. **2** Head frontal, female **3** Head frontal, male **4** Vertex, female **5** Mesosoma dorsal, female **6** Gaster dorsal, female.



Figures 7–12. *Horismenus liturgusae* sp. n. **7** Head frontal, female **8** Head frontal, male **9** Mesosoma dorsal, female **10** Antenna lateral, female **11** Antenna lateral, male **12** Gaster dorsal, female.



Figures 13–14. *Liturgusa* sp. **13** Nymph, length 1 mm **14** Ootheca, length 10 mm.

antennal scrobes joining below frontal suture (Fig. 2). Vertex with engraved and weak reticulation; posterior part with a median groove (Fig. 4). Occipital margin rounded (Fig. 4).

Mesoscutum with engraved reticulation; notauli narrow and distinct throughout (Fig. 5). Scutellum smooth and shiny (Fig. 5). Dorsellum convex and smooth, anterolaterally with two foveae (Fig. 5). Propodeum including median carina smooth and shiny, posterolateral propodeum and anterolateral foveae with weak reticulation, submedian grooves with strong reticulation (Fig. 5); propodeal callus with three setae. Coxae smooth and shiny. Forewing speculum closed below; with 23 admarginal setae; costal cell with 2–5 setae on ventral side close to submarginal vein.

Gaster with first tergite smooth with a reticulate band in posterior part (Fig. 6).

Ratios. DE/DO 1.4; WH/DE 6.5; HE/MS/WM 5.1/1.0/2.3; POL/OOL/POO 5.7/1.0/1.0; WH/WT 1.2; LW/LM/HW 1.8/1.3/1.0; PM/ST 1.0; LC/WC 3.5; WG/WC 0.8; LS/LT 0.19; LP/WP 0.8; MM/LG 0.7–0.8.

Male. Length 1.7 mm.

Similar to female except antenna (Fig. 11) with scape wider and with apical two flagellomeres separated.

Ratios. HE/MS/WM 4.4/1.0/2.3; LP/WP 1.2; MM/LG 1.5–1.6.

Distribution. Brazil.

Hosts. From ootheca of *Liturgusa* sp. (Mantodea: Liturgusidae).

Material examined. Holotype female labeled “BRAZIL: Amazonas, Manaus, Campus I, 21.xi.2012, D.G. Pádua & K. Schoeninger”, “Ex Liturgusa sp.” (INPA). Paratypes: 27 females and 22 males with same data as holotype (7f# 6m# in BMNH, 20f# 16m# in INPA).

Etymology. Named after host.

Acknowledgements

Our thanks to the parataxonomist José Ferreira Ramos for the identification the specimen of Lecythydidae and to Ola Gustafsson, Electron Microscopy Unit at the Department of Biology, Lund University, for help with the scanning electron microscope.

References

- Agudelo AA, Lombardo F, Jantsch LJ (2007) Checklist of the Neotropical mantids (Insecta, Dictyoptera, Mantodea). *Biota Colombiana* 8(2): 105–158.
- Bouček Z (1965) Studies of European Eulophidae, IV: *Pediobius* Walk. and two allied genera (Hymenoptera). *Acta Entomologica Musei Nationalis Pragae* 36: 5–90.
- Ehrmann R (2002) Mantodea-Gottesanberinnen der Welt. Natur und Tier-Verlag, Münster, 519 pp.
- Hansson C (2009) Eulophidae of Costa Rica, 3, the genus *Horismenus*. *Memoirs of the American Entomological Institute* 82: 1–916.
- Narendran TC, Kumar PG, Kazmi SI (2011) A new record of the New World genus *Horismenus* Walker (Hymenoptera: Eulophidae: Entedoninae) from India with description of a new species. *Journal of Environment and Sociobiology* 8(2): 173–176.
- Neto GS, Di Mare RA (2010) Hiperparasitoides em *Cotesia alius* (Mues.) (Hymenoptera: Braconidae) no estado do Rio Grande de Sul, Brasil. *Magistra*, Cruz das Almas-BA 22(3/4): 210–212.
- Thomazini MJ, Albuquerque ES (2005) Ocorrência de *Phyllocnistis citrella* Stainton (Lepidoptera: Gracillariidae) em citros no estado do Acre, Brasil, 35(3): 395–398.

Contributions to the study of the Holarctic fauna of Microgastrinae (Hymenoptera, Braconidae). I. Introduction and first results of transatlantic comparisons

Jose Fernandez-Triana¹, Mark R. Shaw², Sophie Cardinal¹, Peter G. Mason¹

1 Canadian National Collection of Insects, Agriculture and Agri-Food Canada, 960 Carling Ave., Ottawa, ON K1A 0C6, Canada **2** Honorary Research Associate, National Museums of Scotland, Chambers Street, Edinburgh EH1 1JF, U.K.

Corresponding author: Jose Fernandez-Triana (jfr triana@uoguelph.ca)

Academic editor: G. Broad | Received 3 February 2014 | Accepted 4 March 2014 | Published 28 March 2014

Citation: Fernández-Triana J, Shaw MR, Cardinal S, Mason PG (2014) Contributions to the study of the Holarctic fauna of Microgastrinae (Hymenoptera, Braconidae). I. Introduction and first results of transatlantic comparisons. Journal of Hymenoptera Research 37: 61–76. doi: 10.3897/JHR.37.7186

Abstract

Specimens of Microgastrinae (Hymenoptera: Braconidae) from both sides of the Holarctic region (Nearctic and Palaearctic) were sampled for DNA barcoding and examined morphologically. Two species are recorded for the first time for the Nearctic: *Apanteles brunnistigma* Abdinbekova, and *Microgaster raschkiellae* Shaw. Another European species, *Apanteles xanthostigma* (Haliday), previously introduced as a biological control agent, is confirmed to be present in North America. For another 13 species significant range extension is documented, including new records for France, Canada, United States, and Sweden. New host data are also provided for several species. The species name *Apanteles masmithi* Fernández-Triana is considered a **syn. n.** of *Dolichogenidea britannica* (Wilkinson).

Keywords

Microgastrinae, DNA barcoding, morphology, Holarctic, Palaearctic, Nearctic

Introduction

Microgastrinae wasps (Hymenoptera: Braconidae) are one of the most important groups in the biological control of Lepidoptera caterpillar pests of forestry and agriculture (Whitfield 1997). They are also the second largest subfamily of Braconidae, with 2,233 described species (Yu et al. 2012), and many thousands more awaiting description (e.g. Mason 1981; Rodriguez et al. 2012).

According to the latest version of Taxapad (Yu et al. 2012) there are 757 species of Microgastrinae in the Palaearctic (529 of them recorded from the Western Palaearctic, and 496 from the Eastern Palaearctic), and 320 described species in the Nearctic (for the limits of the Nearctic and Palaearctic regions, we follow O'Hara et al. 2009).

Altogether, the Nearctic plus the Palaearctic (i.e., the Holarctic region) have 1029 species, accounting for 46% of the described microgastrines worldwide. This, of course, is an artifact due to most studies being historically focused on the north-temperate areas of the planet. There is a significant diversity waiting to be described in the tropics, totalling several thousand new species (e.g., Rodriguez et al. 2012). Regardless of that, the information currently available for the Holarctic allows for some analyses and comparisons to be made.

While the Palaearctic has twice the number of known species as the Nearctic, the final figures might be much closer. Most of the European (i.e. Western Palaearctic) species are already known, with the remaining diversity to be discovered being mostly morphologically cryptic species. On the other hand, the Eastern Palaearctic is much less studied, and it is likely that a significant number of additional species remain to be found and described there, although we are not aware of any published information providing estimates. The most updated list of species for the Palaearctic can be found in *Fauna Europaea* (van Achterberg 2012), although that list uses a more condensed generic classification than the one followed here, which is based on Mason (1981) largely as interpreted by Papp (1988).

As for the Nearctic region, it is clear that a considerable number of species are still unknown. For example, Fernández-Triana (2010) estimated that just for the northern part of the Nearctic (i.e. Canada and Alaska) the known species (approximately 200) only represent half of the actual diversity. For the southern Nearctic, which is warmer and more diverse, it is reasonable to expect that 50% or more of the species remain unknown and/or undescribed there too. Clearly there is still much to be discovered, even in the relatively poorly diverse, temperate regions. The most updated lists of species for the Nearctic can be found in Whitfield (1995) and Fernández-Triana (2010).

According to the published data, only 272 (26%) of the 1,029 Holarctic species of Microgastrinae are shared between the Nearctic and Palaearctic regions. This relatively low percentage might be due to some taxa being described twice, as different species, on the two sides of the Atlantic. The large number of descriptions, and the holotypes being scattered across a large number of collections, make it very difficult to approach the study of this group from a truly Holarctic perspective. Thus, taxonomic revisions

of Microgastrinae have usually focused on either the Palaearctic or the Nearctic, with very few studies covering both regions.

DNA barcoding uses a short standardized region of the mitochondrial gene cytochrome *c* oxidase (COI) as a key character for species-level identification and discovery (Floyd et al. 2002; Hebert et al. 2003a; Hebert et al. 2003b; Janzen et al. 2009; Smith et al. 2006; Smith et al. 2007; Smith et al. 2008). DNA barcoding has been extensively used in biodiversity and taxonomic studies of Microgastrinae during the past few years (summarized in Fernández-Triana et al. 2014), due to the recent availability of over 20,000 sequences from more than 75 countries (e.g., Smith et al. 2013). Those resources have allowed us to compare sequences of specimens from different areas and unravel potentially new distribution patterns – which were previously overlooked, or unknown until now. All new distribution records reported here have been corroborated through careful comparisons with holotypes or authenticated specimens deposited in major collections.

Methods

This paper is mostly based in the study of DNA barcoded specimens of Microgastrinae from the Canadian National Collection, Ottawa (CNC), and the National Museums of Scotland, Edinburgh (NMS). Additionally, some barcoded specimens from the Swedish Malaise Trap Project (SMTP) were available for study; the SMTP aims to provide species determinations for all the 80 million insect specimens obtained from Malaise traps sampling at a wide range of landscapes and habitats in Sweden (<http://www.stationlinne.se/en/research/the-swedish-malaise-trap-project-smtp/>). Pictures of barcoded specimens housed in the Biodiversity Institute of Ontario, Guelph were also analyzed. Examination of holotypes deposited in the National Museum of Natural History, Washington D.C. (NMNH), and the Natural History Museum, London (BMNH), was made in some cases – mostly when necessary to verify identifications of specimens in the CNC and NMS.

One of us (MRS) provided samples of reliably determined Microgastrinae from Europe for barcoding, reared from identified hosts that are in many cases the very hosts from which the species in question was originally described. This provides a framework of fixed reference points from which to assess the specific identity of other specimens, whether reared or not and from both the Nearctic and the Palaearctic, initially through their barcodes. When host names are given for specimens in NMS, we append “Det.” and then the name of the person who reared the caterpillars, because it was (s)he who was responsible for the host determination.

To uncover new distribution patterns, we first scanned the tree presented in Smith et al. (2013), which contained all Microgastrinae sequences available at the time of its publication, and searched for clusters of closely related sequences (2% divergence or less) that contained both identified and unidentified specimens. These unidentified specimens were then morphologically studied to see if they were the same species as the identified specimens. To further uncover new distribution patterns, we generated

new barcode sequences from authenticated material from the NMS and CNC with the hope that some of these sequences would cluster with unidentified sequences found in BOLD. We used the Identification Engine tool (http://www.boldsystems.org/index.php/IDS_OpenIdEngine) in the Barcode of Life Data Systems (BOLD) to compare our newly generated sequences to all sequences available in BOLD. When our sequences matched previously unidentified sequences with a probability of placement above 98%, we morphologically studied the specimens to see if they were the same species. In some cases, unidentified specimens differed morphologically from the identified specimens they were clustering with based on molecular barcoding data. These cases will be studied further and results will be published in following papers.

Newly generated DNA barcodes were obtained using DNA extracts prepared from single legs using a glass fibre protocol (Ivanova et al. 2006). Extracts were re-suspended in 30 µl of dH₂O, and a 658-bp region near the 5' terminus of the COI gene was amplified using standard primers (LepF1–LepR1) following established protocols (Smith et al. 2006; Smith et al. 2007; Smith et al. 2008). All newly generated sequences were edited in Geneious v.6.1.6 created by Biomatters (<http://www.geneious.com/>) and submitted to Genbank (see Table 1 for Genbank accession numbers). All sequences from Smith et al. (2013) can also be retrieved from BOLD (Ratnasingham and Hebert 2007).

Sequences were considered as “barcode-compliant” when they had 500 or more base pairs and had less than 1% ambiguous characters (Barcode Compliance standards as in http://www.boldsystems.org/index.php/resources/handbook?chapter=6_managingdata.html§ion=record_list).

Genera (and species within a genus) are presented in alphabetical order. Each new distribution record is discussed within the context of the previously known distribution of the species. For Canadian provinces and territories, and states of the United States we use acronyms consisting of two capital letters following Canada Post (<http://www.canadapost.ca/tools/pg/manual/PGaddress-e.asp>).

Table 1. Details of specimens from the National Museums of Scotland (NMS) with DNA barcode sequences newly obtained – and not yet available in the Barcode of Life Data Systems (BOLD). Collection codes for NMS and the Canadian National Collection of Insects (CNC), as well as GenBank accession numbers are included.

Wasp species	Host species	Locality	Emergence date	NMS code	CNC code	GenBank accession numbers
<i>Apanteles brunnistigma</i>	<i>Pyausta aurata</i>	France: Aveyron, Livinhac-le-Haut	18.vi.2012	MRS 0183	CNCHYM49298	KJ459123
<i>Apanteles brunnistigma</i>	<i>Pyausta aurata</i>	France: Aveyron, Livinhac-le-Haut	11.vi.2012	MRS 0184	CNCHYM49319	KJ459223
<i>Dolichogenidea britannica</i>	<i>Ptocheuusa paupella</i>	England: Hants, Portsmouth	vii.2011	MRS 0217	CNCHYM45321	KJ459126
<i>Microgaster raschkiellae</i>	<i>Mompha raschkiella</i>	Scotland: Skye, Armadale	4.vii.2012	MRS 0192	CNCHYM45380	KJ459161
<i>Pbolytesor viminetorum</i>	<i>Elachista poae</i>	England: W. Yorks, Copley	28.iv.2012	MRS 0166	CNCHYM45332	KJ459179

Photos were taken with a Keyence VHX-1000 Digital Microscope, using a lens with a magnification range of 13–130×. Multiple images through the focal plane were taken of a structure and these were combined to produce a single in-focus image, using the software associated with the Keyence System.

Results

Two species previously known only from the Palaearctic are here recorded for the first time for the Nearctic. Another European species, previously introduced as a biological control agent but not known to be established, is here confirmed to be still present in North America. Additionally, another 13 species have been found to have a wider range than previously known – in some cases the new data reported here significantly expand the known distributions.

Most of the range expansions recorded were towards northern areas (e.g. Alaska, Manitoba, Nunavut, and Yukon Territory) and may reflect an increase in the availability of material recently collected in arctic and sub-arctic localities of North America (e.g., Fernández-Triana et al. 2011; Stahlhut et al. 2013). Other new records fill gaps in the known distribution of species.

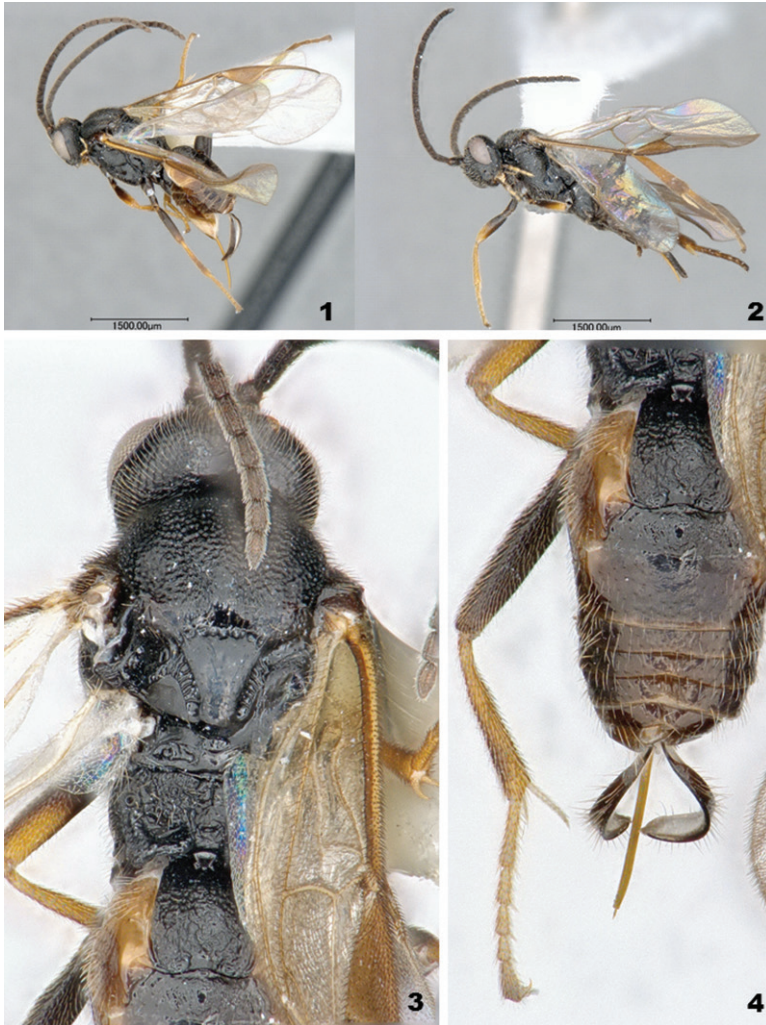
1) *Apanteles brunnistigma* Abdinbekova, 1969

Figs 1–4

Previously, this species was known to be widely distributed in the Palaearctic (Yu et al. 2012). Here it is recorded for the first time for the Nearctic (**Canada**: MB, Churchill, 51 specimens; and NL, Cap St-George, one specimen). The specimens from Manitoba were named as “*Apanteles jft02*” in a previous paper (Fernández-Triana et al. 2011). In the Palaearctic it is recorded for the first time from **Sweden** (all from the SMTP: Haninge Municipality, Stockholm County, one specimen; and Gällivare Municipality, Norrbotten County, four specimens) and from **France** (Aveyron, Livinhac-le-Haut, two specimens from the NMS).

Apanteles brunnistigma had been previously recorded as a parasitoid of Depressariidae (*Agonopterix umbellana* (Fabricius), *Depressaria ultimella* Stainton), and Tortricidae (*Aphelia viburnana* (Denis & Schiffermüller), *Archips rosana* (Linnaeus), *Eucosma rubescana* (Constant) (as *catoptrana*), and *Gynnidomorpha vectisana* (Humphries and Westwood)), as summarized in Yu et al. (2012). Specimens in the NMS were reared from the following (all of them are new host records): Epermeniidae (*Epermenia chaerophyllella* (Goeze) (Det. A. N. B. Simpson)), Tortricidae (*Rhopobota naevana* (Hübner) (Det. J. M. Chalmers-Hunt)), and Crambidae (*Pyrausta aurata* (Scopoli) (Det. R. J. Heckford, M. R. Shaw)).

We analyzed 61 barcode sequences available for this species (59 of them barcode compliant), representing 11 haplotypes from Canada, France, Sweden, and Ukraine.



Figures 1–4. *Apanteles brunnistigma*. **1** Habitus, lateral view, Swedish specimen with CNC code CNCH1798 **2** Habitus, lateral view, Canadian specimen with CNC code 07PROBE-23429 **3** Head, mesosoma and mediotergites 1-2, dorsal view, specimen CNCH1798 **4** Metasoma, dorsal view, specimen CNCH1798.

The difference between haplotypes ranged from one to 10 base pairs (0.2–1.5%), with most sequences differing by five base pairs or less.

2) *Apanteles ensiger* (Say, 1836)

This species was known to be widely distributed in the Nearctic (Yu et al. 2012). Here it is recorded for the first time, from numerous specimens, in five additional

provinces/territories of Canada (AB, Banff National Park; NB, Kouchibouguac National Park; NL, Corner Brook; Plum Point; St-Andrew's; St-David's; NT, Wood Buffalo National Park; PE, Blooming Point; and SK, Prince Albert National Park), and three states of the United States (AK, Anchorage; Trapper Creek, Petersville Road at 62°N; FL, Kissimmee Prairie Preserve State Park; and MA, Barnstable Country, Woods Hole). The records from Alaska considerably expand westwards and northwards the known distribution of the species.

This species had been previously recorded from the Lepidoptera families Tortricidae (*Choristoneura occidentalis* Freeman), and Crambidae (*Fissicrambus mutabilis* (Clemens), and *Neodactria zeella* (Fernald)), as summarized in Yu et al. (2012). Here a new host from Tortricidae is recorded, *Epiblema strenuana* (Walker) from one Canadian specimen (ON, Grimsby) deposited in the CNC.

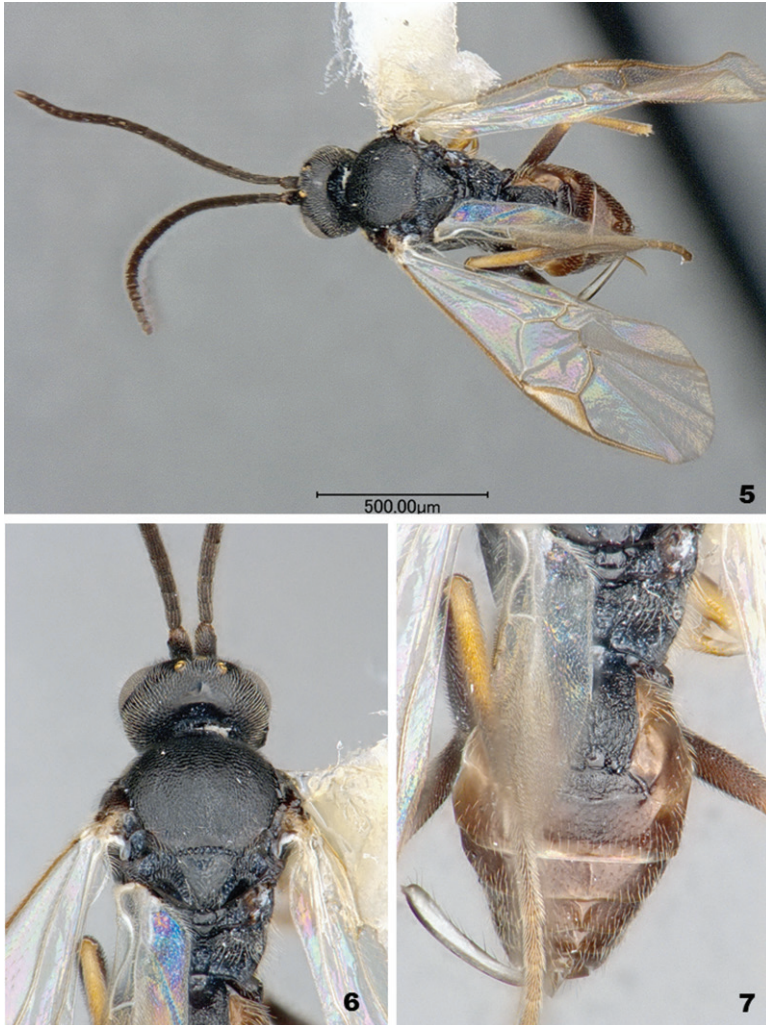
We analyzed 178 barcode sequences available for this species (166 of them barcode compliant), representing 20 haplotypes from Canada and the United States. The difference between haplotypes ranged from one to eight base pairs (0.2–1.2%).

3) *Apanteles xanthostigma* (Haliday, 1834)

Figs 5–7

Previously, the species was known to be widely distributed in the Palaearctic (Yu et al. 2012), with one record from tropical Africa (De Saeger 1944). In 1963, 290 specimens were released in St. John's, Newfoundland, Canada (Williamson 1963); however, until now it was not known if the species became established there (Fernández-Triana 2010). Here we confirm for the first time its continued presence in the Nearctic, from 17 specimens collected in three provinces of western Canada (MB, Churchill; SK, Prince Albert National Park; and BC, Sorrento). The specimens from Manitoba were named as "*Apanteles jft03*" in a previous paper (Fernández-Triana et al. 2011).

In the NMS there are authenticated specimens reared from the following Lepidoptera families and species: Choreutidae (*Choreutis diana* (Hübner) (R. J. Heckford)), Gracillariidae (*Caloptilia betulicola* (Hering) (Det. S. D. Beavan, K. P. Bland, R. J. Heckford, J. R. Langmaid, M. R. Shaw, P. A. Sokoloff), *Caloptilia elongella* (Linnaeus) (Det. K. P. Bland, M. R. Shaw), *Caloptilia stigmatella* (Fabricius) (Det. P. J. Johnson, J. R. Langmaid, S. E. Whitebread), *Povolnya leucapennella* (Stephens) (Det. R. J. Heckford) new host record, *Parornix devoniella* (Stainton) (Det. M. R. Shaw) new host record, and *Parornix scoticella* (Stainton) (Det. M. R. Shaw) new host record), Pyralidae (*Acrobasis suavella* (Zincken) (Det. M. F. V. Corley, R. J. Heckford) new host record), Tortricidae (*Acleris hastiana* (Linnaeus) (Det. P. J. Johnson) new host record, *Adoxophyes orana* (Fischer von Röslerstamm) (Det. A. Wilson), *Rhopobota naevana* (Hübner) (Det. M. R. Young)), and Yponomeutidae (*Swammerdamia caesiella* (Hübner) (Det. M. R. Shaw), *Swammerdamia pyrella* (Villers) (Det. J. L. Gregory), *Paraswammerdamia albicapitella* (Scharfenberg) (Det. J. L. Gregory, N. Hall)).



Figures 5–7. *Apanteles xanthostigma*. **5** Habitus, dorsal view, Swedish specimen with CNC code CNCH1804 **6** Head and mesosoma, dorsal view, specimen CNCH1804 **7** Propodeum and metasoma, dorsal view, specimen CNCH1804.

Yu et al. (2012) summarized recorded hosts for *A. xanthostigma*, including 11 families and 63 species of Lepidoptera. Even allowing for the probability that some records are erroneous (as must surely be the case for the two records from Diptera (Cecidomyiidae)), the historical data demonstrate an extremely broad host range comprising semi-concealed arboreal microlepidoptera larvae feeding on the foliage of trees and shrubs. Including the new records reported here, there are now 68 host species of Lepidoptera recorded, with the best represented host families being Tortricidae (28 species), Gracillariidae (14), Yponomeutidae (6), Gelechiidae (4), Pyralidae (4), and Choreutidae (3) – a pattern of representation that is to a rather large extent just a

reflection of the number of host species available to the parasitoid within its essentially ecologically defined host range.

We analyzed 12 barcode sequences available for this species (10 of them barcode compliant), representing four haplotypes from Canada, the Netherlands, Russia, and Sweden. The difference between haplotypes ranged from one to eight base pairs (0.2–1.2%), with most sequences differing by six base pairs or less.

The fact that new Canadian records come from several localities, all far apart (more than 3,000 km) from the original site of introduction in Newfoundland, suggests that the species was probably already established in North America prior to the 1963 introduction.

4) *Cotesia crambi* (Weed, 1887)

This species was previously known from northeast and central United States (Yu et al. 2012) and one locality in Canada (QC, Frelighsburg) (Fernández-Triana et al. 2009). Here it is recorded for a second locality and province in Canada (ON, Ottawa, three specimens). Three species of Crambidae have been recorded as hosts of the species (Yu et al. 2012).

We analyzed six barcode sequences available for this species (two of them barcode compliant), representing 3 haplotypes from Canada and the United States. The difference between haplotypes was one base pair (0.2%).

5) *Cotesia parastichtidis* (Muesebeck, 1921)

Previous records show a wide distribution within the Nearctic, although records are scarce and sparse over North America. Here it is recorded for the first time in three additional Canadian provinces/territories (AB, Waterton Lakes National Park, one specimen; MB, Churchill, four specimens; and YT, Top of the World Highway, km 82, one specimen) and one state of the United States (AK, Anchorage, three specimens). The new records expand northward the known distribution of the species. Some of the specimens from Manitoba were named as “*Cotesia jft04*” in a previous paper (Fernández-Triana et al. 2011). Five species within three families of Lepidoptera (Geometridae, Noctuidae, and Tortricidae) have been recorded as hosts of the species (Yu et al. 2012).

We analyzed 16 barcode sequences available for this species (seven of them barcode compliant), representing five haplotypes from Canada. The difference between haplotypes ranged from one to 13 base pairs (0.2–2.0%).

6) *Cotesia rufocoxalis* (Riley, 1881)

This species was previously known from eastern and central United States and the Canadian province of Nova Scotia. Here it is recorded for the first time for two additional states of the United States (NJ, Metuchen, one specimen; and AL, Mobile County,

Country Road 1, one specimen). Five species of Lepidoptera, one in Lasiocampidae and four in Noctuidae, have been recorded as hosts of the species (Yu et al. 2012).

We analyzed six barcode sequences available for this species (two of them barcode compliant), representing 3 haplotypes from Canada and the United States. The difference between haplotypes ranged from one to three base pairs (0.2–0.5%).

7) *Cotesia selenevora* Shaw, 2009

This species was previously known from Belgium and Finland. Here recorded for the first time for Sweden (Småland, Nybro kommun, Bäckebo, Grytsjöns naturreservat, Lat/Lon: 63.1766, 15.3005, one specimen from the SMTP).

The reared material (the type series) in NMS is from *Boloria selene* (Dennis & Schiffermüller) (Lepidoptera: Nymphalidae) (C. Turlure, J. Chouett), so far the only known host of *C. selenevora*. There are no records additional to those given by Shaw (2009).

We analyzed two barcode sequences available for this species (both barcode compliant), representing 1 haplotype from Belgium and Sweden.

8) *Dolichogenidea britannica* (Wilkinson, 1941)

Apanteles masmithi Fernández-Triana, 2010. **Syn. n.**

After comparing the type material of *Dolichogenidea britannica* and *Apanteles masmithi*, we conclude that both are the same species – and thus the latter name becomes a synonym of the first. This represents the first record of *D. britannica* for the Nearctic. The evidence from morphology is also supported by DNA barcoding – which indeed had suggested the synonymy in the first place. The difference was only three base pairs (0.5%) between the two available haplotypes (one haplotype from eight Canadian specimens (three specimens barcode compliant), the other haplotype from one English specimen (barcode compliant) reared from the same host species as the type). This species is an example of the need to study the Holarctic fauna as a whole, whenever possible; otherwise the same species is likely to be described twice (or more) on both sides of the Atlantic.

The type series of *D. britannica* was reared from the gelechiid now known as *Ptocheuusa paupella* (Zeller). An additional host record given by Yu et al. (2012) is from Tortricidae (*Enarmonia formosana* (Scopoli)). Reared material in NMS is from Gelechiidae (*Ptocheuusa paupella* (Det. E. S. Bradford, J. R. Langmaid, M. S. Parsons, P. A. Sokoloff), almost certainly *Isophrictis striatella* (Dennis and Schiffermüller) (Det. E. C. Pelham-Clinton) new host record), and Cosmopterigidae (*Limnaecia phragmitella* Stainton (Det. B. Goodey, I. Sims, P. A. Sokoloff, I. A. Watkinson) new host record of family and species). It is noteworthy that some of the Canadian specimens were also reared from *L. phragmitella*.

9) *Dolichogenidea melanopa* (Viereck, 1917)

This species was previously known in the Nearctic from three rather separate areas (CT in the United States, BC and PE in Canada). Here it is recorded for the first time, from numerous specimens, from six additional provinces/territories in Canada (AB, Banff National Park; MB, 22 km S of Camperville; Churchill; 1 km N of Winnipeg; NL, Corner Brook; Port Saunders; St-Andrew's; QC, Belle-Anse; SK, Grasslands National Park; and YT, Whitehorse); and one state in the United States (AK, S of Anchorage). The new records show the species is rather widely distributed within the Nearctic north of 40°N. Specimens were previously named as *Dolichogenidea* jft09 in Fernández-Triana et al. (2010). The only recorded host is *Pieris rapae* (Linnaeus) (Lepidoptera: Pieridae).

We analyzed 70 barcode sequences available for this species (64 of them barcode compliant), representing 12 haplotypes from Canada and the United States. The difference between haplotypes ranged between one and three base pairs (0.2–0.5%).

10) *Microgaster raschkiellae* Shaw, 2012

Figs 8–12

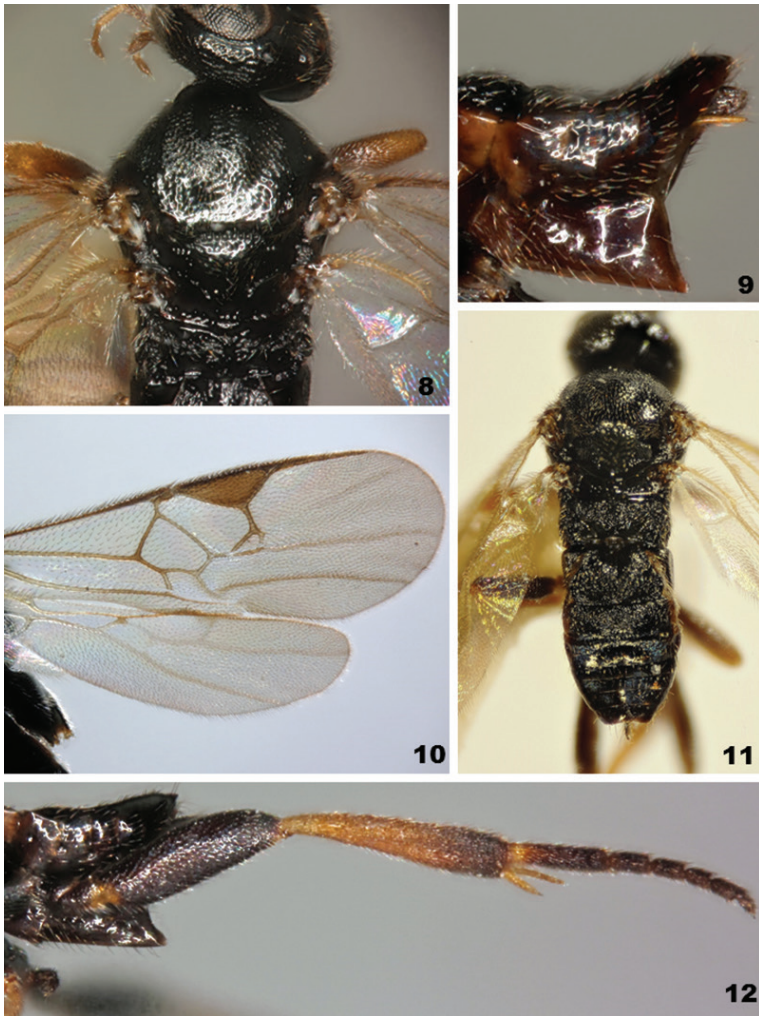
This species was recently described from Great Britain (England, Scotland and Wales), where it was widely recovered as the commonest parasitoid of *Mompha raschkiella* (Zeller) (Lepidoptera: Momphidae). Because it has not been reared from any other species of *Mompha*, Shaw (2012) considered that the species is probably monophagous, at least in Great Britain. Here it is recorded for the first time for the Nearctic, from Canada (MB, Churchill); *Mompha raschkiella* also occurs in Canada, but is not considered to be native there (J.F. Landry, personal communication). The difference between the two available haplotypes (one haplotype from several Canadian specimens, the other from one Scottish specimen) ranged between four and five base pairs (0.6–0.8%).

This species was described too late for inclusion in Yu et al. (2012). The reared material in NMS is all from the only known host, *Mompha raschkiella* (Det. K. P. Bland, E. S. Bradford, R. J. Heckford, E. C. Pelham-Clinton, M. R. Shaw, P. A. Sokoloff, M. R. Young).

11) *Microplitis kewleyi* Muesebeck, 1922

This species is widely distributed within the Nearctic. Here it is recorded for the first time in three additional Canadian provinces (NL, Corner Brook; NS, Kentville Research Station; Cape Breton Highlands National Park, MacIntosh Brook; and PEI, Harrington), and one state in the United States (NJ, Metuchen). Three species of Noctuidae have been recorded as hosts of the species (Yu et al. 2012).

We analyzed 38 barcode sequences available for this species (35 of them barcode compliant), representing 1 haplotype from Canada.



Figures 8–12. *Microgaster raschkiellae* (all photos from specimens from the United Kingdom part of the original description of the species) **8** Mesoscutum and scutellum **9** Metasoma in lateral view **10** Wings **11** Habitus, dorsal view **12** Hind leg (excluding coxa).

12) *Pholetesor bedelliae* (Viereck, 1911)

This species is widely distributed within the Nearctic, and is also reported from Finland (Hellén 1977), Peru (de Huiza 1995), and was introduced to Hawaii (Fullaway 1950). Here it is recorded for the first time from one additional province in Canada (SK, Grasslands National Park); and one province in the United States (AK, Anderson, Highway 3; Delta Junction; Sutton on Glen Highway). Around 20 host species within seven families of Lepidoptera have been recorded as hosts of the species (Yu et al. 2012).

We analyzed 66 barcode sequences available for this species (60 of them barcode compliant), representing seven haplotypes from Canada and the United States. The difference between haplotypes ranged between one and five base pairs (0.2–0.8%).

13) *Pholetesor masoni* Whitfield, 2006

This species is widely distributed within the Nearctic, and also reported from Chiapas, Mexico (Whitfield 2006). Here it is recorded for the first time from two additional provinces/territories in Canada (MB, Churchill, several specimens; 22 km S of Camperville, one specimen; and YT, Pelly Crossing, one specimen). The new records expand the known distribution of the species northwards. Only the genus *Bucculatrix* (Lepidoptera: Bucculatricidae) is known as host for this wasp species.

We analyzed eight barcode sequences available for this species (seven of them barcode compliant), representing four haplotypes from Canada. The difference between haplotypes ranged between one and seven base pairs (0.2–1.0%).

14) *Pholetesor rhygoplitoides* Whitfield, 2006

Previously known records for this species show a wide distribution within the Nearctic, although records are scarce and sparse over North America. Here it is recorded for the first time from two additional provinces in Canada (AB, Banff National Park, one specimen; and NL, Gros Morne National Park, Western Brook Pond, Hiking Trial, one specimen). No host is known for this species.

We analyzed three barcode sequences available for this species (two of them barcode compliant), representing one haplotype from Canada.

15) *Pholetesor salicifoliellae* (Mason, 1959)

This species is widely distributed within the Nearctic. Here it is recorded for the first time from two additional provinces in Canada (YT, Champagne; Takhini River road; and NT, Inuvik), and one province in the United States (AK, King Salmon, Naknek River; Nome). The new records expand the known distribution of the species northward. Around 16 host species of Gracillaridae and one species in Elachistidae (Lepidoptera) have been recorded as hosts of the species (Yu et al. 2012).

We analyzed 40 barcode sequences available for this species (39 of them barcode compliant), representing 13 haplotypes from Canada and the United States. The difference between haplotypes ranged between one and eight base pairs (0.2–1.2%).

16) *Pholetesor viminetorum* (Wesmael, 1837)

This species is widely distributed in the Holarctic (Yu et al. 2012). Here it is recorded for the first time from numerous specimens from four additional provinces/territories in Canada (NL, Cap St-George; Plum Point; Sally's Cove; South Branch; St-David's; NB, vicinity of Tracy; NT, Ford Lake; and SK, N of Rocanville, Qu'Appelle Road). More than 40 host species within 13 families of Lepidoptera have been recorded as hosts of the species (Yu et al. 2012), along with two records of Diptera (Agromyzidae and Tephritidae) which we consider to be almost certainly erroneous. The numerous reared specimens in NMS, all from species of *Elachista* (Lepidoptera: Elachistidae), are enumerated by Shaw (2012).

We analyzed 85 barcode sequences available for this species (76 of them barcode compliant), representing 28 haplotypes from Canada. The difference between haplotypes ranged between one and 12 base pairs (0.2–1.9%).

Acknowledgements

Teresa Martin did the lab work required to obtain the new sequence data. Agriculture and Agri-Food Canada provided funding for the sequencing of some specimens from the CNC and NMS. MRS is grateful to all those who donate reared specimens to him for the NMS collection. Jeremy deWaard, Jayme Sones, Paul Hebert, and Alex Smith kindly allowed JFT to access sequences and examine photographs of specimens collected by and deposited in the Biodiversity Institute of Ontario. Pelle Magnusson and his colleagues at the Swedish Museum of Natural History in Stockholm and the Station Linné in Öland (Sweden) sent specimens of Microgastrinae collected as part of the Swedish Malaise Trap Project. The reviews of Julia Sigenberg and an anonymous reviewer improved the final version of the manuscript.

References

- Achterberg C van (2012) Fauna Europaea: Microgastrinae. Fauna Europaea version 2.5, <http://www.faunaeur.org>
- De Saeger H (1944) Microgasterinae (Hymenoptera: Apocrita). Exploration du Parc National Albert. Mission G.F. de Witte. 47: 1–342.
- Fernández-Triana J, Goulet H, Bostanian N, Boudreault C (2009) Diversity of Microgastrinae (Hymenoptera: Braconidae) in apple orchards of southern Quebec, Canada. *Biocontrol Science and Technology* 19 (3): 237–248. doi: 10.1080/09583150802684406
- Fernández-Triana J (2010) Eight new species and an annotated checklist of Microgastrinae (Hymenoptera: Braconidae) from Canada and Alaska. *ZooKeys* 63: 1–53. doi: 10.3897/zookeys.63.565
- Fernández-Triana J, Smith MA, Boudreault C, Goulet H, Hebert PDN, Smith AC, Roughley R (2011) A poorly known high-latitude parasitoid wasp community: unexpected diversity and dramatic changes through time. *PLoS ONE* 6(8): e23719. doi: 10.1371/journal.pone.0023719

- Fernández-Triana J, Whitfield JB, Rodriguez JJ, Smith MA, Janzen DH, Hallwachs W, Hajibabaei M, Burns JM, Solis MA, Brown J, Cardinal S, Goulet H, Hebert PDN (2014) Review of *Apanteles* sensu stricto (Hymenoptera: Braconidae, Microgastrinae) from Area de Conservación Guanacaste, northwestern Costa Rica, with keys to all described species from Mesoamerica. *Zookeys* 383: 1–565. doi: 10.3897/zookeys.383.6418
- Floyd R, Abebe E, Papert A, Blaxter M (2002) Molecular barcodes for soil nematode identification. *Molecular Ecology* 11: 839–850. doi: 10.1046/j.1365-294X.2002.01485.x
- Fullaway DT (1950) *Apanteles* in Hawaii. *Proceedings of the Hawaiian Academy of Sciences* 25: 7.
- Hebert PDN, Cywinska A, Ball SL, DeWaard JR (2003a) Biological identifications through DNA barcodes. *Proceedings of the Royal Society B* 270: 313–321. doi: 10.1098/rspb.2002.2218
- Hebert PDN, Ratnasingham S, DeWaard JR (2003b) Barcoding animal life: cytochrome c oxidase subunit I divergences among closely related species. *Proceedings of the Royal Society B* 270 (Suppl. 1): S96–S99. doi: 10.1098/rspb.2002.2218
- Hellén W (1977) För Finlands fauna nya *Apanteles*-arter (Hymenoptera, Braconidae). *Notulae Entomologicae* 57: 9–10.
- de Huiza R (1995) Diversidad de Braconidae (Hymenoptera) en el Peru. *Revista Peruana de Entomología* 37: 11–22.
- Ivanova NV, Dewaard JR, Hebert PDN (2006) An inexpensive, automation-friendly protocol for recovering high-quality DNA. *Molecular Ecology Notes* 6 (4): 998–1002. doi: 10.1111/j.1471-8286.2006.01428.x
- Janzen DH, Hallwachs W, Blandin P, Burns JM, Cadiou J, Chacon I, Dapkey T, Deans AR, Epstein ME, Espinoza B, Franclemont JG, Haber WA, Hajibabaei M, Hall JPW, Hebert PDN, Gauld ID, Harvey DJ, Hausmann A, Kitching I, Lafontaine D, Landry J, Lemaire C, Miller JY, Miller JS, Miller L, Miller SE, Montero J, Munroe E, Rab Green S, Ratnasingham S, Rawlins JE, Robbins RK, Rodriguez JJ, Rougerie R, Sharkey MJ, Smith MA, Solis MA, Sullivan JB, Thiaucourt P, Wahl DB, Weller SJ, Whitfield JB, Willmott KR, Wood DM, Woodley NE, Wilson JJ (2009) Integration of DNA barcoding into an ongoing inventory of complex tropical biodiversity. *Molecular Ecology Resources* 9 (Supplement 1): 1–26. doi: 10.1111/j.1755-0998.2009.02628.x
- Mason WRM (1981) The polyphyletic nature of *Apanteles* Foerster (Hymenoptera: Braconidae): A phylogeny and reclassification of Microgastrinae. *Memoirs of the Entomological Society of Canada* 115: 1–147. doi: 10.4039/entm113115fv
- O'Hara J, Shima H, Zhang C (2009) Annotated Catalogue of the Tachinidae (Insecta: Diptera) of China. *Zootaxa* 2190: 1–236.
- Papp J (1988) A survey of the European species of *Apanteles* Först. (Hymenoptera, Braconidae: Microgastrinae). 11. “Homologization” of the species-groups of *Apanteles* s.l. with Mason's generic taxa. Checklist of genera. Parasitoid/host list 1. *Annales Historico-Naturales Musei Nationalis Hungarici* 80: 145–175.
- Ratnasingham S, Hebert PDN (2007) BOLD: The Barcode of Life Data System (www.barcodinglife.org). *Molecular Ecology Notes* 7: 355–364. doi: 10.1111/j.1471-8286.2007.01678.x
- Rodriguez JJ, Fernández-Triana J, Smith MA, Janzen DH, Hallwachs W, Erwin TL, Whitfield JB (2012) Extrapolations from field studies and known faunas converge on dramatically

- increased estimates of global microgastrine parasitoid wasp species richness (Hymenoptera: Braconidae). *Insect Conservation and Diversity* 6: 530–536. doi: 10.1111/icad.12003
- Shaw MR (2009) *Cotesia* Cameron (Hymenoptera: Braconidae: Microgastrinae) parasitoids of Heliconiinae (Lepidoptera: Nymphalidae) in Europe, with description of three new species. *British Journal of Entomology and Natural History* 22: 133–146.
- Shaw MR (2012) Notes on some European Microgastrinae (Hymenoptera: Braconidae) in the National Museums of Scotland, with twenty species new to Britain, new host data, taxonomic changes and remarks, and descriptions of two new species of *Microgaster* Latreille. *Entomologist's Gazette* 63: 173–201.
- Smith MA, Woodley NE, Janzen DH, Hallwachs W, Hebert PDN (2006) DNA barcodes reveal cryptic host-specificity within the presumed polyphagous members of a genus of parasitoid flies (Diptera: Tachinidae). *Proceedings of the National Academy of Sciences* 103: 3657–3662. doi: 10.1073/pnas.0511318103
- Smith MA, Wood DM, Janzen DH, Hallwachs W, Hebert PDN (2007) DNA barcodes affirm that 16 species of apparently generalist tropical parasitoid flies (Diptera, Tachinidae) are not all generalists. *Proceedings of the National Academy of Sciences* 104: 4967–4972. doi: 10.1073/pnas.0700050104
- Smith MA, Rodriguez JJ, Whitfield JB, Deans AR, Janzen DH, Hallwachs W, Hebert PDN (2008) Extreme diversity of tropical parasitoid wasps exposed by iterative integration of natural history, DNA barcoding, morphology, and collections. *Proceedings of the National Academy of Sciences* 105: 12359–12364. doi: 10.1073/pnas.0805319105
- Smith MA, Fernández-Triana JL, Eveleigh E, Gómez J, Guclu C, Hallwachs W, Hebert PDN, Hrcék J, Huber JT, Janzen DH, Mason PG, Miller SE, Quicke DLJ, Rodriguez JJ, Rougerie R, Shaw MR, Varkonyi G, Ward D, Whitfield JB, Zaldívar-Riverón A (2013) DNA barcoding and the taxonomy of Microgastrinae wasps (Hymenoptera, Braconidae): impacts after 8 years and nearly 20 000 sequences. *Molecular Ecology Resources* 13: 168–176. doi: 10.1111/1755-0998.12038
- Stahlhut JK, Fernández-Triana J, Adamowicz SJ, Buck M, Goulet H, Hebert PDN, Huber JT, Merilo M, Sheffield CS, Woodcock T, Smith MA (2013) Diversity of Hymenoptera and the dominance of parasitoids in a sub-Arctic environment. *BMC Ecology* 13: 2. doi: 10.1186/1472-6785-13-2
- Whitfield JB (1995) Checklist of the Microgastrinae (Hymenoptera: Braconidae) in America north of Mexico. *Journal of the Kansas Entomological Society* 68: 245–262.
- Whitfield JB (1997) Subfamily Microgastrinae. In: Wharton RA, Marsh PM, Sharkey MJ (Eds). *Manual of the New World genera of the family Braconidae* (Hymenoptera). Special Publication No. 1 International Society of Hymenopterists, Washington, D.C.: 333–364.
- Whitfield JB (2006) Revision of the Nearctic species of the genus *Pholetesor* Mason (Hymenoptera: Braconidae). *Zootaxa* 1144: 1–94.
- Williamson GD (1963) Summary of parasite and predator liberations in Canada and of insect shipments from Canada in 1963. *Canadian Insect Pest Review* 41: 137–151.
- Yu DSK, van Achterberg C, Horstmann K (2012) Taxapad 2012, Ichneumonoidea 2011. Ottawa, Ontario, Canada. Database on flash-drive. www.taxapad.com

The maxillo-labial complex of *Sparasion* (Hymenoptera, Platygastroidea)

Ovidiu Alin Popovici¹, István Mikó², Katja C. Seltmann³, Andrew R. Deans²

1 University “Al. I. Cuza” Iasi, Faculty of Biology, B-dul Carol I, no. 11, RO – 700506; Romania **2** Pennsylvania State University, Department of Entomology, 501 ASI Building, University Park, PA 16802 USA **3** Department of Invertebrate Zoology, American Museum of Natural History, Central Park West at 79th Street, New York, New York 10024, USA

Corresponding author: *István Mikó* (istvan.miko@gmail.com)

Academic editor: *M. Yoder* | Received 25 November 2013 | Accepted 28 February 2014 | Published 28 March 2014

Citation: Popovici OA, Mikó I, Seltmann CK, Deans AR (2014) The maxillo-labial complex of *Sparasion* (Hymenoptera, Platygastroidea). *Journal of Hymenoptera Research* 37: 77–111. doi: [10.3897/JHR.37.5206](https://doi.org/10.3897/JHR.37.5206)

Abstract

Hymenopterans have evolved a rich array of morphological diversity within the maxillo-labial complex. Although the character system has been extensively studied and its phylogenetic implications revealed in large hymenopterans, e.g. in Aculeata, it remains comparatively understudied in parasitoid wasps. Reductions of character systems due to the small body size in microhymenoptera make it difficult to establish homology and limits the interoperability of morphological data. We describe here the maxillo-labial complex of an ancestral platygastroid lineage, *Sparasion*, and provide an ontology-based model of the anatomical concepts related to the maxillo-labial complex (MLC) of Hymenoptera. The possible functions and putative evolutionary relevance of some anatomical structures of the MLC in *Sparasion* are discussed. Anatomical structures are visualized with Confocal Laser Scanning Microscopy.

Keywords

Mouthparts, Hymenoptera Anatomy Ontology, Confocal laser scanning microscopy, maxillary palpus, labial palpus, galea, lacinia, prementum, glossa

Introduction

Despite relatively recent efforts (e.g., Austin and Field 1997, Murphy et al. 2007), the phylogeny of Platygastroidea remains largely unresolved, as such insights from previously unexplored character systems have the potential to make important contributions to our understanding of the groups evolution. As Platygastroidea are usually reduced

in body size, the number of informative characters is limited to those anatomical complexes that cannot be simplified without negatively affecting the wasps' survival. In the case of Platygastroidea two character systems seem to match this requirement: the ovipositor apparatus (Austin 1983, Field and Austin 1994, Austin and Field 1997) and the mouthparts including the maxillo-labial complex. While the former is crucial for the piercing the chorion of host egg and laying the wasp's own eggs, the second structure is vital to the process of feeding. Very little is known about the feeding behavior and diet of adult platygastroids. Some species, e.g., the phoretic mantid egg parasitoid *Mantibaria*, feed also on their hosts' body fluids (Clausen 1976).

Due to the extreme diversity of Hymenoptera foraging strategies homologizing mouthpart structures within the order is a challenging task. Other than palpal formulae (Kieffer 1926, Masner 1976, Kononova and Kozlov 2001) and a relatively superficial survey of the maxillo-labial complex (MLC) in some genera of platygastroids (Popovici and Fusu 2006) data on MLC morphology in platygastroids have never been published.

Sparasion is a fairly speciose genus, with 141 valid species (Johnson 1992, Johnson et al. 2008). These wasps are widespread in Eurasia, Africa, and temperate North America (Johnson et al. 2008), and, as far as is known, these species are egg-parasitoids of Tettigoniinae (Orthoptera: Tettigoniidae) (Johnson et al. 2008). Based on the latest phylogenetic analyses, *Sparasion* is part of a small lineage that is sister to either the vast majority of Scelionidae *sensu* Haliday 1839 (Murphy et al. 2007) or Platygastriidae *sensu stricto* (Austin and Field 1997). Species in this lineage typically exhibit ancestral morphological states (Murphy et al. 2007, Austin and Field 1997), which should facilitate homologization of mouthparts with other hymenopterans. *Sparasion* are also relatively large species, with less anatomical simplification, which makes them more suitable for dissection and observation.

Material and methods

We examined 34 specimens of 10 *Sparasion* species (Appendix 1). All specimens were stored in 70% ethanol prior to dissection. Card-mounted voucher specimens are deposited in the Insect Collection of University "Al.I.Cuza" Faculty of Biology, Iasi, Romania (OPPC), in the C. A. Triplehorn Insect Collection, Ohio State University, Columbus, OH, USA (OSUC) and in the Frost Entomological Museum, Pennsylvania State University, State College, PA, USA (PSUC).

We followed the protocols of Prinsloo (1980) for specimen preparation. The head was boiled in 10% phenol in lactic acid for 30 minutes and rinsed in distilled water. The MLC were separated from the cranium using forceps (Dumont #5) and insect pins (size 2), then were transferred into 10% NaOH and macerated for 30 minutes, than transferred and rinsed in glacial acetic acid for 10 minutes. Clear and neutralized MLC specimens were dehydrated using ethanol series (70%, 96%, and 100% alcohol; 30 min each) and transferred to a clove oil droplet on concave microscope slide. The labium was separated from the right and left maxillae and mounted separately in Canada balsam medium.

MLC specimens were examined under Euromex GE 3045 microscope (400×–1000×). Line drawings were made using Reichart drawing tube attached to the same microscope. Photos were taken using a Leica DFC-500 camera mounted on a Leica M 205A stereomicroscope.

CLSM images were taken on glycerin-stored specimens with Zeiss LSM 710 Confocal Microscope. For visualizing anatomical structures we used excitation wavelength of 488 and emission wavelength of 510–680 nm, detected using two channels visualized separately using two pseudocolors (510–580 nm=green; 580–680 nm=red). For visualizing resilin we used excitation wavelength of 405 nm and emission wavelength of 510–680 nm detected using one channel visualized with blue pseudocolor.

For Scanning Electron Microscopy (SEM) specimens were dried using hexamethyldisilazane (HMDS, Brown 1993), mounted on double adhesive tape and coated with gold. SEM images were taken using VEGA T SCAN SEM.

Anatomical concepts used here are defined and aligned with those of Alam 1951, Beutel and Vilhelmsen 2007, Bugnion 1924, 1925, Cockerell 1924, Crampton 1923, Crosskey 1951, Dhillon 1966; Duncan 1939, Eickwort 1969, Forel 1874, Gotwald 1969, Krenn et al. 2005, Liu 1925; Matsuda 1965, Matsuda 1957, McGinley 1980, Michener 1944, Michener 1984, Plant and Paulus 1987, Prentice 1998, Ross 1937, Ritchie and Peters 1981, Ronquist and Nordlander 1989, Snodgrass 1942, Ulrich 1924, Vilhelmsen 1996, Winston 1979 in the Hymenoptera Anatomy Ontology (HAO, Yoder et al. 2010). Anatomical terms in the Results section are linked to the HAO via the URI table (Appendix 2; see Seltmann et al. 2012 for more information about this approach).

Results

Maxilla (integument)

The cardo (cd: Fig. 1A–B) is triangular. The submedial maxillary process of the hypostoma (hys: Fig 1A) inserts submedially on the proximal part of the cardo (caf: Fig. 1B). The mediodistal cardinal ridge, laterodistal cardinal ridge and basal cardinal ridge are present (lcr, mcr, bcr: Fig. 1D) and the inner and outer cardinal processes are absent. The cardo lays almost parallel to the external surface of the hypostoma and is largely obscured by it even if the maxillo-labial complex is fully protracted (Figs 1A, cd: 4A). The conjunctiva connecting the cardo to the rest of the maxillo-labial complex is resilin rich along the stipitocardinal hinge (sch: Fig. 1C).

The stipes is triangular in cross section distally. The posterior stipital wall of the stipes bears the posterior stipital sclerite (pss: Figs 1A, C, 2B, C), while the partly sclerotised medial wall and the convex and membranous anterolateral wall (conj: Fig. 1B) bears the galeo-lacinial complex (Fig. 2A, B, D; gal-lac: Fig. 1B, C). The posterior stipital sclerite is triangular in posterior view, and is margined by the principal carina of stipes (pcs: Figs 1A–C, 3A), which is less rigid and melanized than other regions of the sclerite and is the most developed medially and distolaterally. The principal carina of stipes is equipped

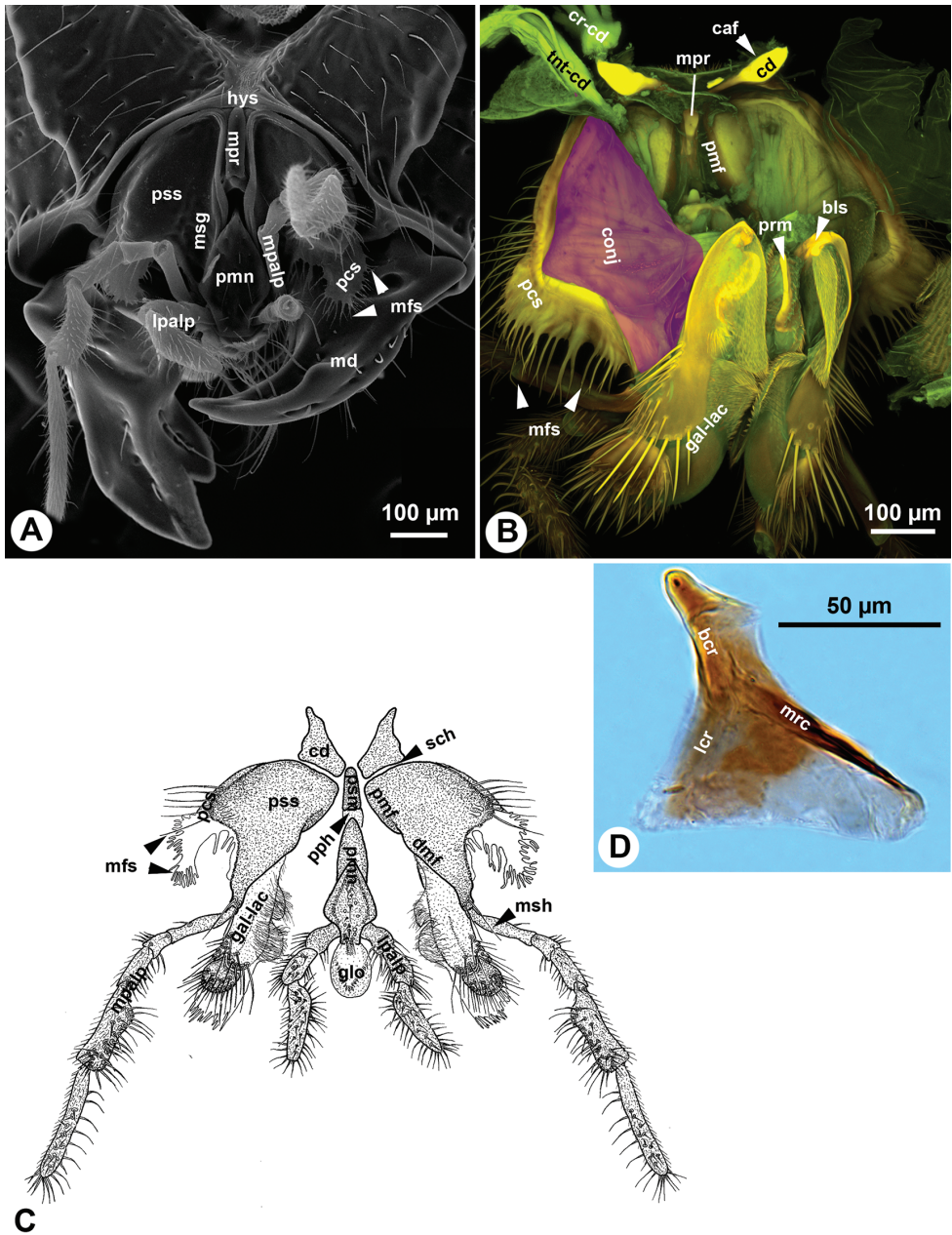


Figure 1. Mouthparts of *Sparasion* sp. **A** SEM micrograph showing the mouthparts, posterior (external) view, distal to the bottom **B** CLSM volume rendered image showing the maxillo-labial complex, anterior (internal) view, distal to the bottom (doi: 10.6084/m9.figshare.861065, doi: 10.6084/m9.figshare.861058) **C** Line drawing showing the maxillo-labial complex, posterior (external), distal to the bottom **D** Bright field image showing the cardo of *Sparasion*, lateral to the left.

distolaterally with the marginal fringe of the stipes (mfs: Figs 1A–C, 2B, C) composed of occasionally branched spines. The extent of the principal carina of the stipes on the distolateral margin is variable in different *Sparasion* species (compare pcs of Fig. 1A with that of Fig. 1B) but it always overlaps the proximomedial surface of the mandible (md: Fig. 1A). The median part of principal carina of the stipes is divided into the proximomedian stipital flange (pmf: Figs 1B, C, 2A) and the distomedial stipital flange (dmf: Figs 1C, 2A, B, C). The proximal part of the distomedial stipital flange posteriorly overlaps the distal part of the proximomedial stipital flange (pmf, dmf: Fig. 1C). The stipes articulates with the postmentum (psm: Figs 1C, 2C) and the distal prementum (pmn: Fig. 1A, C) along the proximomedial stipital flange and with the proximal prementum via the distomedial stipital flange. The medial stipital groove (msg: Figs 1A, 2B) extends medially along the proximomedial stipital flange and distomedial stipital flange and accommodates the first sclerite of the maxillary palp (mpalp: Fig. 1A, C, 3D, E) when it is adpressed against the stipes. The posterior stipital sclerite is glabrous, except a for few, elongate, mechanosensory hairs (msh: Figs 1C, 2B) just proximal of the base of maxillary palp and along the distolateral margin of the stipes abutting the hypostoma. The distal part of the posterior stipital sclerite is equipped with numerous campaniform sensilla (cps: Fig. 2C), which are visible only with transmitted light.

The galeo-lacinal complex has four sclerites and two marginal lobes. The proximal, inverted T-shaped lacinal lever (bls: Fig. 2A, B) and the distal, narrow basal galeal sclerite (bgs: Fig. 2B, D) are situated on the median wall of the stipes and articulate with the posterior stipital sclerite along the distomedial stipital flange. The lacinal bar and lacinal comb are absent. The proximolateral galeal sclerite (pgs: Fig. 2A) is situated in the middle on the lateral wall of stipes and is connected proximally with the lacinal lever and distally with the basal galeal sclerite. The number of mechanosensory hairs in the proximolateral galeal setiferous patch (prs: Fig. 2A) is variable in different *Sparasion* species (Table 1) and overlaps the distolateral galeal sclerite (dgs: Fig. 2A, B, D), which traverses the galeo-lacinal complex and is represented on both its medial and lateral walls (the complex is unilayered at the sclerite). The proximolateral and distolateral galeal sclerites are connected to each other by the lateral galeal crease. The apicomedial galeal plate is absent. The number of setae in the distolateral galeal setiferous patch (dgp: Fig. 2A) is variable in different *Sparasion* species (Table 1). The proximal galeal brush is absent. The single coeloconic sensillum of galea (cfs: Fig. 2B, D) is located distally on the median surface of the distolateral galeal sclerite. The single lacinal lobe (llb: Fig. 2A, B, D) extends anteroproximal whereas the galeal lobe (glb: Fig. 2A, B, D) distal to the proximal galeal sclerites. The lacinal lobe and the proximal part of the galeal lobe are covered with short acanthae (ach: Fig. 2D), which comprise the spiculate patch of the lacinia and the spiculate patch of galea respectively. The galeal comb, galeal lamina and galeal fringe are absent. The velum (vlm: Fig. 2D) is fringed distally in some species (vlm: Fig. 2D). The stipital sclerite is absent from *Sparasion*.

The maxillary palp (1mp: Fig. 2B, D) is connected at the distal apex of the posterior stipital sclerite through the ventral dististipital process (vdp: Fig. 2B) adjacent to the basal galeal sclerite. The maxillary palp is composed of five maxillary sclerites among

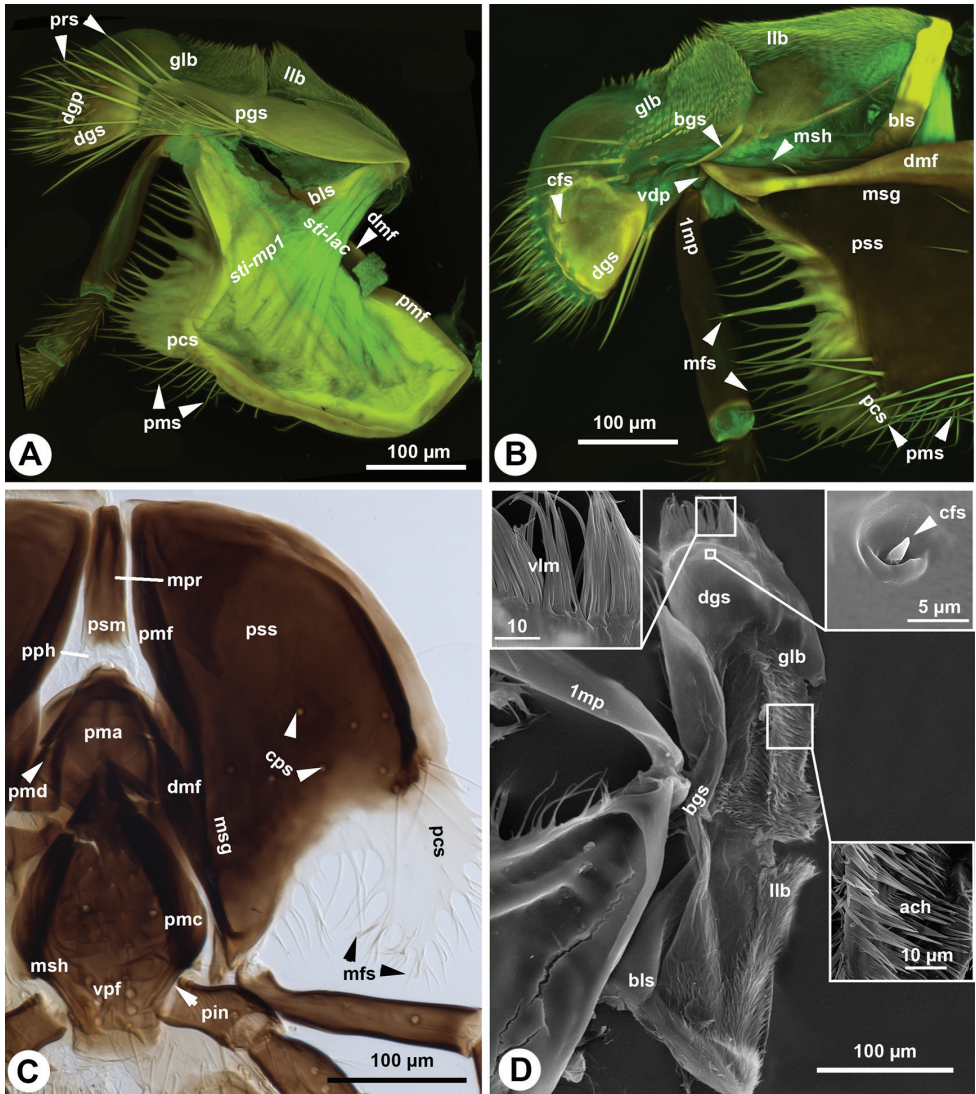


Figure 2. Maxillo-labial complex of *Sparasion*. **A, B** CLSM volume rendered images showing the maxilla: **A**. anterolateral (internal lateral) view (doi: 10.6084/m9.figshare.861060), distal to the left **B** postero-medial (external medial) view (doi: 10.6084/m9.figshare.861057), distal to the left **C** Brightfield image showing the maxillo-labial complex, posterior (external) view, distal to the bottom **D** SEM micrograph showing the maxilla, postero-medial (external-medial) view, distal to the top.

Table I.

Characters	<i>Sparasion</i>								
	sp.1	sp.2	sp.3	sp.4	sp.5	sp.6	sp.7	sp.8	sp.9
The number of setae in the proximal galeal brush	5–7	5–7	5–7	5–7	5–7	5–7	7–10	5–7	6
The number of setae in the distal galeal setiferous patch	18–19	18–20	18–20	11–14	18–20	17	27–34	18–20	22
The number of styloconic sensilla on the glossa	14–15	15–16	10–12	10–12	17	23	18–19	15–16	10

which the second sclerite of the maxillary palp is the shortest, and the fifth sclerite of the maxillary palp is always the longest (5mp: Figs 1A,C, 3D, E). The relative width of the maxillary palpal sclerites varies between *Sparasion* species and in some cases even between different sexes (Table 1). Two different setal types can be differentiated on the maxillary palp, based on their gross morphology. The type 1 seta (ss1: Fig. 3B) is a uniporous sensillum whereas the type 2 seta (ss2: Fig. 3B) is a longer mechanosensory hair. A type 1 seta is present on all but the first sclerite of the maxillary palp, which is glabrous in *Sparasion* sp. 4 and sp. 9 and bears only 1–2 type 2 setae in the rest of the species. Type 1 setae are evenly distributed on the third sclerite of the maxillary palp, on the fourth sclerite of the maxillary palp and on the fifth sclerite of the maxillary palp. Type 1 setae are located in 1–4 whorls of setae on the second sclerite of the maxillary palp. Type 2 setae occur only on the third, fourth sclerite of the maxillary palp and on the fifth sclerite of the maxillary palp. The number of type 2 setae is positively correlated with the width of the third sclerite of the maxillary palp and the fourth sclerite of the maxillary palp: type 2 setae are absent from the third sclerite of the maxillary palp if it is not increased in width relative to the second maxillary palpal sclerite.

Maxilla (skeletal muscles)

The *cranio-cardinal muscle* (*cr-cd*: Figs 1B, 4A, B) arises medially of the posterior site of origins of the tentorium and inserts on the cardo just laterally of the cranial fossa of the cardo (*caf*: Fig. 1B). The *tentorio-cardinal muscle* (*tnt-cd*: Fig. 1B) arises ventrally on the tentorium just laterally of the site of origin of the *tentorio-stipital muscle* (*tnt-sti*: Fig. 4A) and inserts laterally on the stipitocardinal hinge. The tentorio-stipital muscle arises ventrally from the tentorium, medially of the site of origin of the tentorio-cardinal muscle and inserts on the median margin of the posterior stipital sclerite just posterior of the lacinial lever. The *cranio-lacinial muscle* is absent. The *stipito-lacinial muscle* (*sti-lac*: Fig. 2A) arises from along the lateral margin of the posterior stipital sclerite and inserts apically on the lacinial lever. The single *stipito-palpal muscle* (*sti-mp1*: Figs 2A, 3A) and the *stipito-galeal muscle* (*sti-gal*: Fig. 3A) arise medially from the stipito-lacinial muscle, subsequently. The stipito-galeal muscle inserts on the basal galeal sclerite. The *first intrinsic muscle of the maxillary palp*, *third intrinsic muscle of the maxillary palp* and *fourth intrinsic muscle of the maxillary palp* are present, the *second intrinsic muscle of the maxillary palp* was not observed. No muscle was attached to the fifth maxillary sclerite.

Labium, distal hypopharynx (integument)

The postmentum is composed of a single interstipital sclerite that is elongate, rectangular, and is articulated with the posterior stipital sclerites proximolaterally at the proximomedial stipital flange (*psm*, *pmf*: Figs 1B, C, 2C). The median postmental ridge (*mpr*: Figs 1A, B, 2C) is present and the postmental-premental hinge (*pph*: Figs 1C, 2C) is resilin rich.

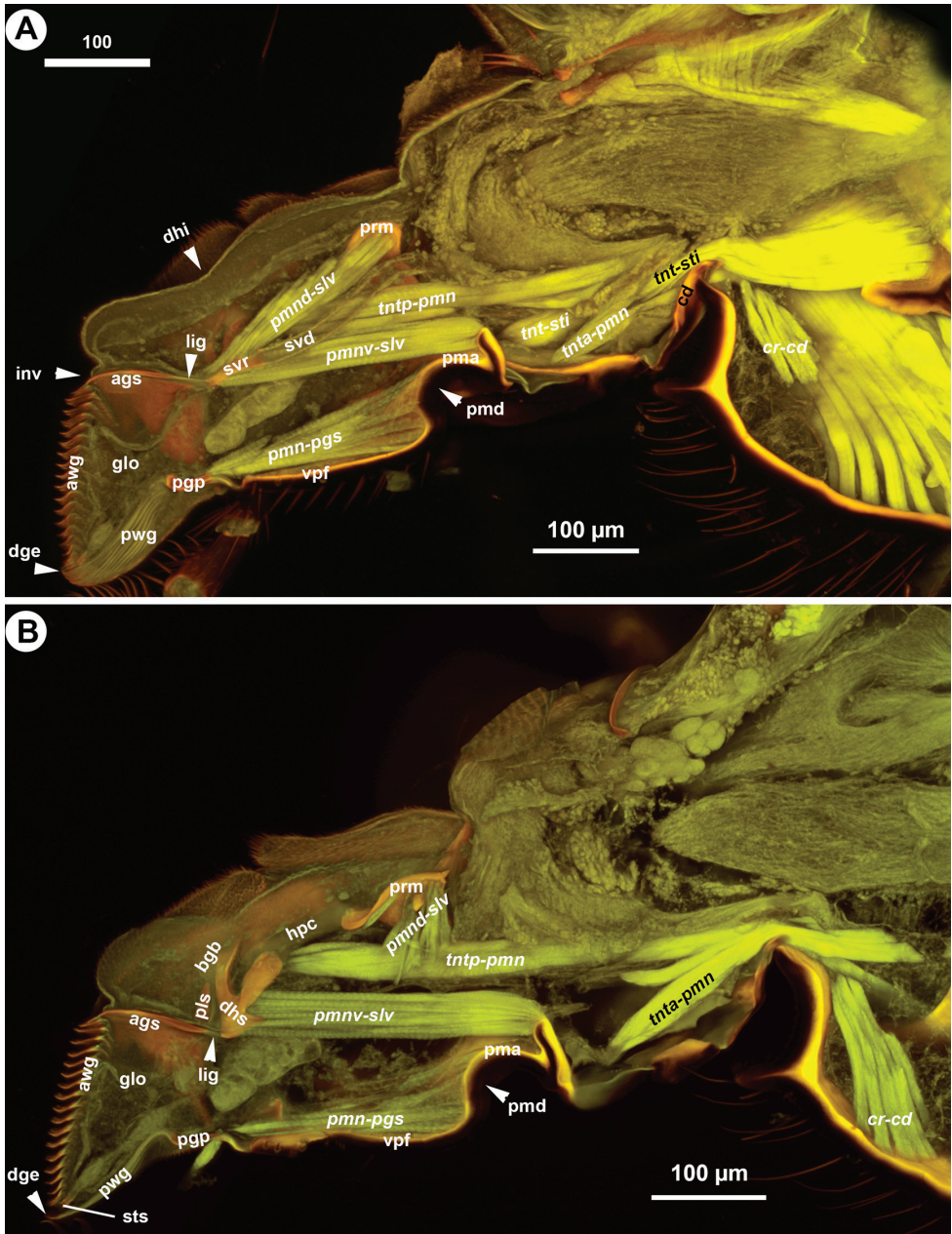


Figure 4. CLSM volume rendered images showing the skeletomuscular system of the labium of *Sparasion*, medial view, distal to the left.

premental carinae (pmc: Fig. 2C and corresponding premental ditches (pmd: Figs 2C, 4A, B, 5C, D, 6A, D) converge proximally and separate the ventral premental face from (vpf: Figs 2C, 3C, 4A, B, 5C, D, 6A, D) the lateral premental face (pma: Figs 2C, 4A, B,

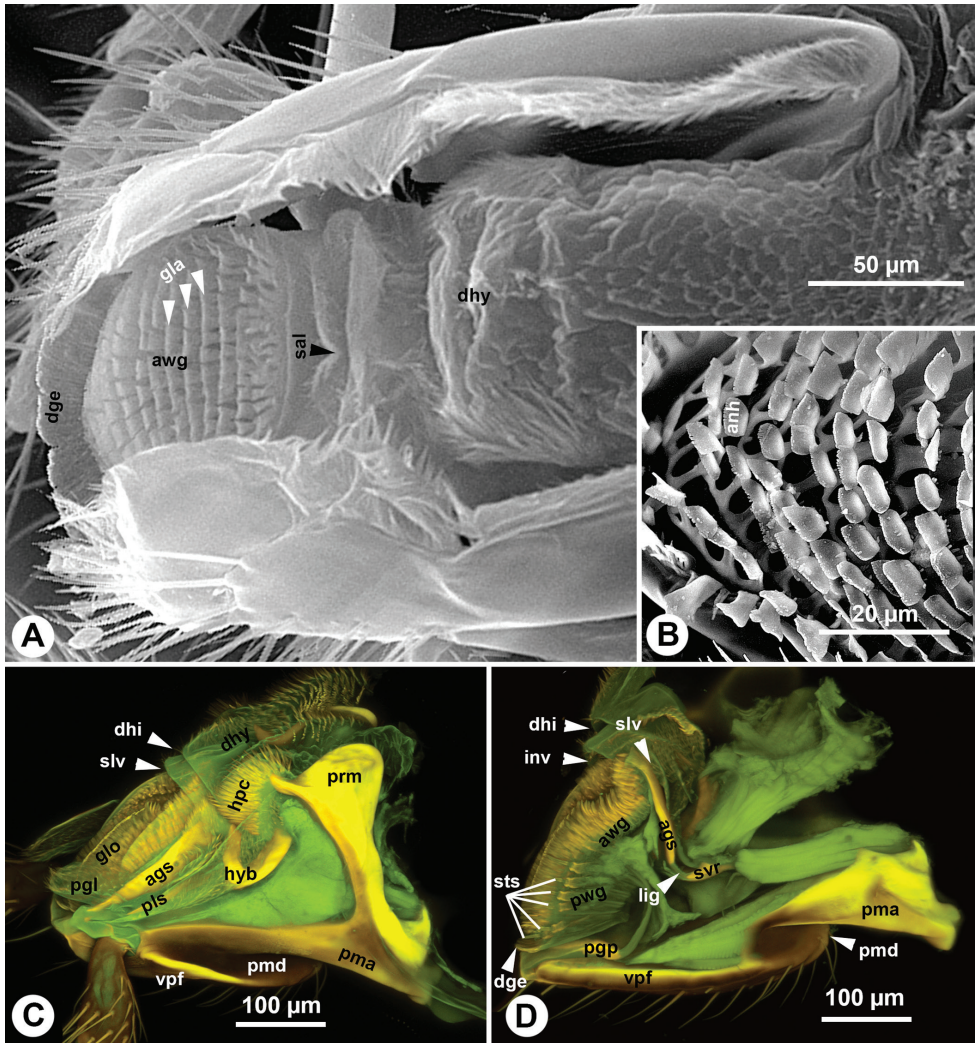


Figure 5. Labium and distal hypopharynx of *Sparasion*. **A** SEM micrograph showing the labium and distal hypopharynx, anterolateral view, distal to the left **B** SEM micrograph showing the glossal annuli, anterior view, distal to the left **C, D** CLSM volume rendered images showing the labium with retracted glossa and paraglossae, distal to the left **C** lateral view (doi: 10.6084/m9.figshare.861064) **D** medial view (doi: 10.6084/m9.figshare.861061).

5C, D, 6A, D). The ventral premental face is flat, diamond-shaped and is equipped with campaniform sensillae of the prementum (cps: Fig. 2C) and distally-oriented mechanosensory hairs (msh: Fig. 2C). The number and pattern of both the campaniform sensilla and mechanosensory hairs and the length of the mechanosensory hairs are variable between different species and sexes (Table 1). The lateral face of the prementum is mostly overlapped ventrally by the distomedial stipital flange (Fig. 1A). The labial palpal excision

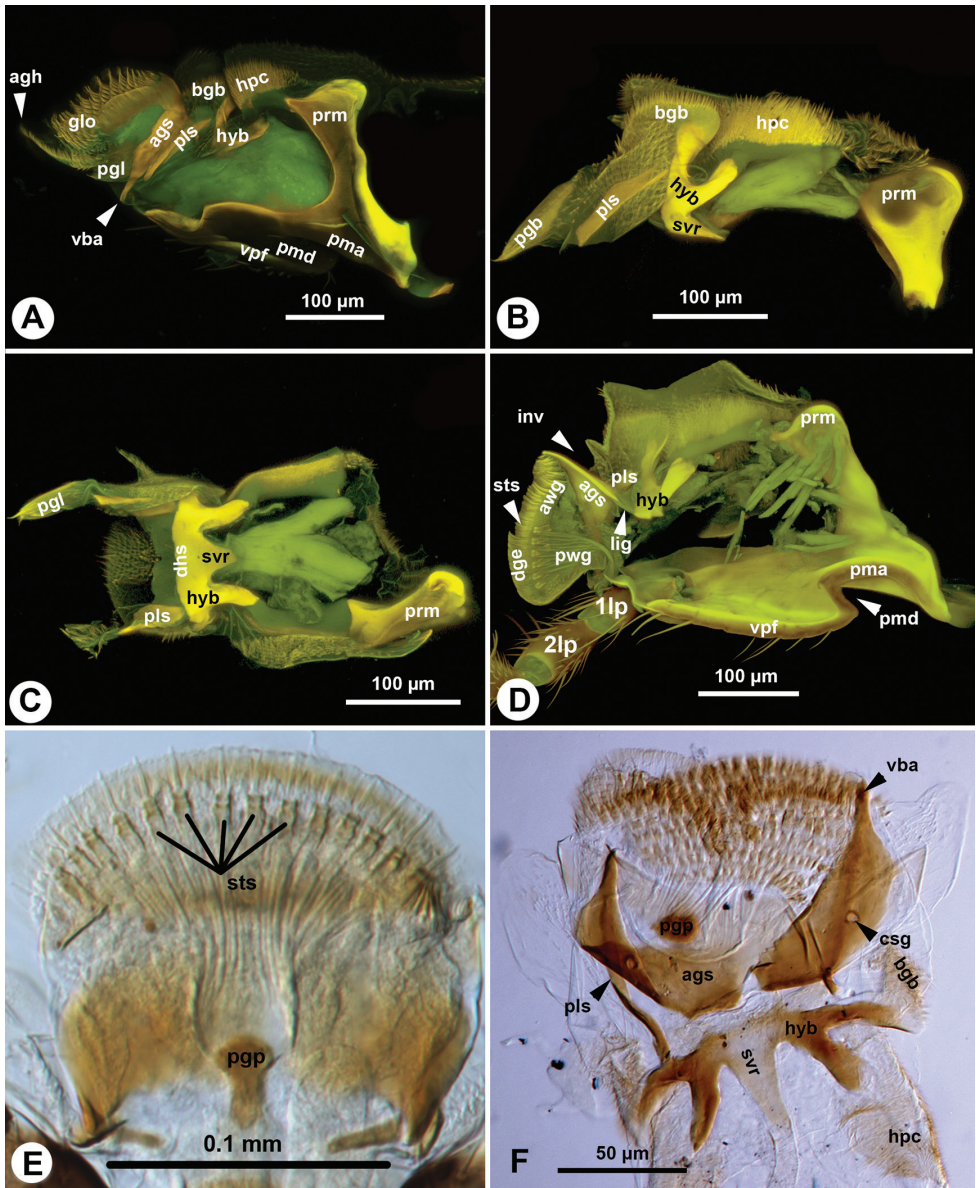


Figure 6. Labium of *Sparasion*. **A** CLSM volume rendered images showing the labium with protracted glossa and paraglossae, lateral view, distal to the left (doi: 10.6084/m9.figshare.861063) **B** CLSM volume rendered images showing the labium, glossa removed, lateral view, distal to the left (doi: 10.6084/m9.figshare.861062, doi: 10.6084/m9.figshare.861066) **C** CLSM volume rendered images showing the labium, glossa removed, posterior view, distal to the left (doi: 10.6084/m9.figshare.861056, doi: 10.6084/m9.figshare.861067) **D** CLSM volume rendered images showing the labium with protracted glossa and paraglossae, medial view, distal to the left (doi: 10.6084/m9.figshare.861059) **E, F** Bright field images showing the labium, posterior view, distal to the top.

(pin: Figs 2C, 3C) accommodating the base of the labial palp is distinct on the distolateral corner of the prementum. The labial palp is composed of three sclerites that are equipped with both the uniporous sensilla (type 1) and mechanosensory hairs (type 2).

The glossa (glo: Figs 1C, 3C, 4A, B, 5C, 6A) is separated anteroproximally from the paraglossae (pgl: Figs 5C, 6A, C) and the distal hypopharynx by the basal glossal invagination (inv: Figs 4A, 5D, 6D) adjacent to the salivarium (svr: 6B, C, F). The anterior glossal sclerites (ags: Figs 3C, 4A, B, 5C, 6A, D) are embedded into the distal wall of the invagination and are connected medially to the ventral wall of the salivarium via a ligament (lig: Figs 4A, B, 5D, 6D). The ventrolateral basiglossal arms are distinct (vba: Fig. 6A, F) and each anterior glossal sclerite is equipped with a single campaniform sensillum of the glossa (csg: Fig. 6F). The posterior glossal plate is composed of a single, median sclerite (pgp: Figs 4A, B, 5D, 6E, F). The flat posterior surface of the glossa (pwg: Figs 3C, 4A, B, 5D, 6D) is glabrous with distinct ventral glossal lines. The distal glossal edge (dge: Figs 3C, 4A, B, 5A, D, 6D) is thicker than the proximal region of the posterior surface of the glossa. The apical glossal hairs are usually present (agh: Fig. 6A). The apical glossal setae (sts: Figs 5D, 6D, E) are styloconic sensilla with variable number in different species (Table 1).

The arched anterior surface of the glossa (awg: Figs 4A, B, 5A, D, 6D) is evenly covered with glossal annuli (gla: Fig. 5A), which are composed of transverse rows of spatulate and anteriorly curving annular hairs, each with a dentate distal margin (anh: Fig. 5B).

The bilobed paraglossae arise proximolaterally of the basal glossal invagination and encircle the proximal part of the glossa. The elongate, triangular basiparaglossal sclerite (pls: Figs 3C, 5C, 6A–D, F) corresponds to a posterior lobe of the paraglossa whereas the larger anterior lobe of the paraglossa bears the distal, less sclerotised paraglossal acroglossal button (pgb: Fig. 6B). Proximally the paraglossa is continuous with the wall of the distal hypopharynx (dhy: Fig. 5A, C) and the paraglossal sclerite is connected to the distal hypopharyngeal sclerite via an elongate ligament. The basiparaglossal brush (bgb: Figs 4B, 6A, B, F) is distinct but the paraglossal sclerite and paraglossal annuli are absent.

The distal hypopharynx is supported laterally by the premental arms and the hypopharyngeal rod (hypr: Fig. 3C), which is continuous with the distal hypopharyngeal sclerite via the hypopharyngeal button (hyb: Figs 3C, 5C, 6A–D). The hypopharyngeal pecten (hpc: Figs 4B, 5C, 6A, B) is distinct and abuts the basiparaglossal brush when the ligula is retracted (hpc: Figs 5C). The hypopharyngeal buttons are connected to each other medially through the ventral wall of the salivarium, that is either sclerotised (svr: Figs 3C, 6B; salivarial sclerite) or is a resilin rich conjunctiva (svr: Fig. 6F). In the former case the hypopharyngeal buttons and the ventral, sclerotised wall of the salivarium compose the distal hypopharyngeal sclerite (dhs: Figs 4B, 6C) encompassing ventrally the salivary duct (svd: Figs 3C, 4A). The distal hypopharyngeal invagination (dhi: Figs 4A, 5C, D) corresponds to the dorsal bend on the hypopharyngeal button.

Labium, distal hypopharynx (skeletal muscles)

The *postmento-premental muscle* is absent. The *posterior tentorio-premental muscle* (*tntp-pmn*: Fig. 4A, B) arises from the tentorium anterolaterally from the site of origin of the *anterior tentorio-premental muscle* (*tnta-pmn*: Fig. 4A, B) and inserts on the proximal part of the hypopharyngeal button. The *anterior tentorio-premental muscle* arises from the tentorium medially of the site of origin of the posterior *tentorio-premental muscle* and inserts proximomedially on the postmental-premental hinge. The *premento-paraglossal muscle* (*pmn-pgs*: Fig. 4A, B) arises medially from the internal edge corresponding to the premental ditch and from the intima of the median premental face anterior to the edge and inserts on the posterior glossal plate. The *dorsal premento-salivarial muscle* (*pmnd-slv*: Fig. 4A, B) arises distomedially from the premental arm and inserts dorsally on the salivarium. The *ventral premento-salivary sclerite muscle* (*pmnv-slv*: Figs 4A, B) arises from the proximal premental area and inserts proximomedially on the distal hypopharyngeal sclerite. The *premento-palpal muscle* arises anterolaterally from the site of origin of the premento-paraglossal muscle. The *first intrinsic muscle of the labial palp* and the *second intrinsic muscle of the labial palp* are present. The premento-glossal muscle is apparently absent.

Discussion

The maxillo-labial complex of *Sparasion*

The term maxillo-labial complex (MLC) is used by Snodgrass (1935). However, many entomologists prefer to use the term labio-maxillary complex, e.g. Duncan (1939), Labandeira (1997), Jervis (1998), Vilhelmsen (1996), Krenn (2007). The reason for using the latter seems to be that it is more easily pronounced (Duncan 1939). In this paper the term maxillo-labial complex is preferred because it corresponds with the anatomical position of the component pieces.

The hymenopteran labium, unlike that of other holometabolans, is so tightly connected to the maxillae by the labiomaxillary hinge that they protract and retract together as a single unit (Duncan 1939, Snodgrass 1942, Vilhelmsen 1996, Krenn 2007). While the labiomaxillary hinge connects their proximal parts, the distal, more sclerotised regions of the maxillae and the labium still are able to move with some freedom in basal Hymenoptera (Vilhelmsen 1996, Beutel and Vilhelmsen 2007) and in a few apocritan taxa (e.g. in *Gasteruption*, *Evania* (Evanoidea) (Fig. 8) and *Gryon* (Platygastridae) Mikó, pers. obs.). However, in *Sparasion* and some other apocritan taxa (*Ibalia* (Cynipoidea) Ronquist & Nordlander, 1989, *Vespula* (Vespoidea) Duncan, 1939) where the posterior wall of the labium and maxilla are almost exclusively sclerotised, the freedom of the independent movement between the appendages is restricted: they can not be separated from each other and sometimes – e.g. in *Sparasion*

— not even from the hypostoma. The development of rigid connections between sclerites that are flexibly connected in basal Hymenoptera seems to be an apocritan evolutionary trend, which is arguably related to their more sclerotised body (Vilhelmsen 2000a, 2000b, Vilhelmsen et al. 2010).

Although the MLC of *Sparasion* is reduced in size and highly sclerotized, we were able to homologize most of its anatomical structures to those of other Hymenoptera (Appendix 2, Figs 7–9). We hypothesize that the platygastroid MLC is an anatomical system with enough phenotypic diversity to serve as a source of morphological characters for phylogenetic analyses and species diagnosis.

Maxilla

One consequence of the more heavily sclerotised and less moveable MLC is that the cardo remains relatively simple in *Sparasion*, retaining its main function: providing rigid attachment of the MLC to the cranium. The inner and outer processes of the cardo (Winston 1979) that articulate with the stipes are missing from *Sparasion*, similarly to other Proctotrupomorpha (e.g., *Ibalia* and *Pelecinus* pers. obs.). Because the stipito-cardinal articulation is absent, the cardo seemingly interacts with the posterior stipital sclerite only by the resilin rich stipito-cardinal hinge. Similarly to *Sparasion*, the cardo is not visible externally in these taxa and even if the MLC is in a protracted position, the cardo is obscured by the proximal portion of the principal carina of the stipes.

Different levels of sclerotization can be observed on the intercardinal and interstipital areas in different hymenopteran taxa. Only the intercardinal area contains a sclerite in basal Hymenoptera (Ross 1937), while both intercardinal or interstipital sclerites may be present in Apocrita. The intercardinal and interstipital areas are separated from each other by the labial suture (Snodgrass 1935, Prentice 1998). The median area of the MLC posterior to the suture contains an anterior and a posterior sclerite in some holometabolans (i.e. Coleoptera), the submentum and the mentum. This condition never occurs in Hymenoptera (see references listed in materials and methods section). Even in those Aculeata where two medial sclerites are in the postmental area, one is always anterior to the labial suture. Based on their position relative to the stipites and cardines, the intercardinal postmentum of basal Hymenoptera might be homologous with the postmentum in other insects and the interstipital postmentum of Apocrita is most likely not homologous to these structures. The postmental area is fully membranous in many Apocrita (*Evania*, psm: Fig. 8; *Vespula*, Duncan 1939; *Stenobracon*, Alam 1951). Only the intercardinal sclerite is present in *Ibalia* (Ronquist and Nordlander 1989) leading Ritchie and Peters (1981) to homologize this structure with the mentum of other holometabolans.

Only the interstipital postmentum (Prentice 1998) is present in *Sparasion*. This sclerite is not connected with muscles, nor is it articulated with any other sclerites. Its only function might be to separate the posterior stipital sclerites from each other.

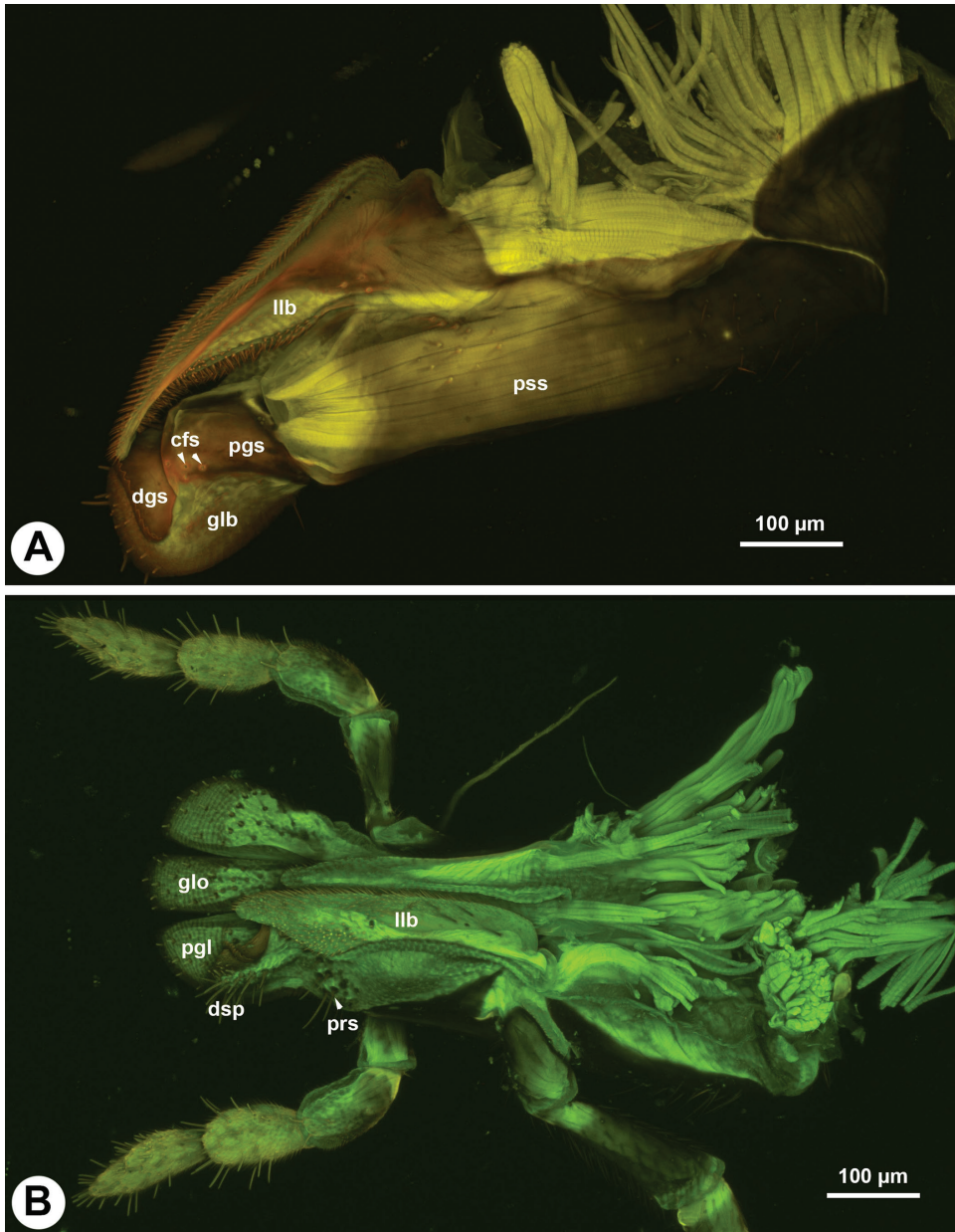


Figure 7. CLSM volume rendered images showing the MLC of *Athalia rosae*. **A** maxilla, medial view, doi: 10.6084/m9.figshare.956279 **B** MLC, anterior view, distal to the left, doi: 10.6084/m9.figshare.956279

The development of the principal carina arguably correlates with the presence of rigid connection between the stipes and neighboring sclerites. In those taxa, where the stipes articulates with the hypostoma, but not with the labium, the principal carina is present only laterally (*Evania*, pcs: Fig. 8).

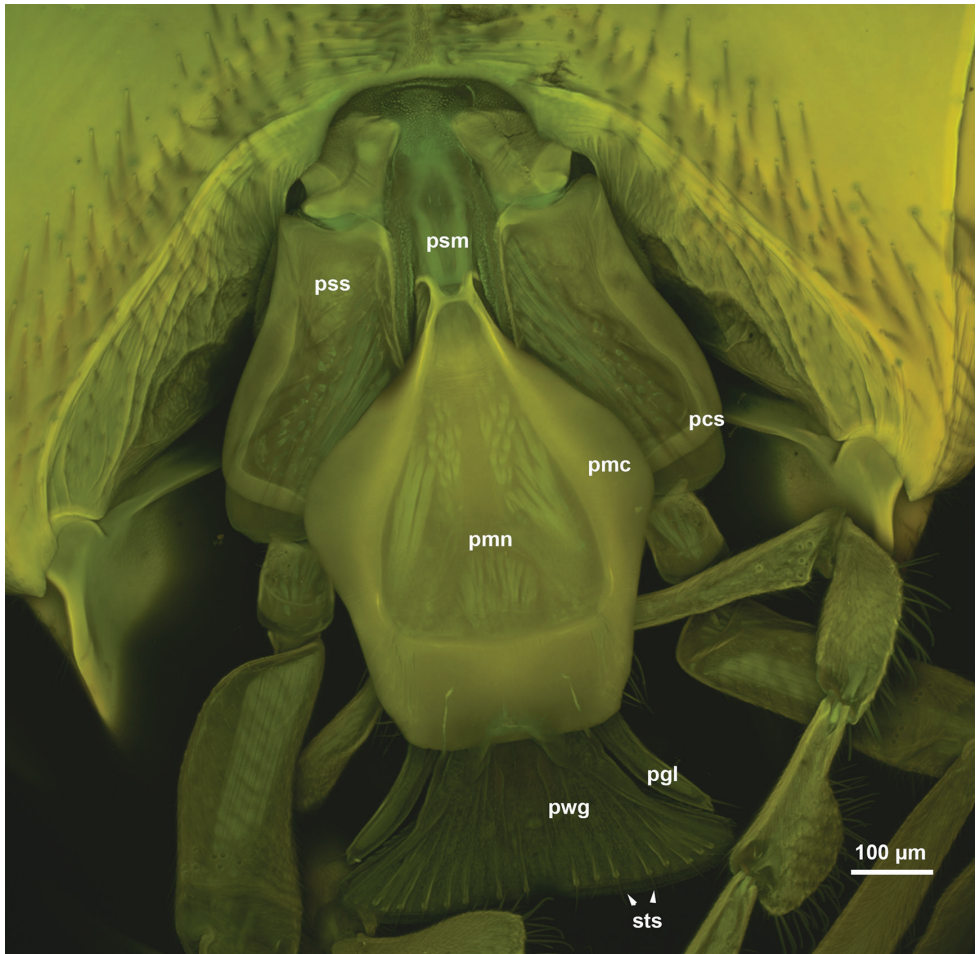


Figure 8. CLSM volume rendered image showing the mouthparts of *Evania* sp, posterior view, distal to the bottom, doi: 10.6084/m9.figshare.956280

Both the medial and lateral portions of the carina are well developed in *Sparasion*, having two unique characteristics that were not found in other Hymenoptera (see references listed in the materials and methods section):

1. The median portion of the carina is divided into two sections that overlap each other and accommodate the proximal and distal part of the lateral premental margin.
2. The presence of an “apical fringe”, a branched flattened evagination along the distolateral margin of the carina. While the first specialization might be the consequence of the articulation between the posterior stipital sclerite and the prementum, the second is most probably related to the unique movement of the mandible in *Sparasion*. While pivotal axis of the mandible is anteroposterior in most Hymenoptera taxa (dorsoventral in a prognathous head) it is directed medi-



Figure 9. CLSM volume rendered image showing the maxilla of *Orthogonalyx pulchella*, posteromedial view, distal to the top-left, doi: 10.6084/m9.figshare.956281

olaterally in *Sparasion* and the mandibles are moved parallel to the body axis (Mikó et al. 2007). Due to this unique, oblique position of the mandible, the distolateral, fringed margin of the principal carina is positioned inside the internal concavity of the mandible and seemingly acts as a cleaning “brush”. Similar movement of the mandible has been reported from many other Hymenoptera taxa, including

two platygastroid genera, *Tyrannoscelio* and *Encyrtocelio*. It would be worthwhile to study the MLC of these taxa and to clarify whether the fringed lateral portion of the principal carina is unique for *Sparasion* or whether it can be found in other genera with modified mandible movement.

The presence of the campaniform sensillum of the stipes was considered as one of the synapomorphies of the clade composed of Platygastridae and Cynipoidea (Sharkey et al. 2012). Although the sensillum is present in *Sparasion* and some other platygastroid taxa (Sharkey et al. 2012), it is absent from *Triteleia*, *Calliscelio*, *Macroteleia*, *Apepus*, *Duta*, *Psilanteris*, *Anteris* (Popovici and Fusu 2006), which implies that this character might be useful for generic classification in Platygastridae.

Prentice (1998) reported the presence of two apical sclerites on the galea, the apicolateral and apicomedial stipital plates. We were able to locate only one apical sclerite, the distolateral galeal sclerite on the galeo-lacinial complex of *Sparasion*. This sclerite traverses the complex and bears both the distolateral galeal setiferous patch and the medial coelomic sensillum that define the apicolateral and apicomedial stipital plates respectively.

Appendage segments and annuli are ring-like and repetitive sclerites of the legs, antenna, labial palps and maxillary palps. While appendage segments have muscles attaching to them, annuli do not. Annuli are traditionally differentiated from appendage segments by names with the suffix “-mere” e.g. flagellomere and tarsomere. Among the five maxillary palpal sclerites of *Sparasion* the fifth one does not have muscle attachments. We observed a similar condition in *Orthogonalys* (Trigonaliidae), where the fifth and sixth sclerites lack any muscle attachment (Fig. 9). If we apply the annuli vs. segment terminology system to these taxa, we should call the first four sclerites “palpal segments” and fifth sclerite in *Sparasion* and the fifth and sixth sclerites in *Orthogonalys* “palpomeres”. To avoid misinterpretations of the segment identity of the palpi, and keeping a simple and easily applicable terminology we prefer to use palpal sclerites for the ring-like sclerites of the palpi.

Sparasion has five maxillary palpal sclerites that is the highest in Platygastridae (Masner 1976). Since the presence of five maxillary palpal sclerites is a possible synapomorphy for Proctotrupomorpha (Sharkey et al. 2012), and is also shared by other, putatively basal lineages of Platygastridae (i.e. *Archaeoteleia*, *Nixonia* and *Plaumannion*, Johnson et al. 2008) it is most probable that this condition is plesiomorphic for Platygastridae.

The maxillary palp is located medially on the lateral margin of the posterior stipital sclerite in basal Hymenoptera distantly from the apical end of the sclerite bearing the base of the galea (Fig. 7B., Vilhelmsen 1996, Beutel and Vilhelmsen 2007). In *Sparasion* the palp is connected to the apical vertex of the posterior stipital sclerite, adjacent to the base of the galeo-lacinial complex. This distal position makes it difficult to interpret the presence of minute anatomical structures such as the palpifer (“flexible and transparent, very difficult to detect structure” at the base of the maxillary palp, Prentice 1989).

The 2nd, 3rd and 4th maxillary palpal sclerites are distinctly wider than the more proximal or distal maxillary palpal sclerites in some *Sparasion* species (Figures 3D, E).

The number and position of these modified sclerites are sexually dimorphic in some *Sparasion* species and are seemingly useful for species groups definitions. A widened 4th palpal sclerite was found in most species of the plesiomorphic platygastrid genus *Nixonia*, and representatives of *Plaumannion*, *Archaeoteleia*, *Sceliomorpha* and *Neuroscelio* (Johnson and Masner 2006, Johnson et al. 2008); the presence of enlarged 3rd maxillary palpal sclerites have been reported from *Sparasion* (Johnson et al. 2008) and enlarged 2nd and 3rd sclerites from the putatively most primitive extant platygastrid genus, *Huddlestonium* (Masner et al. 2007).

Although the position of enlarged palpal sclerites in the maxillary palp has often been used for the classification of different Hymenoptera taxa (i.e. Evaniidae, Deans and Huben 2003; Aculeata, Bohart and Menke 1976), our knowledge about their possible function is rather incomplete. Albeit our study confirms Prentice's (1998) observation that enlarged sclerite size corresponds to larger muscle mass, the role of this modification in the mechanics of palpal movement is still unrevealed.

Although the presence of only two stipito-palpal muscles is considered as the Hymenoptera groundplan (stia-mp1, stip-mp1: Fig. 9; Beutel and Vilhelmsen 2007), similarly to *Sparasion*, only one maxillary palpal muscle has been reported from many Hymenoptera taxa (Snodgrass 1942, Matsuda 1957, Prentice 1998). The presence of resilin-rich conjunctiva at the base of the maxillary palpus in *Sparasion* supports Prentice's hypothesis that the expansion of the maxillary palpus is facilitated by a resilin rich region between the posterior stipital sclerite and the palpus in taxa with a single stipito-palpal muscle.

The terms, galea and lacinia refer usually to the evaginated distal, sclerotised regions of the maxillar cuticle that are adjacent to the sites of insertions for the stipito-lacinal, cranio-lacinal and the stipito-galeal muscles in insects. Although these muscles are present in most hymenopterans (sti-gal, sti-lac: Fig. 7A, and more proximal and more distal lobes can almost always be differentiated, the proximal limits of the galea and lacinia are difficult to define and thus these structures are difficult to homologize to that of other insects where the galea and lacinia are well sclerotised. Therefore we preferred to use galeal lobe and lacinal lobe instead of galea and lacinia in the present paper.

Two distinct setiferous areas can be defined on the lateral area of the galeal lobe in *Athalia*: a proximal row of setae traversing the galea (prs: Fig. 7B) and a more distal setiferous patch (dsp: Fig. 7B). The presence of these two setiferous areas seems to be consistent within Hymenoptera (Prentice 1998) and can be used for the delimitation of areas of the galeo-lacinal complex.

In *Sparasion*, similarly to some other, more derived Hymenoptera taxa these setiferous areas correspond to two sclerites, the proximolateral and distolateral sclerites of the galea (Prentice 1998, Ronquist and Nordlander 1989). Two distal sclerites are located on the medial wall of the galeo-lacinal complex in *Athalia* (pgs, dgs: Fig. 7A), with some campaniform sensillae (cfs: Fig. 7A). Based on the presence of the sensilla on the medial wall of the distal galeal sclerite of *Sparasion* it is possible that the distal galeal sclerite, or at least its medial part (the sclerite traverses the galeo-lacinal complex) is homologous with one of the apical galeal sclerites of *Athalia*.

Although the velum is well developed in numerous other Hymenoptera (Prentice 1998), we are not aware of any case in the order where the lobe is fringed apically as it was found in some *Sparasion* species (vlm: Fig. 2D).

The galeal comb and the galeal lamina are important characters that have been used in aculeate systematics (Prentice 1998, “comb of galea” in Michener 1944, “Borstenkamm” in Ulrich 1924). Although neither of these structures are present in *Sparasion*, they are present in some other scelionines (*Encyrtoscelio*, *Teleas*, *Trimorus* Popovici pers. obs.).

Labium

The prementum is articulated with the stipes via the premento-stipital articulation that is composed of the premental ditch, premental carinae, and the principal carina of the stipes. Duncan (1939) reported a similar connection between the stipes and the prementum and considered its importance in the simultaneous movement of these two structures. Although we are unaware of other hymenopterans with a complete premento-stipital articulation, the premental carinae are present in some Evaniidae (pmc: Fig. 8) and in some platygastroid genera (illustrations in Popovici and Fusu 2006).

Vilhelmsen (1996) proposed the presence of acanthae on the hypopharyngeal rod as a possible synapomorphy for Apocrita. In *Sparasion* and in some other apocritans (e.g. *Vespula*, Duncan 1939; in Apoidea, =spiculate patch of the hypopharynx in Prentice 1989, *Evania* pers. obs.) two regions of the hypopharyngeal rod, the hypopharyngeal pecten (hpc: Fig. 10) and the basiparaglossal brush (bgb: Fig. 10) are extensively covered with acanthae. Contraction of the posterior tentorio-premental muscle might protract, whereas contraction of the ventral premento-salivarial muscle retract the hypopharyngeal buttons. The distal hypopharyngeal invagination, which is apparently unique for Platygastroidea, is defined by the hypopharyngeal button. Protraction and retraction of the button, therefore, might actually control the orientation of the invagination. We were not able to locate an infrabuccal pouch (Fig. 10) in *Sparasion* between the transverse line connecting the tips of the lateral arms of the prementum and the sitophore in basal Hymenoptera (Vilhelmsen 1996).

The maximum number of labial palpal sclerites in Apocrita is four (some Formicidae (Gotwald, 1969), Braconidae (Belokobylskij, 2006), Vespinae (Duncan, 1939)). In *Sparasion*, the labial palp is composed of three sclerites that are moved directly by muscles. In those Hymenoptera where the labial palp is composed of four sclerites (Vilhelmsen and Beutel 2007, Gotwald 1969, Belokobylskij and Chen 2006, Duncan 1939) the apical sclerite has no muscles and is considered to be a secondary subdivision of the apical segment. The presence of four labial palp sclerites is considered a hymenopteran synapomorphy (Vilhelmsen and Beutel 2007) and the ground plan of almost all other apocritan superfamilies (Sharkey et al. 2012). The ground plan of a three-segmented labial palp of Platygastroidea is probably the result of the secondary loss of the apical palpal sclerite.

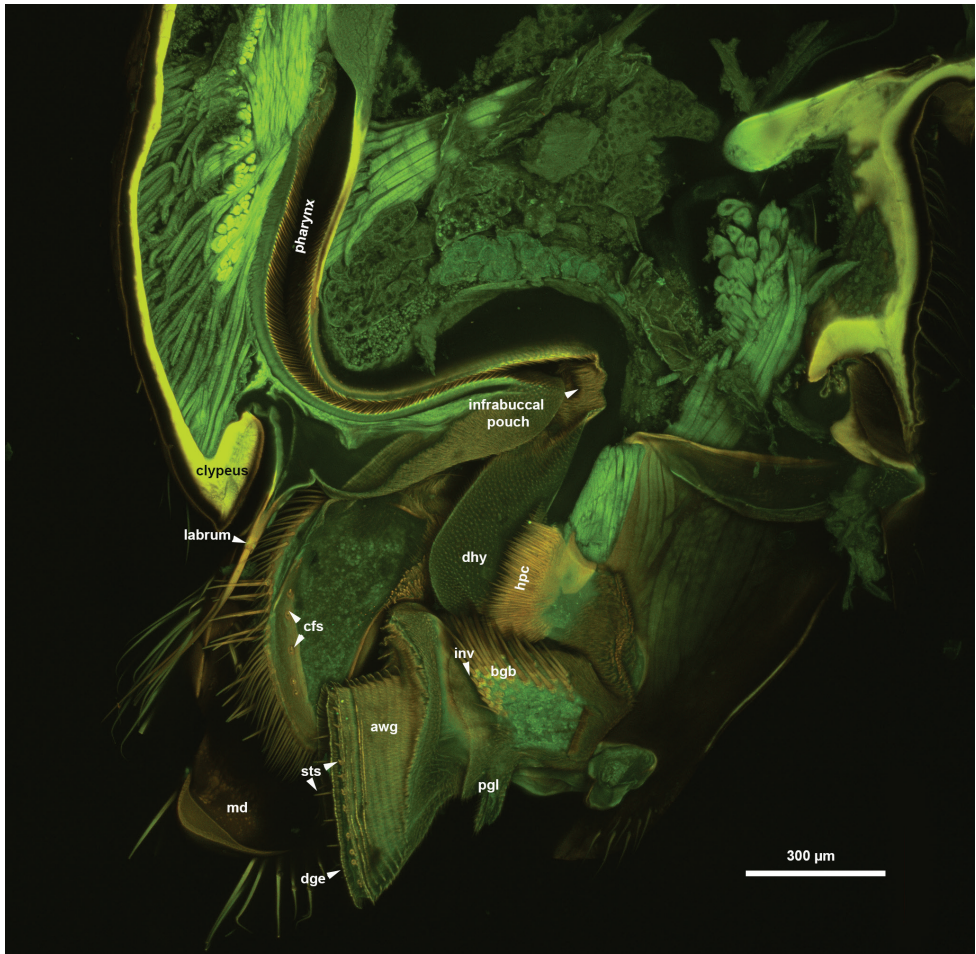


Figure 10. CLSM volume rendered image showing the ventral region of the head of *Evania* sp., medial view, distal to the bottom, doi: 10.6084/m9.figshare.956282

Duncan (1939) hypothesized that the glossal annuli have rasping function or are involved in retaining liquids in Vespinae. Glossal annuli with elongated and well developed spatulate annular hairs are present in most Apocrita (Duncan 1939, Prentice 1998, Ronquist and Nordlander 1989, Dangerfield et al. 2001, Popovici and Fusu 2006) while are present only in a few basal Hymenoptera taxa (Cephoidea, Megalodontoidea and Orussoidea, Vilhelmsen 1996).

Along the proximal margin of distal edge of glossa in *Sparasion*, a row of 9–23 apical glossal setae can be observed. These setae are styloconic sensilla, which are considered to be bimodal contact chemo-mechanosensillae (Shields 2010). Although they have never been mentioned elsewhere, these styloconic setae are present in other Hymenoptera (*Evania*, sts: Figs 8, 10, *Gasteruption*, *Ibalia*, Mikó pers. obs.) and might play crucial role in the chemo- and mechanosensation in Apocrita.

The ventral glossal lines have been reported only from a few Hymenoptera (Salman 1929, Prentice 1998, *Evania*, Fig. 8). The lines radiate from the posterior glossal plate and extend toward the apical glossal hairs and therefore might be related to the presence of these styloconic sensilla. We have found the lines present in taxa which apical styloconic sensilla.

Acknowledgements

We wish to thank Mariana Popovici and Gordon Ramel for gift specimens, Irina Gostin and Răileanu for the SEM pictures, Eva Johannes (NCSU-NSCORT, Department of Plant Biology) for her assistance in Confocal Laser Scanning Microscopy, Lubomír Masner, Lucian Fusu, Mircea Mitroiu, and Lars Vilhelmsen for their valuable comments, and Norman F. Johnson and Luciana Musetti for maintaining the sites “The genera of Platygastroidea (Hymenoptera) of the World” and “Hymenoptera On-line Database”. The material is based on work supported, in part, by a grant of the Romanian National Authority for Scientific Research, CNCS-UEFISCDI, project number PN-II-RU-TE-2012-0057 to O. Popovici. This research is also based on work supported by the National Science Foundation (grant numbers DBI-0850223, DEB-0842289, DEB-0956049, and EF-0905606); and the National Evolutionary Synthesis Center and benefited from discussions initiated through the Phenotype Research Coordination Network. Any opinions, findings, and conclusions or recommendations expressed in this material are those of the authors and do not necessarily reflect the views of the National Science Foundation.

References

- Alam SM (1951) The skeleto-muscular mechanism of *Stenobracon deesae* Cameron (Braconidae, Hymenoptera) - An ectoparasite of sugarcane and juar borers of India Part I Head and thorax. Aligarh Muslim University Publications (Zoological Series) on Indian Insect Types 3: 1–174.
- Austin AD (1983) Morphology and mechanics of the ovipositor system of *Ceratobaeus* Ashmead (Hymenoptera: Scelionidae) and related genera. International Journal of Insect Morphology Embryology 12: 139–155. doi: 10.1016/j.bbr.2011.03.031
- Austin AD, Field SA (1997) The ovipositor system of scelionid and platygastroid wasps (Hymenoptera: Platygastroidea): comparative morphology and phylogenetic implications. Invertebrate Taxonomy 11: 1–87. doi: 10.1071/IT95048
- Belokobylskij AJ, Chen X (2006) *Hecabolomorpha* n. gen., a new Asian genus from the tribe Hecabolini (Hymenoptera: Braconidae: Doryctinae). Annales de la Société Entomologique de France (n.s.), 42(1): 107–111.
- Beutel GB, Vilhelmsen L (2007) Head anatomy of Xyelidae (Hexapoda: Hymenoptera) and phylogenetic implications. Organisms Diversity & Evolution 7: 207–230. doi: 10.1016/j.ode.2006.06.003

- Bohart RM and Menke AS (1976) Sphecid Wasps of the World A Generic Revision. University of California Press, Berkeley, 696 pp.
- Brown BV (1993) A further chemical alternative to critical-point-drying for preparing small (or large) flies. *Fly Times* 11: 10.
- Bugnion E (1924) Le sac infrabuccal et le pharynx des fourmis. *Comptes rendus des séances de la Société de biologie* 91: 998–1000.
- Bugnion E (1925) Notes relatives a la terminologie des organes buccaux des insectes. *Bulletin de la Société zoologique de France* 50: 352–358.
- Clausen CP (1976) Phoresy among entomophagous insects. *Annual Review of Entomology* 21: 343–368. doi: 10.1146/annurev.en.21.010176.002015
- Cockerell T (1924) Notes on the structure of Bees. *Proceedings of the Entomological Society of Washington* 26: 77–85.
- Crampton GC (1923) A phylogenetic comparison of the maxillae throughout the orders of insects. *Journal of the New York Entomological Society* 31: 77–107.
- Crosskey RW (1951) The morphology, taxonomy, and biology of the British Evaniidae (Hymenoptera). *Transactions of the Royal Entomological Society of London* 102: 247–301. doi: 10.1111/j.1365-2311.1951.tb00749.x
- Deans AR, Huben M (2003) Descriptions of three new ensign wasp genera (Hymenoptera: Evaniidae), *Decevania*, *Rothevania*, and *Vernevania*, with a key and diagnoses for the genera of the world. *Proceedings of the Entomological Society of Washington* 105 (4): 859–875.
- Dangerfield P, Austin A, Baker G (2001) Biology, ecology and systematics of Australian *Scelio*, wasp parasitoids of locust and grasshopper eggs. CSIRO, Collingwood, Victoria, 254 pp.
- Dhillon SS (1966) Morphology and biology of *Athalia proxima*. Aligarh Muslim University Publications (Zoological Series) on Indian Insect Types 7: 1–170.
- Duncan CD (1939) A Contribution to the biology of North American Vespine wasps. Stanford University Publications University Series Biological Science 8: 1–272.
- Eickwort GC (1969) A comparative morphological study and generic revision of the augochlorine bees (Hymenoptera: Halictidae). *University of Kansas Science Bulletin Vol. 48*: 325–524.
- Field SA, Austin AD (1994) Anatomy and mechanics of the telescopic ovipositor system of *Scelio* Latreille (Hymenoptera: Scelionidae) and related genera. *International Journal of Insect Morphology and Embryology* 23: 135–58. doi: 10.1016/0020-7322(94)90007-8
- Forel A (1874) Les fourmis de la Suisse. *Soc. Helvetique Sci. Natur. Mem.* 26: 452 pp.
- Gotwald WH (1969) Comparative morphological studies of the ants, with particular reference to the mouthparts (Hymenoptera: Formicidae). *Cornell University Agriculture Experiment Station Memoirs* 408, 150 pp.
- Jervis M (1998) Functional and evolutionary aspects of mouthpart structure in parasitoid wasps. *Biological Journal of the Linnean Society* 63: 461–493. doi: 10.1111/j.1095-8312.1998.tb00326.x
- Johnson NF (1992) Catalog of world Proctotrupeoidea excluding Platygastridae. *Memoirs of the American Entomological Institute* 51: 1–825.
- Johnson NF, Masner L (2006) Revision of world species of the genus *Nixonia* Masner (Hymenoptera: Platygastridae, Scelionidae). *American Museum Novitates* 3518: 1–32. doi: 10.1206/0003-0082(2006)3518[1:ROWSOT]2.0.CO;2

- Johnson NF, Masner L, Musetti L (2008) Review of genera of the tribe Sparasionini (Hymenoptera, Scelionidae), and description of two genera from the New World. *American Museum Novitates* 3629: 1–24. doi: 10.1206/578.1
- Kieffer JJ (1926) Scelionidae. *Das Tierreich*. Vol. 48. Walter de Gruyter & Co., Berlin, 885 pp.
- Kononova SV, Kozlov MA (2001) [Scelionidae (Hymenoptera) of Palaearctics. Subfamilies Teleasinae, Baeinae.] *Academperiodika*, Kiev, 438 pp.
- Krenn HW (2007) Evidence from mouthpart structure on interordinal relationships in Endopterygota? *Arthropod Systematics & Phylogeny* 65(1): 7–14.
- Labandeira CC (1997) Insect mouthparts: ascertaining the paleobiology of insect feeding strategies. *Annual Review of Ecology and Systematics* 28: 153–193. doi: 10.1146/annurev.ecolsys.28.1.153
- Liu CL (1925) Observations on the acroglossal buttons and on the submentum of Hymenoptera. *Annals of the Entomological Society of America* 18: 445–455.
- Masner L (1976) Revisionary notes and keys to world genera of Scelionidae (Hymenoptera: Proctotrupoidea). *Memoirs of the Entomological Society of Canada* 97, 87 pp.
- Masner L, Johnson NF, Polaszek AD (2007) Redescription of *Archaeoscelio* Brues and description of three new genera of Scelionidae (Hymenoptera): a challenge to the definition of the family. *American Museum Novitates* 3550, 24 pp.
- Matsuda R (1957) Morphology of the head of a sawfly, *Macrophya pluricincta* Norton (Hymenoptera, Tenthredinidae). *Journal of Kansas Entomological Society* 30(3): 99–108.
- McGinley R (1980) Glossal Morphology of the Colletidae and Recognition of the Stenotritidae at the Family Level (Hymenoptera: Apoidea). *Journal of the Kansas Entomological Society* 53: 539–552.
- Michener CD (1944) Comparative external morphology, phylogeny, and a classification of the bees (Hymenoptera). *Bulletin of the American Museum of Natural History* 82: 157–326.
- Michener (1984) A comparative study of the mentum and lorum of bees (Hymenoptera: Apoidea). *Journal of the Kansas Entomological Society* 57: 705–714.
- Mikó I, Vilhelmsen L, Johnson NF, Masner L, Péntzes Z (2007) Skeletomusculature of Scelionidae (Hymenoptera: Platygastridae): head and mesosoma. *Zootaxa* 1571: 1–78.
- Murphy NP, Carey D, Castro LR, Dowton M (2007) Phylogeny of the platygastroid wasps (Hymenoptera) based on sequences from the 18S rRNA, 28S rRNA and cytochrome oxidase I genes: implications for the evolution of the ovipositor system and host relationships. *Biological Journal of the Linnean Society* 91: 653–669. doi: 10.1111/j.1095-8312.2007.00825.x
- Popovici O, Fusu L (2006) Contribution to the knowledge of the maxillo-labial complex of some Scelionidae species. *Lucrarile Simpozionului „Entomofagii și rolul lor în păstrarea echilibrului în natură”*. Iași, 39–46.
- Plant JD, Paulus HF (1987) Comparative morphology of the postmentum of bees (Hymenoptera: Apoidea) with special remarks on the evolution of the lorum. *Sonderdruck aus Z. f. zool. Systematik und Evolutionsforschung* 25: 81–103. doi: 10.1111/j.1439-0469.1987.tb00594.x
- Prentice M A (1998) The comparative morphology and phylogeny of Apoid wasps (Hymenoptera: Apoidea) Thesis (Ph D in Entomology)-University of California, Berkeley.
- Prinsloo GL (1980) An illustrated guide to the families of African Chalcidoidea. Republic of South Africa Department of Agriculture and Fisheries Science Bulletin 395: 1–66.

- Ritchie AJ, Peters TM (1981) The external morphology of *Diplolepis rosae* (Hymenoptera, Cynipidae, Cynipinae). *Annales of the Entomological Society of America* 74: 191–199.
- Ronquist F, Nordlander F (1989) Skeletal morphology of an archaic cynipoid. *Ibalia rufipes* (Hymenoptera: Ibalidae). *Entomologica Scandinavica Supplement* 33, 60 p.
- Ross HH (1937) A generic classification of the Nearctic sawflies (Hymenoptera, Symphyta). *Illinois Biological Monographs* 15(2), 172pp.
- Salman K (1929) The external morphology of *Pepsis elegans* Lepeletier (Hymenoptera: Psammocharidae). *Transactions of the American Entomological Society* 55: 119–153.
- Seltmann K, Yoder M, Miko I, Forshage M, Bertone M, Agosti D, Austin A, Balhoff J, Borowiec M, Brady S, Broad G, Brothers D, Burks R, Buffington M, Campbell H, Dew K, Ernst A, Fernandez-Triana J, Gates M, Gibson G, Jennings J, Johnson N, Karlsson D, Kawada R, Krogmann L, Kula R, Mullins P, Ohl M, Rasmussen C, Ronquist F, Schulmeister S, Sharkey M, Talamas E, Tucker E, Vilhelmsen L, Ward PS, Wharton R, Deans A (2012) A hymenopterists' guide to the Hymenoptera Anatomy Ontology: utility, clarification, and future directions. *Journal of Hymenoptera Research* 27: 67–88. doi: 10.3897/jhr.27.2961
- Sharkey MJ, Carpenter JM, Vilhelmsen L, Heraty J, Liljeblad J, Dowling APG, Schulmeister S, Murray D, Deans AR, Ronquist F, Krogmann L, Wheeler CW (2012) Phylogenetic relationships among superfamilies of Hymenoptera. *Cladistics* 28: 80–112. doi: 10.1111/j.1096-0031.2011.00366.x
- Shields VDC (2010) Fine structure of the galeal styloconic sensilla of larval *Lymantria dispar* (Lepidoptera: Lymantriidae). *Annals of the Entomological Society of America* 102(6): 1116–1125. doi: 10.1603/008.102.0621
- Snodgrass RE (1935) *Principles of Insect Morphology*. McGraw-Hill Book Company, New York, 667 pp.
- Snodgrass RE (1942) The skeleto-muscular mechanisms of the honey bee. *Smithsonian Miscellaneous Collections* 28: 1–120.
- Ulrich W (1924) Die Mundwerkzeuge der Spheciden (Hym., Foss.). *Zeitschr. Morph. OkoL Tiere* 1: 539–636. doi: 10.1007/BF00407472
- Vilhelmsen L (1996) The preoral cavity of lower Hymenoptera (Insecta): comparative morphology and phylogenetic significance. *Zoologica Scripta* 25: 143–170. doi: 10.1111/j.1463-6409.1996.tb00156.x
- Vilhelmsen LB (2000a) Before the wasp-waist: Comparative anatomy and phylogenetic implications of the skeleto-musculature of the thoraco-abdominal boundary region in basal Hymenoptera (Insecta). *Zoomorphology* 119: 185–221. doi: 10.1007/PL00008493
- Vilhelmsen LB (2000b) Cervical and prothoracic skeleto-musculature in the basal Hymenoptera (Insecta): Comparative anatomy and phylogenetic implications. *Zoologischer Anzeiger* 239: 105–138.
- Vilhelmsen LB, Mikó I, Krogmann L (2010) Beyond the wasp waist: structural diversity and phylogenetic significance of the mesosoma in apocritan wasps (Insecta: Hymenoptera). *Zoological Journal of the Linnean Society* 159: 22–194. doi: 10.1111/j.1096-3642.2009.00576.x
- Winston ML (1979) The proboscis of the long-tongued bees: A comparative study. *University of Kansas Science Bulletin* 51: 631–667.
- Yoder MJ, Mikó I, Seltmann KC, Bertone MA, Deans AR (2010) A Gross Anatomy Ontology for Hymenoptera. *PLOS ONE* 5(12): e15991. doi: 10.1371/journal.pone.0015991

Appendix I

Specimens examined.

Taxon	Number of specimens	Data labels
<i>Anteris</i> sp.	1	ROMANIA: Botosani, 10.viii.2004, leg. O. Popovici
<i>Anteris</i> sp.	1	ROMANIA: Iasi, 26.vi.2004, leg. O. Popovici
<i>Apepus</i> sp.	1	ROMANIA: Iasi, 30.vi.2004, leg. O. Popovici
<i>Athalia rosae</i>	1	Wildtype culture, 2005, M. Hatakeyama
<i>Behya</i> sp.	2	ROMANIA: Iasi, 10.ix.2005, leg. O. Popovici
<i>Calliscelio</i> sp.	1	ROMANIA: Bacău, 31.viii.2002, leg. O. Popovici
<i>Calliscelio</i> sp.	1	ROMANIA: Holboca (Iași), 30.06.2002, leg. I. Moglan
<i>Duta</i> sp.	1	ROMANIA: Bacau, 17.vii.2004, leg. O. Popovici
<i>Evania</i> sp.	2	Costa Rica, 21.II.2005 15/M/16/016 1500-site Costa Rica Heredia, 9km NE Vara Blanca, 10°14'N (INBIO)
<i>Gasteruption</i> sp.	2	USA WV, Hardy Co., 11–22.v.2006, MT, D. Smith
<i>Ibalia</i> sp.	1	USA: Virginia, Fairfax Co., Great Falls, 18–30.v. 2007, leg. D. Smith
<i>Ibalia</i> sp.	1	USA: Montgomery Co., 21.v. 2010, leg. N. E. Woodley
<i>Ibalia</i> sp.	1	USA: Virginia, Fairfax Co., Great Falls, 31.v.-13.vi.2007, leg. D. Smith
<i>Macroteleia</i> sp.	1	ROMANIA: Iasi, 17.viii.2004, leg. O. Popovici
<i>Macroteleia</i> sp.	1	ROMANIA: Iasi, 13.viii.2000, leg. M. Mitroiu
<i>Macroteleia</i> sp.	1	ROMANIA: Iasi, 25.vii.2005, leg. L. Fusu
<i>Orthogonahys pulchella</i>	4	USA, WV, Hardy Co. 3mi NE Mathias, 38°55'N, 78°49'W, 2–15.vii.2004, Malaise trap. D. Smith
<i>Paramesius</i> sp.	1	ROMANIA: Iasi, 10.ix.2005, leg. O. Popovici
<i>Pelecinus polyturator</i>	1	USA: VA: Fairfax Co., Great Falls, 27.vii–4.viii. 2006, leg. D. Smith
<i>Pelecinus polyturator</i>	1	USA: VA: Fairfax Co., Turkey Run, 5–24.viii.2006, leg. D. Smith
<i>Proctotrupes</i> sp.	1	GREECE: Kerkini Nat. Res., 15–17.vii.2007, leg. G. Ramel
<i>Proctotrupes</i> sp.	1	ROMANIA: Iasi, 7.x.2004, leg. O. Popovici
<i>Proctotrupes</i> sp.	1	ROMANIA: Vorona, 21.v.2007, leg. C. Lisenchi
<i>Psilanteris</i> sp.	1	ROMANIA: Bacau, 17.vii.2004, leg. O. Popovici
<i>Ropronia</i> sp.	2	USA: Virginia, Fairfax Co., 18–30.v.2007, leg. D. Smith
<i>Scelio</i> sp.	3	ROMANIA: Iasi, 24.viii.2004, leg. O. Popovici
<i>Spanasion</i> sp.1	2	ROMANIA: Iasi county, Bărnova forest, meadow in glade; 12.vii.2007 N46°59.617'; E27°35.452', Leg. Popovici O. & Popovici Mariana YPT
<i>Spanasion</i> sp.2	1	ROMANIA: Iasi county, Bărnova forest, meadow in glade; 12.vii.2007 N46°59.617'; E27°35.452', Leg. Popovici O. & Popovici Mariana YPT
<i>Spanasion</i> sp.2	2	ROMANIA: Iasi county, Botanical Garden; N47°11.167'; E27°32.983'; 26.vii.2007; Leg. Popovici O. YPT
<i>Spanasion</i> sp.3	3	ROMANIA: Constanta county; sand dune natural reservation from Agigea; 27–29.vii.2008; N44°5.184'; E28°38.517'; Leg. Popovici O. & Popovici Mariana YPT
<i>Spanasion</i> sp.4	10	ROMANIA: Constanta county; sand dune natural reservation from Agigea; 27–29.vii.2008; N44°5.184'; E28°38.517'; Leg. Popovici O. & Popovici Mariana YPT
<i>Spanasion</i> sp.5	1	ROMANIA: Tulcea county; forest border, 9 km S of Babadag; 6–7.vii.2009; N44°48.817'; E28°42.41'; Leg. Popovici O. & Fusu L. YPT
<i>Spanasion</i> sp.6	1	ROMANIA: Tulcea county; forest border, 9 km S of Babadag; 6–7.vii.2009; N44°48.817'; E28°42.41'; Leg. Popovici O. & Fusu L. YPT

Taxon	Number of specimens	Data labels
<i>Sparasion</i> sp.7	1	ROMANIA: Tulcea county; forest border, 9 km S of Babadag; 6–7.vii.2009; N44°48.817'; E28°42.41'; Leg. Popovici O. & Fusu L. YPT
<i>Sparasion</i> sp.7	2	GREECE: Kerkini Lake, N.P. Lithotopos, 1–7.viii.2006 leg. G. Ramel
<i>Sparasion</i> sp.8	2	JAPAN: Kitahira, Otsu-shi Shiga-ken, 19–22.vii.2008, leg. T. Yoshida.
<i>Sparasion</i> sp.9	1	UGANDA: Kibale, N.P. Kanyawara Biol. Station, 14–21.xi.2010, leg. S. Katusabe & Co.
<i>Sparasion</i> sp.	1	USA: NC, Raleigh 03.VII.2009 Winkler, Benoit
<i>Sparasion</i> sp.	7	USA: West Virginia, Hardy Co. VIII-11–28–06, D. Smith
<i>Triteleia</i> sp.	1	ROMANIA: Iasi, 8.ix.2004, leg. O. Popovici
<i>Vanhornia</i> sp.	3	USA: VA: Loudoun Co., 1.vi–17.vii.2000, leg. D. Smith

Appendix 2

Anatomical terms used, cross-referenced to an ontological (formal) definition (Hymenoptera Anatomy Ontology; URI = Uniform Resource Identifier).

Abbreviation	Term	Ontological definition	URI
	acanthae	The process that corresponds to a single epidermal cell.	http://purl.obolibrary.org/obo/HAO_0002119
anh	annular hair	The spine on the distal part of ligula that is connected proximolaterally to the neighboring glossal hair by a carina.	http://purl.obolibrary.org/obo/HAO_0002205
ags	anterior glossal sclerite	The sclerite of the anterior glossal plate that is lateral to the median conjunctiva of the anterior glossal plate.	http://purl.obolibrary.org/obo/HAO_0000112
asg	anterior surface of the glossa	The area of the glossa that is between the distal glossal edge and the anterior glossal plate.	http://purl.obolibrary.org/obo/HAO_0002208
tnta-pmn	anterior tentorio-premental muscle	The muscle that arises anteriorly from the cranium and inserts on the posterior margin of the prementum.	http://purl.obolibrary.org/obo/HAO_0001064
stia-mp1	anterior stipito-palpal muscle	The stipito-palpal muscle that arises medially on the proximal part of the stipes and inserts anteroproximally on the first maxillary sclerite.	http://purl.obolibrary.org/obo/HAO_0000909
conj	anterolateral wall of the stipes	The area that extends between anterior margin of the median wall of the stipes and the lateral margin of the posterior wall of the stipes and the base of the mandible and the labrum.	http://purl.obolibrary.org/obo/HAO_0002215
agh	apical glossal hair	The spines that are on the distal glossal edge.	http://purl.obolibrary.org/obo/HAO_0002209
sts	apical glossal setae	The row of setae of the glossa that is adjacent to the distal glossal edge.	http://purl.obolibrary.org/obo/HAO_0002210
	apicomedial galeal plate	The sclerite that is located on the medial surface of the galeo-lacinal complex and bears the coeloconic sensillum of galea.	http://purl.obolibrary.org/obo/HAO_0002142
bcr	basal cardinal ridge	The cardinal ridge that is median.	http://purl.obolibrary.org/obo/HAO_0002083
bgs	basal galeal sclerite	The sclerite that receives the site of insertion of the stipito-galeal muscle.	http://purl.obolibrary.org/obo/HAO_0002143
inv	basal glossal invagination	The anterior invagination of the labium that is adjacent with the distal end of the salivarium and separates the glossa proximally from the distal hypopharynx and the paraglossae.	http://purl.obolibrary.org/obo/HAO_0002231

bgb	basiparaglossal brush	The anteroproximal area of the paraglossa that is covered with long acanthae and corresponds to the ligament connecting the acroglossal button with the basiparaglossal sclerite.	http://purl.obolibrary.org/obo/HAO_0002199
pls	basiparaglossal sclerite	The sclerite that is located medially on the paraglossa and articulates with the anterior glossal plate and is continuous with the hypopharyngeal rod..	http://purl.obolibrary.org/obo/HAO_0002201
cps	campaniform sensillum	The aporous sensillum without a hairlike cuticular component.	http://purl.obolibrary.org/obo/HAO_0001973
cfs	coeloconic sensillum of galea	The coeloconic sensillum that is located on the medial surface of the galeo-lacinal complex distal to the base of the lacinal lobe.	http://purl.obolibrary.org/obo/HAO_0002141
csg	campaniform sensillum of glossa	The campaniform sensillum of the anterior surface of the glossa that is located proximal to the glossal annuli.	http://purl.obolibrary.org/obo/HAO_0002212
cps	campaniform sensillum of the prementum	The campaniform sensillum that is on the ventral premental face.	http://purl.obolibrary.org/obo/HAO_0002244
	cardinal articular condyle of the cranium	The condyle that is located on the cranium and articulates with the cranial fossa of the cardo.	http://purl.obolibrary.org/obo/HAO_0002074
	cardinal lever	The process that receives the site of attachment of the crano-cardinal muscle.	http://purl.obolibrary.org/obo/HAO_0002075
cd	cardo	The sclerite that is articulated with the cranium at the crano-cardinal articulation, is connected to the stipes distolaterally via the stipitocardinal hinge and receives the site of attachment of the crano-cardinal muscle.	http://purl.obolibrary.org/obo/HAO_0000187
	conjunctiva	The area of the integument that is weakly sclerotized, with thin exocuticle.	http://purl.obolibrary.org/obo/HAO_0000221
caf	cranial fossa of the cardo	The fossa that is located on the cardo and articulates with the cardinal condyle of the cranium.	http://purl.obolibrary.org/obo/HAO_0002219
cr-cd	crano-cardinal muscle	The maxillar muscle that arises medially from the occiput dorsally of the occipital foramen and inserts on the proximolateral part of the cardo.	http://purl.obolibrary.org/obo/HAO_0001592
	crano-lacinal muscle	The maxillar muscle that arises from the occiput and inserts on the proximal part of the lacinal lobe.	http://purl.obolibrary.org/obo/HAO_0001593
dge	distal glossal edge	The transverse edge that extends distally on the glossa.	http://purl.obolibrary.org/obo/HAO_0002206
dhi	distal hypopharyngeal invagination	The invagination on the distal hypopharynx that is adjacent to the concavities of the hypopharyngeal rods.	http://purl.obolibrary.org/obo/HAO_0002213
dhy	distal hypopharynx	The area that is located on the anterior surface of the hypopharyngeal wall and is delimited proximally by the infrabuccal pouch or the distal margin of the sitophore, distally by the salivarial orifice and laterally by the lateral parts of the prementum and the hypopharyngeal rods.	http://purl.obolibrary.org/obo/HAO_0001575
dhs	distal hypopharyngeal sclerite	The sclerite that receives the site of insertions of the dorsal and ventral premento-salivarial muscles and is continuous with the hypopharyngeal rod.	http://purl.obolibrary.org/obo/HAO_0002228

dgs	distolateral galeal sclerite	The sclerite that is located distolaterally on the lateral wall of the galeo-lacinal complex and bears the apicolateral galeal setae.	http://purl.obolibrary.org/obo/HAO_0002127
dgp	distolateral galeal setiferous patch	The setiferous patch that is located distolaterally on the galeo-lacinal complex	http://purl.obolibrary.org/obo/HAO_0002128
dmf	distomedial stipital flange	The medial part of the principal carina of the stipes that is overlapped by the premental carina and overlaps the lateral premental face.	http://purl.obolibrary.org/obo/HAO_0002217
pmd-slv	dorsal premento-salivarial muscle	The salivarial muscle that inserts proximodorsally on the salivary duct.	http://purl.obolibrary.org/obo/HAO_0000274
5mp	fifth sclerite of the maxillary palp	The sclerite that is ringlike and is connected distally to the fourth sclerite of the maxillary palp via conjunctiva.	http://purl.obolibrary.org/obo/HAO_0002220
mp1-mp2	first intrinsic muscle of the maxillary palp	The muscle that arises from the first sclerite of the maxillary palp and inserts on the second sclerite of the maxillary palp.	http://purl.obolibrary.org/obo/HAO_0002114
	first intrinsic muscle of the labial palp	The muscle that arises from the first sclerite of the labial palp and inserts on the second sclerite of the labial palp.	http://purl.obolibrary.org/obo/HAO_0002237
1lp	first sclerite of the labial palp	The sclerite that is ringlike and is connected distolaterally to the prementum via conjunctiva and muscle.	http://purl.obolibrary.org/obo/HAO_0002194
1mp	first sclerite of the maxillary palp	The sclerite that is ringlike and is connected distolaterally to the posterior stipital sclerite via conjunctiva and muscle.	http://purl.obolibrary.org/obo/HAO_0002109
	fourth intrinsic muscle of the maxillary palp	The muscle that arises from the third sclerite of the maxillary palp and inserts on the fourth sclerite of the maxillary palp.	http://purl.obolibrary.org/obo/HAO_0002222
4mp	fourth sclerite of the maxillary palp	The sclerite that is ringlike and is connected distally to the third sclerite of the maxillary palp via conjunctiva.	http://purl.obolibrary.org/obo/HAO_0002113
	galeal comb	The row of setae that is located on the medial wall of the galeo-lacinal complex proximal to the coeloconic sensilla of galea.	http://purl.obolibrary.org/obo/HAO_0002243
	galeal fringe	The row of setae that extends along the margin of the galeo-lacinal complex, distal to the lacinal lobe.	http://purl.obolibrary.org/obo/HAO_0002133
	galeal lamina	The lobe that is located medially on the internal wall of the galeo-lacinal complex and margined by the galeal comb.	http://purl.obolibrary.org/obo/HAO_0002136
glb	galeal lobe	The lobe that is located on the stipes at the distal part of the posterior stipital sclerite distolateral to the lacinia.	http://purl.obolibrary.org/obo/HAO_0000368
gal-lac	galeo-lacinal complex	The area of the stipes that is delimited proximomedially by the stipito-premental conjunctiva, proximolaterally by the stipito-mandibular conjunctiva and posteroproximally by the margin of the posterior stipital sclerite.	http://purl.obolibrary.org/obo/HAO_0002126
glo	glossa	The lobe of the labium that is limited posteroproximally by the prementum, anteroproximally by the fold traversing the salivary orifice and laterally by the paraglossae.	http://purl.obolibrary.org/obo/HAO_0000376
gla	glossal annuli	The anatomical cluster of the glossa that is composed of annular hairs.	http://purl.obolibrary.org/obo/HAO_0002204
hyb	hypopharyngeal button	The bent area of the hypopharyngeal rod that receives the site of insertion of the posterior tentorio-premental muscle.	http://purl.obolibrary.org/obo/HAO_0002234

hpc	hypopharyngeal pecten	The anterolateral area of the distal hypopharynx that is adjacent with the proximal part of the hypopharyngeal rod proximal to the hypopharyngeal button and is covered with acanthae.	http://purl.obolibrary.org/obo/HAO_0002214
hypr	hypopharyngeal rod	The ligament that connects the proximolateral margin of the prementum with the proximal part of the ligula.	http://purl.obolibrary.org/obo/HAO_0000408
hys	hypostoma	The area that extends on the posterior (ventral) margin of the oral foramen along the site of attachments of the conjunctiva connecting the cranium with the maxillae and is delimited laterally by the pleurostomal fossa.	http://purl.obolibrary.org/obo/HAO_0000411
	integument	The anatomical system that forms the covering layer of the animal, ectodermal in origin and composed of epidermal cells producing the cuticle.	http://purl.obolibrary.org/obo/HAO_0000421
	intercardinal area	The area that is located between the cardines and limited proximally and distally by the anatomical line that extends between the proximal and distal ends of the left and right cardines.	http://purl.obolibrary.org/obo/HAO_0002145
	interstipital area	The area of the postmental area that is limited laterally by the median margins of the stipites, proximally by the anterior margin of the intercardinal area and distally by the proximal margin of the prementum.	http://purl.obolibrary.org/obo/HAO_0002146
	interstipital sclerite	The sclerite that is located on the interstipital area and is connected to the prementum via conjunctiva.	http://purl.obolibrary.org/obo/HAO_0002223
	invagination	The area where the cuticle is invaginated.	http://purl.obolibrary.org/obo/HAO_0002021
	labial palp	The anatomical structure that is distal to the proximal margin of the first sclerite of the labial palp.	http://purl.obolibrary.org/obo/HAO_0000450
pin	labial palpal excision	The notch that is located distolaterally on the prementum and receives the base of the labial palp.	http://purl.obolibrary.org/obo/HAO_0002153
	labium	The appendage that is encircled by the area that is proximally delimited by the lateral margins of the cardo and the posterior stipital sclerite laterally, and the anatomical line that is tangential to the salivary duct and traverses the salivary orifice anteriorly.	http://purl.obolibrary.org/obo/HAO_0000453
	lacinial bar	The sclerite that is located on the lateral wall of the lacinial lobe.	http://purl.obolibrary.org/obo/HAO_0002117
	lacinial comb	The row of setae on the lacinial lobe that is marginal.	http://purl.obolibrary.org/obo/HAO_0002124
bls	lacinial lever	The sclerite that is located on the medial stipital wall and receives the site of insertion of the stipito-lacinial muscle.	http://purl.obolibrary.org/obo/HAO_0002093
llb	lacinial lobe	The lobe that extends proximally on the distal margin of the medial stipital wall, is adjacent to the basal lacinial sclerite, overlaps the proximal part of the galea.	http://purl.obolibrary.org/obo/HAO_0000457
pma	lateral premental face	The area of the prementum, that lays parallel and connected via conjunctiva to the medial stipital wall.	http://purl.obolibrary.org/obo/HAO_0002152

lcr	laterodistal cardinal ridge	The cardinal ridge that arises distally from the basal cardinal ridge and is oriented distolaterally.	http://purl.obolibrary.org/obo/HAO_0002084
	ligament	The area of the cuticle that is resilin rich.	http://purl.obolibrary.org/obo/HAO_0002229
	ligula	The anatomical cluster that is composed of the glossa and paraglossae.	http://purl.obolibrary.org/obo/HAO_0000496
	lobes	The evagination that is mostly membranous.	http://purl.obolibrary.org/obo/HAO_0001587
md	mandible	The sclerite that is connected to the cranium along the anterior margin of the oral foramen via the anterior and posterior cranio-mandibular articulations.	http://purl.obolibrary.org/obo/HAO_0000506
mfs	marginal fringe of the stipes	The anatomical cluster that is composed of the spines on the distal margin of the distolateral portion of the principal carina of the stipes.	http://purl.obolibrary.org/obo/HAO_0002216
	maxilla, maxillae	The appendage that is encircled by the area that is proximally delimited by the hypostoma posteriorly, the median margin of the mandible laterally, the labrum anterolaterally and the labium medially.	http://purl.obolibrary.org/obo/HAO_0000513
mpalp	maxillary palp	The anatomical structure that is distal to the proximal margin of the first sclerite of the maxillary palp.	http://purl.obolibrary.org/obo/HAO_0000515
	maxillary palpal sclerite	The sclerite that is part of the maxillary palp.	http://purl.obolibrary.org/obo/HAO_0002183
	maxillary process of the hypostoma	The articular process that bears the cardinal condyle of the cranium.	http://purl.obolibrary.org/obo/HAO_0002073
	maxillo-labial complex	The anatomical cluster that is composed of the maxillae and the labium and is connected by conjunctivae laterally to the cranium along the hypostoma, to the mandible along the proximomedial margin of the mandible and proximally to the hypopharynx.	http://purl.obolibrary.org/obo/HAO_0000452
msh	mechanosensory hair	The aporous sensillum that has a hair-like cuticular component.	http://purl.obolibrary.org/obo/HAO_0001039
msg	medial stipital groove	The depression that extends medially and adjacent to the medial portion of the principal carina of stipes.	http://purl.obolibrary.org/obo/HAO_0002106
	medial wall	The area that is medial and lays parallel with the lateral wall of the prementum.	http://purl.obolibrary.org/obo/HAO_0002092
	median conjunctiva of the anterior glossal plate	The median conjunctiva of the anterior glossal plate that is parallel with the anteroposterior body axis.	http://purl.obolibrary.org/obo/HAO_0002203
mpr	median postmental ridge	The ridge that is limited laterally by the stipital articular surfaces of the postmentum.	http://purl.obolibrary.org/obo/HAO_0002225
mcr	mediodistal cardinal ridge	The cardinal ridge that arises distally from the basal cardinal ridge and is oriented distomedially.	http://purl.obolibrary.org/obo/HAO_0002085
pgl	paraglossa	The lobe that is connected to the distal margin of the prementum posteroproximally, to the premental hypopharynx proximolaterally and anteroproximally, to the glossa proximomedially and bears the basiparaglossal brush and the paraglossal sclerite.	http://purl.obolibrary.org/obo/HAO_0000686

pgb	paraglossal acroglossal button	The sclerite that is located distally on the paraglossa.	http://purl.obolibrary.org/obo/HAO_0002232
	paraglossal annuli	The anatomical cluster of the paraglossa that is composed of connected annular hairs.	http://purl.obolibrary.org/obo/HAO_0002233
	paraglossal sclerite	The anteroproximal sclerite of the paraglossa that bears the basiparaglossal brush.	http://purl.obolibrary.org/obo/HAO_0002200
Pgp	posterior glossal plate	The sclerite that is connected to the distal margin of the prementum and receives the site of insertion of the premento-paraglossal muscles.	http://purl.obolibrary.org/obo/HAO_0000747
pss	posterior stipital sclerite	The sclerite that is located on the posterior stipital wall, articulates with the cardo and with the labial palp, is connected by conjunctiva distolaterally to the galeo-lacinal complex, proximally to the hypostoma and the cardo, proximolaterally to the mandible.	http://purl.obolibrary.org/obo/HAO_0002097
stip-mp1	posterior stipito-palpal muscle	The stipito-palpal muscle that arises medially on the proximal part of the stipes and inserts posteroproximally on the first maxillary palpal segment.	http://purl.obolibrary.org/obo/HAO_0001814
	posterior wall	The area that is limited medially by the medial stipital wall and limited proximolaterally by the margin of the posterior stipital sclerite.	http://purl.obolibrary.org/obo/HAO_0002097
pwg	posterior surface of the glossa	The area of the glossa that is between the distal margin of the prementum and the distal glossal edge.	http://purl.obolibrary.org/obo/HAO_0002207
tntp-pmn	posterior tentorio-premental muscle	The tentorio-labial muscle that arises from the cranium and inserts distally on the labium adjacent to the level of the salivary orifice.	http://purl.obolibrary.org/obo/HAO_0000264
	postmental area	The area that is limited distally by the posterior margin of the prementum and laterally by the median margins of the cardines and the stipes.	http://purl.obolibrary.org/obo/HAO_0002144
pph	postmental-premental hinge	The conjunctiva that is between the postmentum and prementum.	http://purl.obolibrary.org/obo/HAO_0002226
	postmento-premental muscle	The labial muscle that is unpaired, arises from the postmentum and inserts on the proximal margin of the prementum.	http://purl.obolibrary.org/obo/HAO_0000803
psm	postmentum	The anatomical cluster that is composed of the sclerites that are on the postmental area.	http://purl.obolibrary.org/obo/HAO_0000785
prm	premental arms	The area of the lateral premental face that receives the site of origin of the dorsal premento-salivarial muscle.	http://purl.obolibrary.org/obo/HAO_0002155
pmc	premental carina	The flange that is adjacent with the border between the ventral and lateral premental faces and that overlaps externally the median part of the posterior stipital sclerite.	http://purl.obolibrary.org/obo/HAO_0002157
pmd	premental ditch	The scrobe of the prementum that is adjacent to and extends lateral to the premental carina and accommodates the medial part of the posterior stipital sclerite.	http://purl.obolibrary.org/obo/HAO_0002227
	premento-glossal muscle	The labial muscle that arises on the ventral part of the prementum, laterally to the ventral premento-salivarial muscle and inserts on the anterior glossal plate.	http://purl.obolibrary.org/obo/HAO_0000377

	premento-palpal muscle	The labial muscle that arises from the prementum and inserts on the first sclerite of the labial palp.	http://purl.obolibrary.org/obo/HAO_0000314
pmn-pgs	premento-paraglossal muscle	The labial muscle that arises from the ventral part of the prementum, anterior to the origin of the premento-glossal muscle and ventral premento-salivarial muscle and inserts just distally of the distal margin of the prementum.	http://purl.obolibrary.org/obo/HAO_0000687
pmn	prementum	The sclerite that is median, is connected via conjunctiva along its proximolateral margins to the stipites, is articulated with the labial palps, is continuous along its distal margin with the ligula and distolateral margins with the distal hypopharynx and receives the site of attachments of the extrinsic labial palp muscles.	http://purl.obolibrary.org/obo/HAO_0000804
pcs	principal carina of the stipites	The flange that extends along the margin of the posterior stipital wall.	http://purl.obolibrary.org/obo/HAO_0002099
	proximal galeal brush	The row of setae that is on the distal margin of the proximolateral galeal sclerite.	http://purl.obolibrary.org/obo/HAO_0002135
pgs	proximolateral galeal sclerite	The sclerite that is located on the lateral wall of the galeo-lacinial complex and bears the proximolateral galeal setiferous patch.	http://purl.obolibrary.org/obo/HAO_0002130
prs	proximolateral galeal setiferous patch	The setiferous patch that is located on the lateral wall of the galeo-lacinial complex proximally of the distolateral setiferous patch.	http://purl.obolibrary.org/obo/HAO_0002129
pmf	proximomedial stipital flange	The medial part of the principal carina of the stipites that is overlapped distally by the distomedial stipital carina and overlaps the lateral premental face and the proximal part of the prementum.	http://purl.obolibrary.org/obo/HAO_0002218
svr	salivarium	The area that is at the proximal end of the salivary duct and corresponds to the site of insertion of the dorsal and ventral premento-salivarial muscles.	http://purl.obolibrary.org/obo/HAO_0000906
svd	salivary duct	The duct that leads from the salivary gland.	http://purl.obolibrary.org/obo/HAO_0002236
	salivarial sclerite	The sclerite that is located in the ventral wall of the salivarium and corresponds to the site of insertion of the ventral premento-salivarial muscle.	http://purl.obolibrary.org/obo/HAO_0001682
	sclerite	The area of the integument that is strongly sclerotised, with thick exocuticle and is surrounded by conjunctivae.	http://purl.obolibrary.org/obo/HAO_0000909
	second intrinsic muscle of the maxillary palp	The muscle that arises from the first sclerite of the maxillary palp and inserts on the third sclerite of the maxillary palp.	http://purl.obolibrary.org/obo/HAO_0002115
	second intrinsic muscle of the labial palp	The muscle that arises from the second sclerite of the labial palp and inserts on the third sclerite of the labial palp.	http://purl.obolibrary.org/obo/HAO_0002238
	second sclerite of the labial palp	The sclerite that is ringlike and is connected distally to the first sclerite of the labial palp via conjunctiva and muscle.	http://purl.obolibrary.org/obo/HAO_0002195
	second sclerite of the maxillary palp	The sclerite that is ringlike and is connected distolaterally to the first sclerite of the maxillary palp via conjunctiva and muscle.	http://purl.obolibrary.org/obo/HAO_0002111

	seta	The sensillum that is multicellular and consists of trichogen, tormogen, and sense cells and the cuticle secreted by and adjacent to the trichogen cell.	http://purl.obolibrary.org/obo/HAO_0000935
	skeletal muscle	The muscle that is attached at either end to the cuticle.	http://purl.obolibrary.org/obo/HAO_0001922
	spiculate patch of galea	The area on the galeo-lacinal complex distal to the lacinal lobe that is covered with acanthae.	http://purl.obolibrary.org/obo/HAO_0002139
	spiculate patch of the lacinia	The area on the lacinal lobe that is covered with acanthae.	http://purl.obolibrary.org/obo/HAO_0002138
	spine	The process that lacks non-sclerotised ring at the base.	http://purl.obolibrary.org/obo/HAO_0000949
	stipes, stipites	The appendage that is connected posteroproximally to the hypostoma, anteroproximally and lateroproximally to the mandible and medioproximally to the labium and the hypopharynx via conjunctiva, is connected to the cranium via muscles and that bears the maxillary palp.	http://purl.obolibrary.org/obo/HAO_0000958
	stipital sclerite	The sclerite that is on the medial stipital wall, bears the medial stipital process.	http://purl.obolibrary.org/obo/HAO_0002096
sti-gal	stipito-galeal muscle	The maxillary muscle that arises from the posterior sclerite of the stipes medial to the site of origin of the stipito-lacinal muscle and inserts on the median wall of the galeo-lacinal complex distal to the stipito-lacinal muscle.	http://purl.obolibrary.org/obo/HAO_0001661
sti-lac	stipito-lacinal muscle	The maxillary muscle that arises along the lateral margin of the posterior stipital sclerite and inserts proximally on the median wall of the stipes just proximal to the lacinal lobe.	http://purl.obolibrary.org/obo/HAO_0001660
sti-mp1	stipito-palpal muscle	The maxillary muscle that arises from the posterior stipital sclerite and inserts on the first sclerite of the maxillary palp.	http://purl.obolibrary.org/obo/HAO_0002110
	stipito-premental conjunctiva	The conjunctiva that extends along the posterior (dorsal) margin of the premental arm and the proximal margin of the medial stipital wall.	http://purl.obolibrary.org/obo/HAO_0002125
sch	stipitocardinal hinge	The membranous area linking the cardo and stipes.	http://purl.obolibrary.org/obo/HAO_0002076
sts	styloconic sensillum	The seta that is on a process.	http://purl.obolibrary.org/obo/HAO_0002211
tnt-cd	tentorio-cardinal muscle	The maxillary muscle that arises from the anterior region of the cranium and inserts adjacent to the cardino-stipital hinge.	http://purl.obolibrary.org/obo/HAO_0001638
tnt-sti	tentorio-stipital muscle	The maxillary muscle that arises on the posteroventral part of the anterior tentorial arm and inserts on the median wall of the stipes.	http://purl.obolibrary.org/obo/HAO_0001002
	tentorium	The apodeme that has its sites of origin marked by the anterior and posterior tentorial pits and gular sulci.	http://purl.obolibrary.org/obo/HAO_0001003
	third intrinsic muscle of the maxillary palp	The muscle that arises from the second sclerite of the maxillary palp and inserts on the third sclerite of the maxillary palp.	http://purl.obolibrary.org/obo/HAO_0002116
	third sclerite of the labial palp	The sclerite that is ringlike and is connected distally to the second sclerite of the labial palp via conjunctiva and muscle.	http://purl.obolibrary.org/obo/HAO_0002196

3mp	third sclerite of the maxillary palp	The sclerite that is ringlike and is connected distally to the second segment of the maxillary palp via conjunctiva and muscle.	http://purl.obolibrary.org/obo/HAO_0002112
ss1	uniporous sensilla, Type 1 seta	The sensillum whose cuticular component has one cuticular pore.	http://purl.obolibrary.org/obo/HAO_0002221
vlm	velum	The flange that is transparent, and extends along the anterodistal margin of the galeo-lacinal complex distal to the lacinal lobe.	http://purl.obolibrary.org/obo/HAO_0002140
vdp	ventral dististipital process	The projection that is located distally on the posterior stipital sclerite and encircles the base of the maxillary palp.	http://purl.obolibrary.org/obo/HAO_0002102
	ventral glossal lines	The carinae that radiates from the posterior glossal plate towards the apical glossal setae.	http://purl.obolibrary.org/obo/HAO_0002230
vpf	ventral premental face	The area of the prementum that is delimited laterally by the lateral premental face.	http://purl.obolibrary.org/obo/HAO_0002156
pmnv-slv	ventral premento-salivary sclerite muscle	The salivarial muscle that arises from the proximal end of the ventral part of the prementum and inserts on the salivarial sclerite.	http://purl.obolibrary.org/obo/HAO_0001072
vba	ventrolateral basiglossal arm	The projection that is located proximolaterally on the anterior glossal plate and articulates with the basiparaglossal sclerite.	http://purl.obolibrary.org/obo/HAO_0002202

Appendix 3

Volume rendered CLSM media files on figshare.com

doi: 10.6084/m9.figshare.861056
doi: 10.6084/m9.figshare.861057
doi: 10.6084/m9.figshare.861058
doi: 10.6084/m9.figshare.861060
doi: 10.6084/m9.figshare.861061
doi: 10.6084/m9.figshare.861062
doi: 10.6084/m9.figshare.861063
doi: 10.6084/m9.figshare.861064
doi: 10.6084/m9.figshare.861065
doi: 10.6084/m9.figshare.861066
doi: 10.6084/m9.figshare.861067
doi: 10.6084/m9.figshare.861119
doi: 10.6084/m9.figshare.956282
doi: 10.6084/m9.figshare.956281
doi: 10.6084/m9.figshare.956280
doi: 10.6084/m9.figshare.956279
doi: 10.6084/m9.figshare.956278

Organ-specific patterns of endopolyploidy in the giant ant *Dinoponera australis*

Daniel R. Scholes¹, Andrew V. Suarez¹, Adrian A. Smith¹,
J. Spencer Johnston², Ken N. Paige¹

1 School of Integrative Biology, University of Illinois at Urbana-Champaign, 505 S. Goodwin Ave., Urbana, IL, USA 61801 **2** Department of Entomology, Texas A&M University, College Station, TX, USA 77843

Corresponding author: Daniel R. Scholes (scholes2@illinois.edu)

Academic editor: J. Neff | Received 16 December 2013 | Accepted 4 March 2014 | Published 28 March 2014

Citation: Scholes DR, Suarez AV, Smith AA, Johnston JS, Paige KN (2014) Organ-specific patterns of endopolyploidy in the giant ant *Dinoponera australis*. Journal of Hymenoptera Research 37: 113–126. doi: [10.3897/JHR.37.6824](https://doi.org/10.3897/JHR.37.6824)

Abstract

Endoreduplication is an alternative cell cycle that omits cell division such that cellular ploidy increases, generating “endopolyploidy”. Endoreduplication is common among eukaryotes and is thought to be important in generalized cell differentiation. Previous research on ants suggests that they endoreduplicate in body segment-dependent manners. In this study, we measured endopolyploidy of specific organs within ant body segments to determine which organs are driving these segment-specific patterns and whether endopolyploidy is related to organ function. We dissected fourteen organs from each of five individuals of *Dinoponera australis* and measured endopolyploidy of each organ via flow cytometry. Abdominal organs had higher levels of endopolyploidy than organs from the head and thorax, driven by particularly high ploidy levels for organs with digestive or exocrine function. In contrast, organs of the reproductive, muscular, and neural systems had relatively low endopolyploidy. These results provide insight into the segment-specific patterns of endopolyploidy previously reported and into the specific organs that employ endoreduplication in their functional development. Future work aimed at quantifying the metabolic and gene expression effects of endoreduplication will clarify how this often overlooked genomic event contributes to the development and function of specialized organs across the breadth of taxa that are known to endoreduplicate.

Keywords

Endoreduplication, ploidy, Hymenoptera, digestion, exocrine, development

Introduction

Endoreduplication is the replication of the nuclear genome without cell division such that cellular ploidy increases with each round of replication, generating endopolyploidy. This process can proceed independently among cells and create a mosaic of ploidy levels within an organism (Nagl 1976, 1978, Barlow 1978, Lee et al. 2009). Endopolyploidy has been found in a variety of animals, including many insect orders (Nagl 1976, White 1977, Johnston et al. 2004, Aron et al. 2005). In insects, the occurrence of endopolyploidy is tissue-dependent and is perhaps best characterized in *Drosophila melanogaster*, where ploidy levels as high as 1024C are found among the polytene chromosomes of the salivary glands and follicle cells, with lower levels of endopolyploidy occurring throughout the organism (Balbiani 1881, Mulligan and Rasch 1985, Lilly and Duronio 2005, Johnston et al. 2013). The highest level of endopolyploidy observed so far is in the insect *Bombyx mori*, whose silk-producing glands are reported to exceed one million-ploid as a result of intensive artificial selection (Perdix-Gillot 1979).

Given the wide range of taxa and cell types that endoreduplicate, endopolyploidy is presumed to have beneficial effects on the basic properties of the cell (Nagl 1976, 1978, Lee et al. 2009). These “nucleotypic effects” (Bennett 1972, 1982) are in part due to the bulk nuclear DNA content that influences cell size, the rate of cell division, and water and nutrient transport efficiency (Nagl 1976, 1982, Barlow 1978, Lee et al. 2009). Other hypothesized benefits of high DNA content, and in particular endopolyploidy, include increased cellular metabolism and gene expression owing to the increase in available gene templates for transcription (Nagl 1976, 1978, Galitski et al. 1999, Osborn et al. 2003). Collectively, the effects of endopolyploidy can influence the development and functioning of highly specialized tissues (Lee et al. 2009) and may occur in response to physiological stress (e.g. Britton and Edgar 1998, Engelen-Egles et al. 2001, Fusconi et al. 2006, Jimenez et al. 2010, Scholes and Paige 2011).

The order Hymenoptera has a long history for studies on intra-individual variation in ploidy (Merriam and Ris 1954, Mittwoch et al. 1966, Rasch et al. 1975). Recently, Aron et al. (2005) demonstrated that haploid males in many hymenoptera generate endopolyploidy such that they are functionally diploid, with the proportion of diploid cells in thoracic, mandibular, and fore-, mid-, and hindleg muscles comparable between males and females of the bumble bee *Bombus terrestris*. Scholes et al. (2013) surveyed endopolyploidy within and between castes of four polymorphic ant species and found that endopolyploidy varied between workers of different body sizes. Additionally, when body segments were examined separately, ploidy levels of the abdomen were significantly greater than those of the head and thorax, which had comparable ploidy levels. Given the presumed roles of endopolyploidy in cell differentiation, we propose that ploidy levels may be greatest in the abdomen to aid in the development, functioning, and metabolism of the specialized tissues therein.

What is now needed is a fine-scale survey of endopolyploidy to document the degree to which ploidy varies within the body segments, and to determine how ploidy

may be differentially affecting organ development, specialization, and function. In this study, we surveyed endopolyploidy of a variety of organs within individuals of the ant *Dinoponera australis* (Hymenoptera: Formicidae: Ponerinae). *D. australis* is a large (mean 105 mg dry mass and > 2 cm in length), queenless ant that occurs in northern Argentina, Paraguay, and southern Brazil (Paiva and Brandão 1995). Colonies are relatively small with a range of 18 to 86 females (Paiva and Brandão 1995). As with other members of the genus, all females are born physiologically capable of reproducing; however, a single dominant “gamergate” is responsible for egg-laying (Monnin and Peeters 1999, Monnin et al. 2003). *D. australis* has a relatively large genome among ants (554.7 Mb / 1C; Tsutsui et al. 2008) that is composed of numerous small chromosomes (57 chromosomes / 1C; Santos et al. 2012). Given its large genome size, endopolyploidy will conceivably have a major effect in this species. We chose *D. australis* for this research to determine whether the patterns of segment-specific endopolyploidy previously reported in numerous ant species (Scholes et al. 2013) are also evident in this unusual ant. Its large size additionally allowed for the extraction of organs from individual ants that were of adequate mass to estimate organ-specific ploidy.

Initial characterization of the patterns of endopolyploidy among *D. australis* body segments made it possible to determine which specific organs were underlying the segment-specific patterns observed. Given the assumption that endopolyploidy is related to cellular differentiation and function (Nagl 1978, Cavalier-Smith 1985, Gregory and Hebert 1999), we additionally tested whether levels of endopolyploidy correlate with organ function to infer whether organs of similar general function also have comparable levels of endopolyploidy regardless of the segment within which they reside. This information provides important insights into organ development, specialization, and function, with potential further implications into the basis for behavior and sociality given a better understanding of insect physiology.

Methods

Organism collection and dissection

We excavated a single colony in August 2011 from Iguazú National Park, Misiones Province, in northeastern Argentina. The colony was maintained in an insectary at the University of Illinois on a diet of sugar water and crickets. Individuals were a minimum of two years old at the time of analysis. We used carbon dioxide from sublimating dry ice to incapacitate five non-reproducing females prior to dissection. For each individual, we dissected as many organs as possible from each of the head, thorax, and abdominal segments. Dissected organs were placed in a 0.2 ml centrifuge tube on ice until preparation for cytometric analysis. A complete list of organs sampled is provided in Table 1.

Table 1. Organs analyzed for nuclear DNA content by flow cytometry. Identity of the 14 organs analyzed, their abbreviations (Abbrev), the segment within which they reside, their demonstrated functions, and the number of nuclei analyzed for each organ (mean ± SE). Symbols designate reference (Ref) or general functional system (Function).

Segment	Organ	Abbrev	Function	# Nuclei	Ref
Head	Brain	BRN	Sensory processing (††)	8861 ± 1589	†
	Mandibular gland	MDG	Pheromone production (‡‡)	287 ± 99	‡
	Mandibular muscle	MDM	Mandibular movement (§§)	517 ± 141	§
Thorax	Foreleg muscle	FLG	Locomotion (§§)	221 ± 83	§
	Thoracic muscle	THM	Locomotion (§§)	1165 ± 435	§
Abdomen	Abdominal segmental muscle	ABM	Articulation of abdomen (§§)	763 ± 272	§
	Dufour's gland	DUF	Pheromone production (‡‡)	384 ± 68	
	Fat body	FAT	Nutrient metabolism, storage ()	704 ± 202	¶
	Foregut (crop)	FOR	Ingestion & storage ()	1357 ± 618	§
	Hindgut	HIN	Absorption & excretion ()	1656 ± 313	§
	Midgut	MID	Digestion & absorption ()	2582 ± 916	§
	Malpighian tubules	MPG	Excretion, osmoregulation ()	435 ± 254	§
	Ovaries	OVA	Egg production (¶¶)	4305 ± 2057	§
Poison gland	POI	Venom production (‡‡)	290 ± 92	#	

† Gronenberg et al. 2008; ‡ Oldham et al. 1994; § Klowden 2007; | Monnin et al. 2002;

¶ Gullan and Cranston 2005; # Johnson et al. 2010

†† Neural; ‡‡ exocrine; §§ muscular; || digestive; ¶¶ reproduction

Cytometric analysis

Flow cytometry methods were modified from those described by Johnston et al. (2004). Each isolated organ was placed into one milliliter of Galbraith buffer (sodium citrate, 3-morpholinopropane-1-sulfonic acid, magnesium chloride, Triton X-100; Galbraith et al. 1983) in a 2 ml Kontes Dounce. Nuclei were released by grinding with ten very gentle strokes with an A pestle. The released nuclei in the buffer were filtered through a 40 µm nylon mesh, brought to a 1 ml total volume with additional buffer, and stained with 25 µl of propidium iodide (0.25 mg PI / ml). After at least 30 minutes of staining in the dark at 4°C, the number of stained nuclei at each ploidy level was scored on the basis of relative fluorescence using a Partec (Münster, Germany) Cyflow cytometer. Care was taken to set the 2C fluorescence peak at channel 25 so that a total of 6 ploidy levels could be scored. Gates set on scatter and peak/area were set up for doublet discrimination and identification of broken nuclei or nuclei with cytoplasmic tags. The total number of counted gated and ungated nuclei at each ploidy level in each organ was based on the analysis of approximately half (0.5 ml) of each prepared sample. The “cycle value” for each sample was then calculated by the equation:

$$\text{Cycle value} = \frac{(n_{2C} \cdot 0 + n_{4C} \cdot 1 + n_{8C} \cdot 2 + n_{16C} \cdot 3 + n_{32C} \cdot 4 + n_{64C} \cdot 5)}{(n_{2C} + n_{4C} + n_{8C} + n_{16C} + n_{32C} + n_{64C})}$$

as the sum of the number of nuclei at each ploidy level multiplied by the number of endocycles required to achieve that ploidy level, divided by the total number of nuclei measured. The cycle value is interpreted as the average number of endocycles undergone per nucleus in the sample, and is thus directly proportional to endopolyploidy (Barow and Meister 2003).

Statistical analysis

Statistical analyses were conducted as mixed models with SAS PROC MIXED (v.9.2, Cary, North Carolina, USA). To assess whether organs differed from each other across the measured ploidy levels, the proportion of nuclei at each ploidy level was compared among organs by ANOVA with individual as a random effect with five levels (individuals 1–5), ploidy level as a fixed effect with six levels (2C, 4C, 8C, 16C, 32C, 64C), and organ as a fixed effect with fourteen levels (14 organs; see Table 1). Body segments were similarly compared but with body segment as a fixed effect with three levels (head, thorax, abdomen). Additionally, to determine whether differences among body segments were due to differences in the proportion of endopolyploid cells, the proportions of endopolyploid (4C–64C) nuclei were compared among body segments via ANOVA with post-hoc linear contrasts. All proportions were arc-sin square-root transformed prior to statistical analysis to satisfy the assumption of $NID(0, \sigma^2)$.

To determine if endoreduplication differed among organs, the composite measure of endoreduplication, the cycle value, was compared among organs by ANOVA with individual as a random effect with five levels (individuals 1–5) and organ as a fixed effect with fourteen levels (14 organs; see Table 1). Comparing endopolyploidy via cycle values rather than across six ploidy levels individually is useful here due to the number of organs compared. Cycle values of body segments were compared similarly with body segment as a fixed effect with three levels (head, thorax, abdomen). For both the organ and body segment models, differences among organs/body segments were determined by Tukey's Studentized range test (i.e. Tukey's Honest Significant Difference) to correct for multiple comparisons (Tukey 1953) with SAS PROC MIXED. The effect of the individual on cycle values was tested via the Random-Effects Analysis in PROC GLM.

To determine whether the level of endopolyploidy is correlated with organ function, cycle values were compared via ANOVA with individual as a random effect with five levels (individuals 1–5) and functional system as a fixed effect with five levels (digestive, exocrine, reproduction, muscular, neural; see Table 1 for a list of organs comprising each system). Differences among functional systems in their cycle values were determined by Tukey's Studentized range test to correct for multiple comparisons (Tukey 1953) with SAS PROC MIXED.

Results

Proportion of nuclei of ploidy levels among organs and body segments

We quantified nuclei via flow cytometry at ploidy levels doubling from 2C to 64C in 14 organs, though not all organs were composed of all six ploidy levels scored (Figure 1). A comparison of gated and ungated counts showed that careful preparation produced less than 2% of counts of doublets and broken or cytoplasmic tagged nuclei (data not shown). Total, ungated counts are therefore reported at each of the ploidy levels. Overall, organs vary significantly in the proportions of nuclei among the ploidy levels ($F(70,320) = 7.13, p < 0.0001$; Figure 1). When assessed across all organs from each body segment, the head, thorax, and abdomen differ in their proportions of nuclei among ploidy levels ($F(10,392) = 10.33, p < 0.0001$), due primarily to the abdomen having more nuclei at endopolyploid levels (4C, 8C, 16C, 32C, and 64C) than the head and thorax (abdomen vs. head 4C–64C: $t(62) = 4.4, p < 0.0001$; abdomen vs. thorax 4C–64C: $t(62) = 5.2, p < 0.0001$; Figure 2). The head and thorax do not differ in their proportion of endopolyploid nuclei ($t(62) = 1.24, p = 0.2198$; Figure 2).

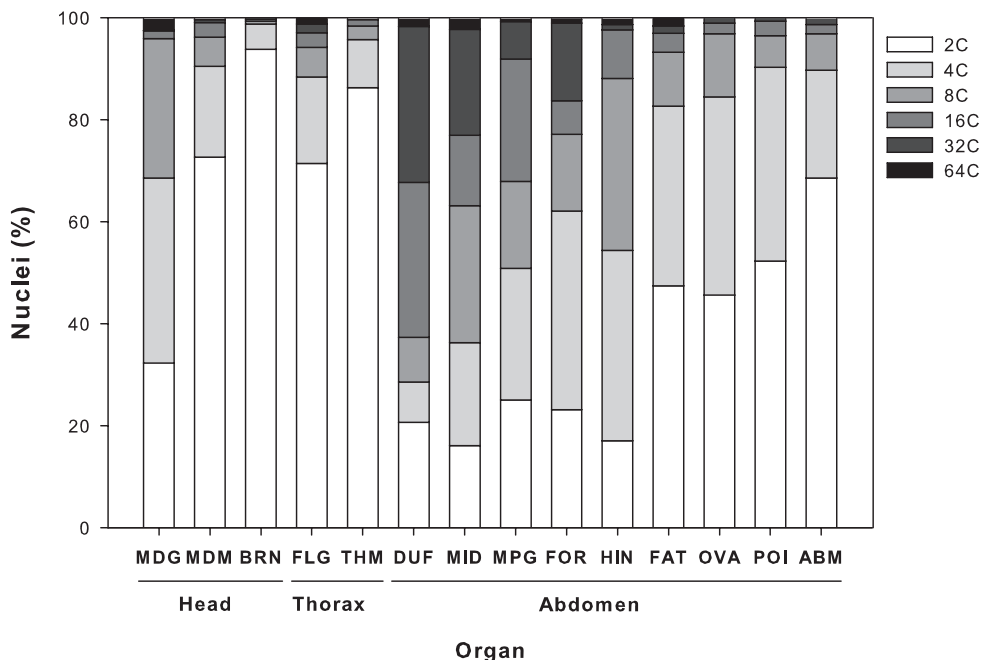


Figure 1. Distribution of ploidy among organs. Percentage of nuclei at each of the ploidy levels observed (2C–64C) within each organ analyzed. Organs are presented by body segment in descending order of cycle value.

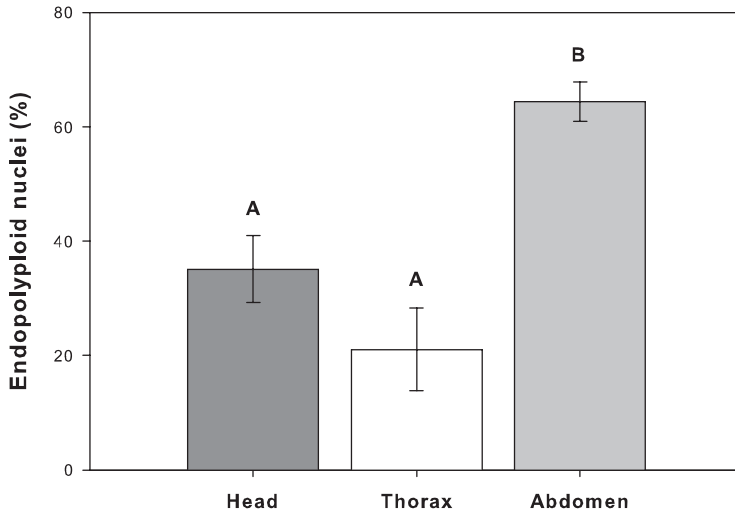


Figure 2. Differences in endopolyploidy among body segments. Percentage of endopolyloid (4C, 8C, 16C, 32C, and 64C) nuclei for each body segment. Shown are means \pm standard error across 5 individuals. Letters indicate significant ($\alpha = 0.05$) differences among body segments. Significance was determined by analysis of arc-sine square-root transformed proportions.

Endopolyploidy among organs and body segments

Organs differ overall in their cycle values ($F(13,51) = 9.57, p < 0.0001$), covering a nearly 31-fold range in ploidy (brain: 0.08, Dufour's gland: 2.47; Figure 3). Overall, these organs comprise two main statistical groups: the Dufour's gland, midgut, Malpighian tubules, foregut, hindgut, and the mandibular gland have the highest cycle values (group A) while the fat body, ovary, poison gland, foreleg muscle, abdominal muscle, mandibular muscle, thoracic muscle, and brain have the lowest cycle values (group D), although there is some overlap in the statistical groupings for organs of intermediate cycle values (Figure 3). There is no significant relationship between the numbers of nuclei counted and the cycle values among organs ($F(1,67) = 2.03, p = 0.159$; Table 1), so differences among organs in their cycle values are not likely due to differences in cell number (i.e. organ size) or technical artifact. We additionally note no significant individual effect on cycle values ($F(4,64) = 0.78, p = 0.5453$), indicating that differences in cycle values are not dependent on the individual from which they were measured. When organs are considered in relation to their body segments, the abdomen has the highest cycle values (abdomen vs. head: $t(62) = 2.88, p < 0.05$; abdomen vs. thorax: $t(62) = 3.49, p < 0.01$), with no difference between cycle values of the head and thorax ($t(62) = 0.88, p = 0.6532$).

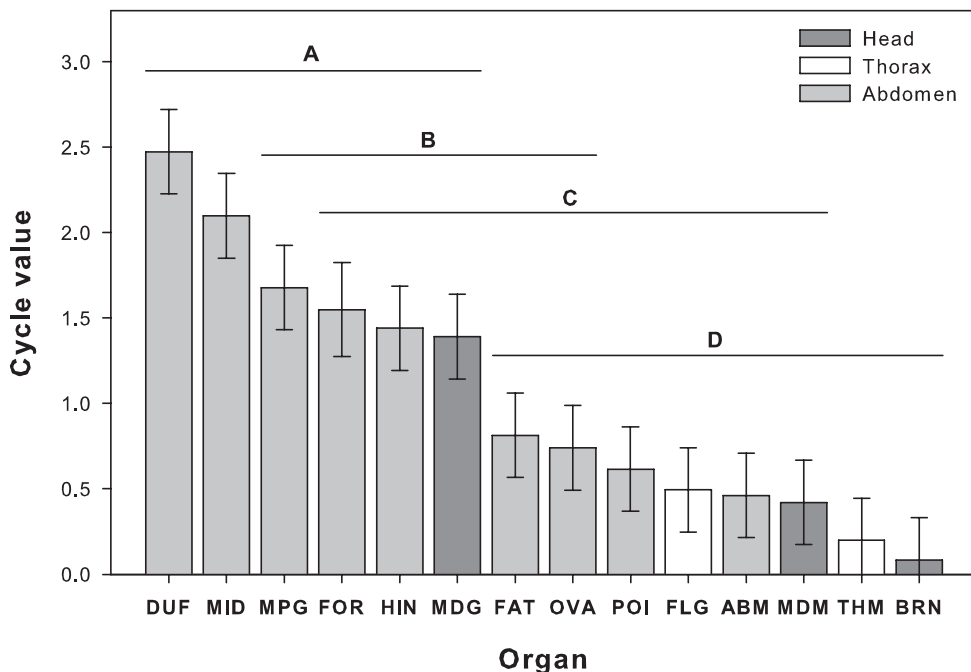


Figure 3. Cycle values for each organ analyzed within each body segment. Shown are means \pm standard error across 5 replicates of each organ within each body segment. Organs are presented in descending order of mean cycle value. Bars labeled with letters denote statistical groups determined by Tukey's Studentized range test (significance tested at $\alpha_{\text{family}} = 0.05$).

Endopolyploidy of organs by function

Upon relating organs to their functional groups (Table 1), endopolyploidy, measured by cycle value, differs among major functional systems ($F(4,60) = 11.83$, $p < 0.0001$). Specifically, systems comprise two main statistical groups—the digestive and exocrine systems have the highest cycle values (group A), while the muscular and neural systems have the lowest cycle values (group B; Figure 4). The reproductive system has an intermediate cycle value and is shared among statistical groups (group AB). Further, while the fat body is typically considered to be part of the digestive system, it is not directly part of the ingestion/excretion pathway (i.e. the gut). Upon exclusion of the fat body from the gut (i.e. the foregut, midgut, hindgut, and Malpighian tubules), the average cycle value of the digestive system increases from a value of 1.51 with the fat body to 1.70. This exclusion changes the significance groups such that the digestive system has the highest cycle value (group A), the muscular and neural systems have the lowest (group C), and the exocrine and reproductive systems have intermediate cycle values (groups AB and BC, respectively).

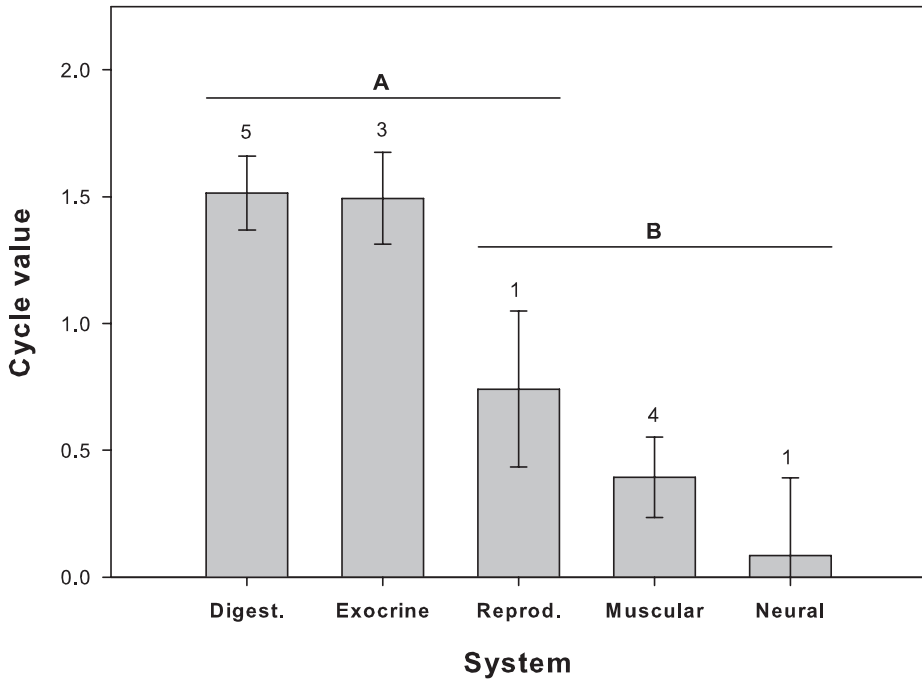


Figure 4. Endopolyploidy of organs by functional system. Cycle value of organs within each functional system (abbreviations “Digest.”: digestive; “Reprod.”: reproductive). Shown are means \pm standard error across 5 replicates of each organ within each system. Systems are presented in descending order of mean cycle value. Bars labeled with letters denote statistical groups determined by Tukey’s Studentized range test (significance tested at $\alpha_{\text{family}} = 0.05$). Numbers above each bar indicate the number of organs that comprise each respective system.

Discussion

Previous studies have documented instances of insect endopolyploidy in a qualitative (White 1977 and references therein) or semi-quantitative (e.g. Johnston et al. 2004, Aron et al. 2005, Scholes et al. 2013) manner. Here, we show that flow cytometry can be utilized to provide a fully quantitative comparison of endopolyploidy within and among organs. Using this technique, we are able to quantify for the first time the extent to which endopolyploidy varies within an insect, with a wide range of ploidy levels detected across the 14 organs examined in the ant *Dinoponera australis*. Specifically, organs from the abdomen collectively had greater endopolyploidy than those of either the head or the thorax. Ploidy levels were highest in organs of the digestive and exocrine systems, and especially of the gut, suggesting that endoreduplication may be particularly important in development and/or organ function in these systems. This information provides the basis from which questions regarding the role of endopolyploidy in insect development, behavior, physiology, body size, caste differentiation, etc. may be addressed.

Our results for this unusual ant support the body segment-specific differences previously reported for four other ant species (Scholes et al. 2013). Specifically, Scholes et al. (2013) determined that regardless of species, caste, or worker body size, the abdomen had consistently greater endopolyploidy than the head and thorax, which had lower, comparable levels. However, our tissue-specific analyses revealed substantial variation in endopolyploidy among organs within body segments. The importance of endoreduplication in segment function and development may therefore be misrepresented if not assessed with regard to specific organs or tissues. For example, the abdomen has high endopolyploidy overall, yet is composed of a variety of organs with relatively high or low endopolyploidy.

Patterns in segment-specific cycle values appear to be driven strongly by organ function. For example, the abdominal organs of the digestive system (and particularly the gut) and the Dufour's gland of the exocrine system have high endopolyploidy. The mandibular gland of the exocrine system also has high endopolyploidy, yet it resides within the head, where the organs otherwise analyzed have very low endopolyploidy and serve other functions. Given endoreduplication's presumed roles in cellular development (Nagl 1976, Lee et al. 2009), endopolyploidy may therefore be particularly beneficial for cells of digestive and exocrine function by increasing metabolic potential and gene expression through increased genome copy number, and/or by increasing cell volume for the production and storage of metabolites (Nagl 1976, 1978, Lee et al. 2009). While ploidy has not yet been related to measures of digestive demands or the production or storage of chemicals within these organs, the extremely high ploidy of the *Bombyx mori* silk gland (Perdix-Gillot 1979), as well as of the *Drosophila melanogaster* nurse cells and salivary gland (Balbani 1881, Mulligan and Rasch 1985), suggests that endoreduplication can be an effective mechanism to support high cell metabolism and specialized function.

The muscular tissues sampled (mandibular, foreleg, thoracic, abdominal) have comparably low levels of endopolyploidy regardless of their body segment (head, thorax, abdomen), likely due to their shared function. Aron et al. (2005) compared muscles of the head and thorax of female bumble bees and found no difference in the distribution of ploidy levels among thoracic, mandibular, fore-, mid-, and hindleg muscles, further suggesting a relationship between endopolyploidy and function for these tissues. Of additional interest is the moderate level of endopolyploidy observed in the *D. australis* ovary—a tissue one might expect to have high metabolic demand. Our results are likely due in part to the presence of both somatic endopolyploid cells (e.g. nurse cells) and meiocytes (1C, 2C, and 4C) with moderate ploidy levels overall.

Endopolyploidy is thought to be particularly important for organisms to compensate for the metabolic and genetic decrements of their small genome sizes (Nagl 1976, 1978, Galbraith et al. 1991, Barow and Meister 2003), yet patterns of endopolyploidy in *D. australis* are comparable to other species examined, including *Pogonomyrmex badius* whose genome is over 2× smaller than that of *D. australis* (*P. badius*: 262.8 Mb / 1C; *D. australis*: 554.7 Mb / 1C; Tsutsui et al. 2008). Karyotypic analysis of four *Dinoponera* species revealed that the genomes in this genus are composed of a large number of very small chromosomes (e.g. *D. australis*: 2n = 114 chromosomes; Santos

et al. 2012), such that the highest ploidy level observed here, 64C, represents 3648 nuclear chromosomes per cell. The discrepancy between the expected and observed relative rates of endoreduplication given the genome size of *D. australis* may therefore suggest that genome organization (i.e. chromosome number and size), in addition to genome size, influences the rate of endoreduplication.

Endopolyploidy is hypothesized to impact cells through associated nucleotypic effects, which are not based on the cell's genotype, and/or genetic effects including genome or gene pathway up-regulation (Bennett 1972, 1982, Nagl 1976, 1978). Endoreduplication may thus promote cell differentiation and specialization in two integrated ways: 1) nucleotypic effects, such as increased cell size, can provide the necessary cell volume, improved transportation efficiency, and other beneficial effects that support cell differentiation generally, while 2) differences among cells in the continuation of endoreduplication beyond this level induce differential gene expression that supports the cell's functional fate through specific impacts on metabolism, chemical production, and/or other processes. Certainly more research is necessary to determine the impact of the organ-specific endoreduplication reported here. For example, the use of whole transcriptome sequencing would allow the examination of gene expression across organs or tissues of interest and help relate endopolyploidy to the functions of specific gene pathways.

Acknowledgements

We thank Bill Wills for help with colony collection, Fred Larabee for help with colony maintenance, and Amy Gervais for help with flow cytometry. For permission to collect and export *Dinoponera australis*, we thank the Administración de Parques Nacionales de Argentina (specifically Parque Nacional Iguazú), Paula Cichero, Karina Schiaffino, Silvia Fabri, and CIES. The ants were imported under USDA APHIS permit number P526P-10-01369. This research was supported by grants from the National Science Foundation (DEB 1020979 to AVS and DEB 1146085 to KNP).

References

- Aron S, de Menten L, Van Bockstaele DR, Blank SM, Roisin Y (2005) When hymenopteran males reinvented diploidy. *Current Biology* 15: 824–827. doi: 10.1016/j.cub.2005.03.017
- Balbani EG (1881) Sur la structure du noyau des cellules salivaires chez les larves de *Chironomus*. *Zoologischer Anzeiger* 4: 637–641.
- Barlow PW (1978) Endopolyploidy: towards an understanding of its biological significance. *Acta Biotheoretica* 27: 1–18. doi: 10.1007/BF00048400
- Barow M, Meister A (2003) Endopolyploidy in seed plants is differentially correlated to systematics, organ, life strategy, and genome size. *Plant, Cell & Environment* 26: 571–584. doi: 10.1046/j.1365-3040.2003.00988.x

- Bennett MD (1972) Nuclear DNA content and minimum generation time in herbaceous plants. *Proceedings of the Royal Society of London B* 181: 109–135. doi: 10.1098/rspb.1972.0042
- Bennett MD (1982) Nucleotypic basis of the spatial ordering of chromosomes in eukaryotes and the implications of the order for genome evolution and phenotypic variation. In: Brandham PE, Bennett MD (Eds) *Genome Evolution*. G. Allen and Unwin (London), 239–261.
- Britton JS, Edgar BA (1998) Environmental control of the cell cycle in *Drosophila*: nutrition activates mitotic and endoreplicative cells by distinct mechanisms. *Development* 125: 2149–2158.
- Cavalier-Smith T (1985) Cell volume and the evolution of eukaryotic genome size. In: Cavalier-Smith T (Ed) *The Evolution of Genome Size*. John Wiley & Sons (New York), 105–184.
- Engelen-Eigles G, Jones RJ, Phillips RL (2001) DNA endoreduplication in maize endosperm cells is reduced by high temperature during the mitotic phase. *Crop Science* 41: 1114–1121. doi: 10.2135/cropsci2001.4141114x
- Fusconi A, Repetto O, Bona E, Massa N, Gallo C, Dumas-Gaudot E, Berta G (2006) Effects of cadmium on meristem activity and nucleus ploidy in roots of *Pisum sativum* L. cv. Frisson seedlings. *Environmental and Experimental Botany* 58: 253–260. doi: 10.1016/j.envexpbot.2005.09.008
- Galbraith DW, Harkins KR, Knapp S (1991) Systemic endopolyploidy in *Arabidopsis thaliana*. *Plant Physiology* 96: 985–989. doi: 10.1104/pp.96.3.985
- Galbraith DW, Harkins KR, Maddox JM, Ayres NM, Sharma DP, Firoozabady E (1983) Rapid flow cytometric analysis of the cell cycle in intact plant tissues. *Science* 220: 1049–1051. doi: 10.1126/science.220.4601.1049
- Galitski T, Saldanha AJ, Styles CA, Lander ES, Fink GR (1999) Ploidy regulation of gene expression. *Science* 285: 251–254. doi: 10.1126/science.285.5425.251
- Gregory TR, Hebert PDN (1999) The modulation of DNA content: proximate causes and ultimate consequences. *Genome Research* 9: 317–324. doi: 10.1101/gr.9.4.317
- Gronenberg W (2008) Structure and function of ant (Hymenoptera: Formicidae) brains: Strength in numbers. *Myrmecological News* 11: 25–36.
- Gullan PJ, Cranston PS (2005) *The insects: an outline of entomology*. Blackwell Malden (Massachusetts).
- Jimenez AG, Kinsey ST, Dillaman RM, Kapraun DF (2010) Nuclear DNA content variation associated with muscle fiber growth in decapod crustaceans. *Genome* 53: 161–171. doi: 10.1139/G09-095
- Johnson SR, Copello JA, Evans MS, Suarez AV (2010) A biochemical characterization of the major peptides from the venom of the giant neotropical hunting ant *Dinoponera australis*. *Toxicon* 55: 702–710. doi: 10.1016/j.toxicon.2009.10.021
- Johnston JS, Ross LD, Beani L, Hughes DP, Kathirithamby J (2004) Tiny genomes and endoreduplication in Strepsiptera. *Insect Molecular Biology* 13: 581–585. doi: 10.1111/j.0962-1075.2004.00514.x
- Johnston JS, Schoener M, McMahon DP (2013) DNA underreplication in the majority of nuclei in the *Drosophila melanogaster* thorax: evidence from Suur and flow cytometry. *Journal of Molecular Biology Research* 2: 47–54. doi: 10.5539/jmbr.v3n1p47

- Klowden MJ (2007) Physiological systems in insects. Elsevier (Amsterdam).
- Lee HO, Davidson JM, Duronio RJ (2009) Endoreplication: polyploidy with purpose. *Genes & Development* 23: 2461–2477. doi: 10.1101/gad.1829209
- Lilly MA, Duronio RJ (2005) New insights into cell cycle control from the *Drosophila* endocycle. *Oncogene* 24: 2765–2775. doi: 10.1038/sj.onc.1208610
- Merriam RW, Ris H (1954) Size and DNA content of nuclei in various tissues of male, female, and worker honeybees. *Chromosoma* 6: 522–538. doi: 10.1007/BF01259952
- Mittwoch U, Kalmus H, Webster WS (1966) Deoxyribonucleic acid values in dividing and non-dividing cells of male and female larvae of the honeybee. *Nature* 210: 264–266. doi: 10.1038/210264a0
- Monnin T, Peeters C (1999) Dominance hierarchy and reproductive conflicts among subordinates in a monogynous queenless ant. *Behavioral Ecology* 10: 323–332. doi: 10.1093/beheco/10.3.323
- Monnin T, Ratnieks FLW, Brandão CRF (2003) Reproductive conflict in animal societies: hierarchy length increases with colony size in queenless ponerine ants. *Behavioral Ecology and Sociobiology* 54: 71–79. doi: 10.1007/s00265-003-0600-9
- Monnin T, Ratnieks FLW, Jones GR, Beard R (2002) Pretender punishment induced by chemical signaling in a queenless ant. *Nature* 419: 61–65. doi: 10.1038/nature00932
- Mulligan WL, Rasch EM (1985) Determination of DNA content in the nurse and follicle cells from wildtype and mutant *Drosophila melanogaster* by DNA Feulgen cytophotometry. *Histochemistry* 82: 233–247. doi: 10.1007/BF00501400
- Nagl W (1976) DNA endoreduplication and polyteny understood as evolutionary strategies. *Nature* 261: 614–615. doi: 10.1038/261614a0
- Nagl W (1978) Endopolyploidy and polyteny in differentiation and evolution. Elsevier/North-Holland Biomedical Press (Amsterdam).
- Nagl W (1982) Cell growth and nuclear DNA increase by endoreduplication and differential DNA replication. *Cell Growth* 38: 619–651. doi: 10.1007/978-1-4684-4046-1_29
- Oldham NJ, Keegans SJ, Morgan ED, Paiva RVS, Brandão CRF, Schoeters E, Billen JPP (1994) Mandibular gland contents of a colony of the queenless ponerine ant *Dinoponera australis*. *Naturwissenschaften* 81: 313–316. doi: 10.1007/BF01131947
- Osborn TC, Pires JC, Birchler JA, Auger DL, Chen ZJ, Lee HS, Comai L, Madlung A, Doerge RW, Colot V, Martienssen RA (2003) Understanding mechanisms of novel gene expression in polyploids. *Trends in Genetics* 19: 141–147. doi: 10.1016/S0168-9525(03)00015-5
- Paiva RVS, Brandão CRF (1995) Nests, worker population, and reproductive status of workers in the giant queenless ponerine ant *Dinoponera roger* (Hymenoptera: Formicidae). *Ethology, Ecology & Evolution* 7: 297–312. doi: 10.1080/08927014.1995.9522938
- Perdix-Gillot S (1979) DNA synthesis and endomitosis in the giant nuclei of the silkgland of *Bombyx mori*. *Biochemie* 61: 171–204. doi: 10.1016/S0300-9084(79)80066-8
- Rasch EM, Cassidy JD, King RC (1975) Estimates of genome size in haploid-diploid species of parasitoid wasps. *Journal of Histochemistry & Cytochemistry* 24: 317.
- Santos IS, Delabie JHC, Silva JG, Costa MA, Barros LAC, Pompolo SG, Mariano CSF (2012) Karyotype differentiation among four *Dinoponera* (Formicidae: Ponerinae) species. *Florida Entomologist* 95: 737–742. doi: 10.1653/024.095.0324

- Scholes DR, Paige KN (2011) Chromosomal plasticity: mitigating the impacts of herbivory. *Ecology* 92: 1691–1968. doi: 10.1890/10-2269.1
- Scholes DR, Suarez AV, Paige KN (2013) Can endopolyploidy explain body size variation within and between castes in ants? *Ecology & Evolution* 3: 2128–2137. doi: 10.1002/ece3.623
- Tsutsui ND, Suarez AV, Spagna JC, Johnston JS (2008) The evolution of genome size in ants. *BMC Evolutionary Biology* 8: 64. doi: 10.1186/1471-2148-8-64
- Tukey JW (1953) *The problem of multiple comparisons*. Princeton University Press (Princeton).
- White MJD (1977) *Animal cytology and evolution*. Cambridge University Press (Cambridge).

Parasitoid wasps from three Jamaican localities: A pilot study

Fadia S. Ceccarelli¹, Dwight E. Robinson²,
Hans Clebsch³, Alejandro Zaldívar-Riverón¹

1 *Colección Nacional de Insectos, Instituto de Biología, Universidad Nacional Autónoma de México, 3er. circuito exterior s/n, Cd. Universitaria, Copilco Coyoacán, A. P. 70-233, C. P. 04510., D. F., México* **2** *Department of Life Sciences, University of the West Indies, Mona, Kingston 7, Jamaica.* **3** *Department of Invertebrate Zoology, Cleveland Museum of Natural History, 1 Wade Oval Circle, Cleveland, OH, USA*

Corresponding author: Fadia S. Ceccarelli (saracecca@hotmail.com)

Academic editor: G. Broad | Received 19 January 2014 | Accepted 3 March 2014 | Published 28 March 2014

Citation: Ceccarelli FS, Robinson DE, Clebsch H, Zaldívar-Riverón A (2014) Parasitoid wasps from three Jamaican localities: A pilot study. *Journal of Hymenoptera Research* 37: 127–135. doi: [10.3897/JHR.37.7081](https://doi.org/10.3897/JHR.37.7081)

Abstract

Parasitoid wasps are an extremely speciose, ecologically and economically crucial group of insects. Despite this, they have received disproportionately little attention from scientists, in particular in certain areas of the world. One such area is the Caribbean, where studies are scarce despite the importance of parasitoid wasps, and the uniqueness and diversity of the Caribbean islands. To verify whether an adequate diversity of parasitoid wasps at family level can be found to warrant future studies, this study carries out preliminary sampling in three localities in Jamaica. A total of 1522 individual parasitoid wasps, belonging to at least 16 different families collected during 16 events provide preliminary evidence there is in fact a high diversity of parasitoid wasps in Jamaica, and that future studies there, as in the rest of the Caribbean are definitely worthwhile.

Keywords

Caribbean, biodiversity, parasitoids

Introduction

Parasitoids are organisms that spend part of their life cycle feeding on or inside a host, eventually killing it. This lifestyle has been adopted by a notable number of insects, and in Hymenoptera approximately 80% of its species are parasitoids (LaSalle and Gauld 1991, Quicke 1997). Parasitoid wasps are widespread and highly abundant, playing an important role not only in ecosystem balancing, but also in biological crop pest control and conservation planning via biodiversity surveys (LaSalle and Gauld 1991, Eggleton and Belshaw 1992, Lewis and Whitfield 1999). Despite their great importance, these wasps are poorly studied. In fact, it has been estimated that even though there are approximately 17,000 described species belonging to the family Braconidae, the total number of species has been estimated at approximately 42,653 (Jones et al. 2009) or between 30,873 and 50,886 (Dolphin and Quicke 2001). In addition to a dire need for taxonomic work on parasitoid wasps, there is an even greater scarcity of studies on their biology and ecology.

The islands of the Caribbean Sea represent a highly interesting part of the world, since they are of complex and varying geological origins: some are volcanic, some tectonic and others continental (Burke 1988, van Benthem et al. 2013). These islands are therefore interesting from a biogeographical perspective as well. To carry out biogeographic as well as other biological and ecological studies of this region, it is necessary to first be familiar with the flora and fauna of these islands. While certain islands are well-studied for select taxa such as anolis lizards (e.g. Losos and Schluter 2000, Ord et al. 2013), there are several taxa on Caribbean islands that are still largely unexplored. For example, parasitoid wasps in Jamaica are definitely understudied, where some of the few existing works include agriculture-related studies of parasitoid wasps as natural enemies of crop pests (e.g. Alam 1990), or taxonomic studies (e.g. Martínez et al. 2012). The fact that such few studies exist is unfortunate considering the ecological importance of the taxon in question, and the exceptional geographical location and topology of Jamaica.

In this study we set out to verify whether collecting efforts in Jamaica would yield high numbers of parasitoid wasps to warrant more detailed future studies, using two of the most common collecting techniques for parasitoid wasps, namely yellow pan trapping (YPT) and sweep netting (e.g. Noyes 1989, Missa et al. 2009, Abrahamczyk et al. 2010). We present preliminary data to show that sampling of parasitoid wasps in the Caribbean islands in general, and Jamaica in particular, is worthwhile for future studies of agriculture, ecology, conservation, systematics and biogeography.

Materials and methods

Parasitoid wasps for this study were collected during the month of November 2010. Three localities were chosen in the Jamaican parishes of St. Andrew, St. Mary and Trelawny (see Figure 1). Within these localities, a total of 16 collecting events took place,

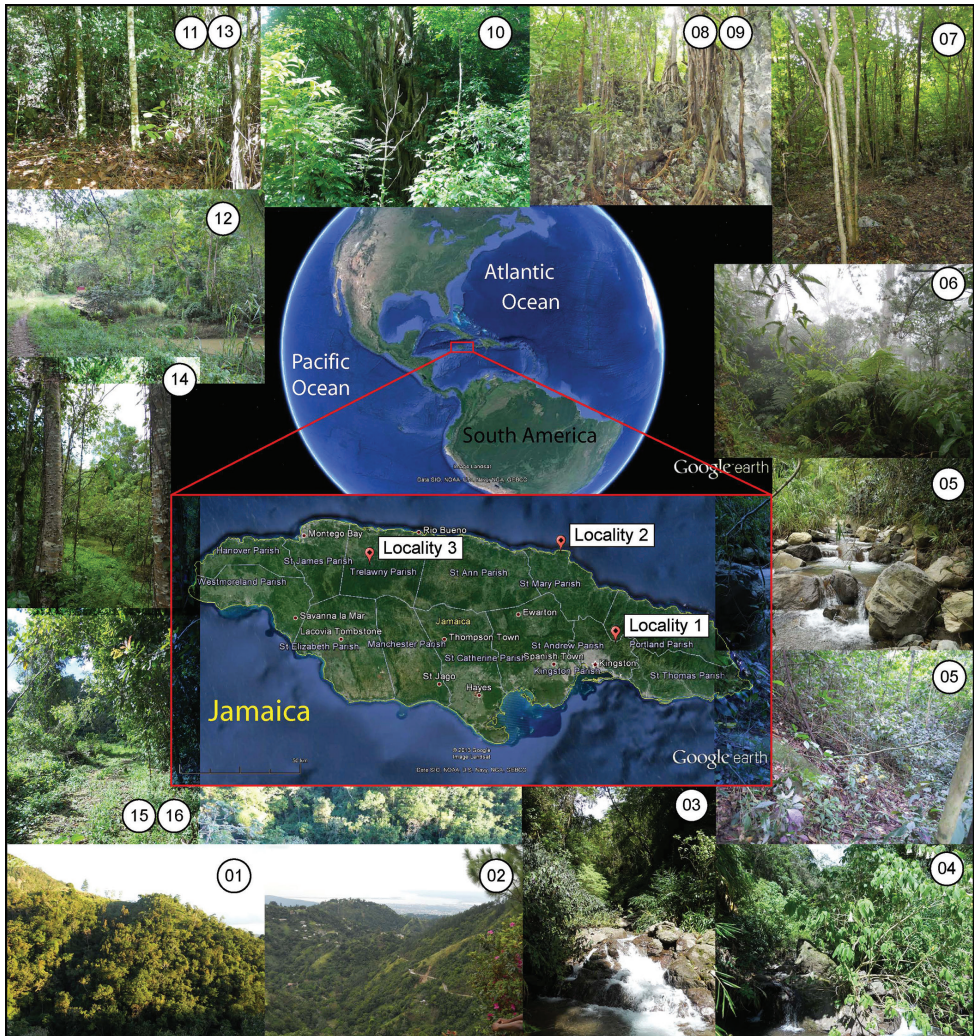


Figure 1. Maps and habitat photographs. Maps in the centre of the figure showing the geographic position of the three localities sampled in this study with surrounding photographs of the habitat types. Numbers in circles represent the collection code as shown in Table 1 without the JAM prefix.

either using a sweep net, or setting yellow pan traps (YPT) (for details see Table 1). The three localities, as well as each collecting event within the localities differed in general habitat type, vegetation cover, topology and climatic conditions, all of which were considered when interpreting the results.

More specifically, locality 1 comprised an area of approximately 0.90 square kilometres (km²) (221.31 acres) in a mountainous area (Blue Mountains), at elevations ranging from 860 to 1205 metres above sea level (m.a.s.l.). As such, most of the collecting sites were on slopes, and the area overall consisted of small patches of primary forest, mostly highly fragmented by human activity. Collecting events JAM01 and

Table I. Collection details for this study.

Code	L	Place	GPS	Alt.	Date	CM
JAM01	1	St. Andrew, Newcastle	18.06840, -076.71190	860	09-11.xi.2010	50 YPT
JAM02	1	St. Andrew, Newcastle	18.06760, -076.71510	956	09-11.xi.2010	50 YPT
JAM03	1	St. Andrew, Newcastle	18.07127, -076.71813	871	10.xi.2010	sweep 11:00–13:00
JAM04	1	St. Andrew, Newcastle	18.06840, -076.70850	1009	10.xi.2010	sweep 15:00–17:00
JAM05	1	St. Andrew, Newcastle	18.06840, -076.71190	860	11.xi.2010	sweep 11:00–12:00
JAM06	1	St. Andrew, Hollywell Park	18.08609, -076.72629	1205	11.xi.2010	sweep 15:30–16:00
JAM07	2	St. Mary, Oracabessa	18.40207, -076.92519	174	14-16.xi.2010	50 YPT
JAM08	2	St. Mary, Oracabessa	18.40324, -076.92727	176	15-17.xi.2010	50 YPT
JAM09	2	St. Mary, Oracabessa	18.40260, -076.92519	167	16.xi.2010	sweep 10:00–11:00
JAM10	3	Trelawny, Windsor	18.35752, -077.65837	97	18.xi.2010	sweep 16:00–17:00
JAM11	3	Trelawny, Windsor	18.35752, -077.66406	82	19-21.xi.2010	50 YPT
JAM12	3	Trelawny, Windsor	18.35823, -077.65675	87	19-21.xi.2010	50 YPT
JAM13	3	Trelawny, Windsor	18.35169, -077.66371	173	19.xi.2010	sweep 14:30–15:30
JAM14	3	Trelawny, Windsor	18.35531, -077.66371	98	20.xi.2010	sweep 11:00–12:00
JAM15	3	Trelawny, Windsor	18.35838, -077.65837	97	20.xi.2010	sweep 15:00–15:30
JAM16	3	Trelawny, Windsor	18.35838, -077.65837	97	21.xi.2010	sweep 15:00–16:30

Code= collecting event, L= locality, Place includes Jamaican parish and town, Alt.= altitude in metres within 5 metres, CM= collecting method (YPT= yellow pan traps, sweep= sweep netting, plus the time of day during which sweep netting was carried out).

JAM03-05 were carried out in the vicinity of fast-flowing mountain streams, with the soil inside the forest patches rich in organic matter. In addition, during collecting events JAM01 to 05 it was sunny, while during event JAM06 there was fog, complicating the sweep netting. Locality 2 consisted of an approximate area of 0.0066 km² (1.63 acres), at altitudes between 167 and 176 m.a.s.l., with collecting carried out mostly inside woodlands with moderate canopy cover on limestone ground. There was no evident water body in the vicinity. The main disturbing factor during collecting events JAM07 and JAM08 was the heavy rain, which flooded the yellow pan traps left out during the night. Locality 3 consisted of an approximately 0.29 km² (70.64 acre) area, at altitudes between 82 and 173 m.a.s.l., within Jamaica's Cockpit Country, an area containing one of the islands' last contiguous rainforests, although collecting events JAM10-12 and JAM15 took place on the edge of the forest. The only registered water body within the locality was a spring near collecting event JAM15, a tributary to the Martha Brae river. No noteworthy climatic events affected the collecting events JAM10-16.

All parasitoid wasps collected were stored in 96% EtOH and subsequently identified in the laboratory using a dissecting microscope. Identifications were made at least to family level and in some cases to genus. However, due to the lack of expertise for most families and due to time constraints, we are at this moment unable to present data at species (or even genus) level for all families, so in the absence of an equal taxonomic treatment of all families, we present the data at family level. The total number of wasp families was recorded for each locality, and calculations were made adjusting the number of wasp families collected for each site to obtain a unit measurement for

collecting effort. For the yellow pan traps the number of wasp families was divided by the number of hours the YPTs were left out, and for the sweep net collection, the number of families was divided by the number of people multiplied by the number of hours spent collecting. All parasitoid wasps collected during this study were deposited at the Colección Nacional de Insectos, Instituto de Biología, Universidad Nacional Autónoma de México, with accession numbers CNIN-JAM0001-1522.

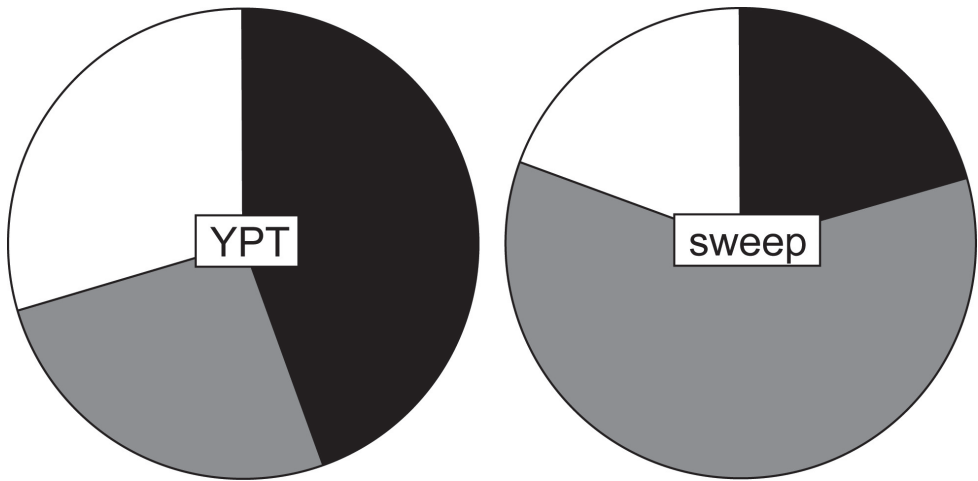
Results

In this pilot study, we collected a total of 1522 individual parasitoid wasps in the three localities belonging to 15 families and one superfamily (for more details see Table 2 and Suppl. metrial 1). To under- rather than overestimate the number of families, we will count the superfamily, Cynipoidea, as one additional family, making the total number of families collected in this study at least 16. The highest proportion of parasitoid wasps collected in locality 1 belong to the family Diapriidae (especially during the collecting events JAM01 and 02 where we used yellow pan traps), in locality 2 to the family Ichneumonidae and in locality 3 to the Pteromalidae. In total, specimens belonging to 13, 10 and 13 parasitoid wasp families were collected in localities 1, 2 and 3, respectively. Specimens belonging to the families Braconidae, Chalcididae, Cynipoidea (superfamily), Diapriidae, Eulophidae, Ichneumonidae, Platygastriidae and Pteromalidae were found in all three localities. Additionally, specimens belonging to the family Mymaridae were only found in localities 1 and 2, specimens belonging to the families Bethyidae and Ceraphronidae were only found in localities 1 and 3, specimens belonging to the family Encyrtidae were only found in localities 2 and 3, specimens belonging to the families Megaspilidae and Proctotrupidae were only found in locality 1 and specimens belonging to the families Agaonidae and Eupelmidae were only found in locality 3.

When accounting for collecting effort, the yellow pan traps were most efficient in locality 1 at family level, meaning that in this locality, using YPTs as a collecting method yielded individuals from more families than in the other two localities. On the other hand, sweep netting was most efficient in locality 3 per unit time (see Figure 2). Parasitoid wasps from most families were collected both in YPTs and sweep nets. The minor differences consisted in the single individuals belonging to the families Agaonidae and Eupelmidae collected by sweep netting but not in YPTs, and the single megaspilid collected by YPT only. Also, in terms of individuals, a higher number of ceraphronids, diapriids, mymarids and platygastriids was collected using YPTs, while for the remaining families more individuals were collected by sweep netting than using YPTs (see Table 3). However, this should not be taken as hard evidence for preferring one method over the other for several reasons. First of all, presenting data in terms of individuals does not equate to species richness; second, collecting effort was not standardised; and thirdly, the numbers we are dealing with in this study are generally low. For these reasons no tests of significance were carried out with regards to differences in productivity between sampling methods.

Table 2. Number of individual wasps collected from each locality for all families.

Family	Locality 1	Locality 2	Locality 3	TOTAL
Agaonidae	0	0	1	1
Bethylidae	2	0	2	4
Braconidae	196	11	94	301
Ceraphronidae	1	0	6	7
Chalcididae	1	1	5	7
Cynipoidea (unidentified families)	26	12	91	129
Diapriidae	225	10	144	379
Encyrtidae	0	1	3	4
Eulophidae	19	1	28	48
Eupelmidae	0	0	1	1
Ichneumonidae	24	40	8	72
Megaspilidae	1	0	0	1
Mymaridae	23	2	0	25
Platygastridae	185	4	37	226
Proctotrupidae	13	0	0	13
Pteromalidae	26	3	275	304
TOTAL INDIVIDUALS	742	85	695	1522
<i>Number of families</i>	<i>13</i>	<i>10</i>	<i>13</i>	<i>16</i>

**Figure 2.** Efficiency of collecting methods. Pie charts representing the efficiency of the two collecting methods used in this study at family level (YPT= yellow pan traps; sweep = sweep net) in units (calculated as described in the Materials and Methods section) for each locality (black= locality 1, grey= locality 2, white= locality 3).

Discussion

The differences between the three localities with regards to the parasitoid wasp families sampled in this study could be attributed to a combination of topology, climate and collecting method. For example, in locality 1 relatively few families were represented in

Table 3. Number of individual wasps collected by the two collecting methods for all families.

Family	Yellow pan traps	sweep netting
Agaonidae	0	1
Bethylidae	1	3
Braconidae	148	153
Ceraphronidae	4	3
Chalcididae	1	6
Cynipoidea (unidentified families)	30	99
Diapriidae	295	84
Encyrtidae	2	2
Eulophidae	22	26
Eupelmidae	0	1
Ichneumonidae	22	50
Megaspilidae	1	0
Mymaridae	23	2
Platygastridae	168	58
Proctotrupidae	7	6
Pteromalidae	151	153
TOTAL INDIVIDUALS	875	647
<i>Number of families</i>	<i>14</i>	<i>15</i>

sweep net collections compared to the other two localities. The reasons for this may be that walking the steep slopes and rugged terrain by mountain streams hindered maximum collecting efficiency with a sweep net while the thick fog during collecting event JAM06 definitely lowered the average for the families collected in locality 1. Similarly, the yellow pan traps appeared to be the least efficient in locality 2, however, the heavy rains washing out most of the specimens collected in the traps definitely skewed the results in favour of localities 1 and 3 for YPTs. The fact that the YPTs were most efficient in locality 1 with a high proportion of Diapriidae collected in this locality supports the fact that Diapriidae are efficiently collected using YPTs (e.g. Noyes 1989) in areas rich in organic matter (Masner and Gracia 2002). As mentioned before, the two collecting methods used in this study are not comparable as to efficiency. However, as in previous studies (e.g. Noyes 1989, Missa et al. 2009), we show that increasing the number of collecting methods may increase the chances of collecting parasitoid wasps from different families, even though according to Missa et al. (2009) habitat type is a more important factor than collecting method in determining the parasitoid wasp species collected.

Given more time and more sampling methods than used in this study, differences in parasitoid wasp family assemblages between localities are more likely to display structuring based on host species assemblages, in turn driven by differences in plant assemblages. Sampling during different seasons throughout the year is also likely to yield different assemblages to those found in this study. Nevertheless, the high numbers of parasitoid wasps belonging to a considerable number of families collected during a

relatively short time using only two basic collecting techniques provide evidence that Jamaica is definitely a place worth sampling for future studies on or including these taxa. In addition to collecting for general ecological studies, hymenopterists wishing to undertake studies on specific families may also be able to verify in this pilot study the most appropriate locality for collecting the specific taxon which they wish to investigate.

Acknowledgements

We thank all the people who facilitated our field work while in Jamaica, especially Oliver Magnus and Time Anson. We also extend our gratitude to Juan José Martínez and Juliano Nunes who helped during the process of wasp identification, and two anonymous referees for comments on a previous version of this manuscript. This work was supported by and a grant given by CONACyT (convocatoria SEP Ciencia Básica 2008) to AZR.

References

- Abrahamczyk S, Steudel B, Kessler M (2010) Sampling Hymenoptera along a precipitation gradient in tropical forests: the effectiveness of different coloured pan traps. *Entomologia Experimentalis et Applicata* 137: 262–268. doi: 10.1111/j.1570-7458.2010.01063.x
- Alam MM (1990) Diamondback moth and its natural enemies in Jamaica and some other Caribbean Islands. In: Talekar NS (Ed) *Diamondback moth and other crucifer pests: Proceedings of the Second International Workshop*. Asian Vegetable Research and Development Center, Shanshua (Taiwan), December 1990: 233–243.
- Burke K (1988) Tectonic evolution of the Caribbean. *Annual Review of Earth and Planetary Sciences* 16: 201–230. doi: 10.1146/annurev.ea.16.050188.001221
- Dolphin K, Quicke DLJ (2001) Estimating the global species richness of an incompletely described taxon: an example using parasitoid wasps (Hymenoptera: Braconidae). *Biological Journal of the Linnean Society* 73 (3): 279–286. doi: 10.1111/j.1095-8312.2001.tb01363.x
- Eggleton P, Belshaw R (1992) Insect parasitoids: an evolutionary overview. *Philosophical Transactions of the Royal Society London B* 337: 1–20. doi: 10.1098/rstb.1992.0079
- Jones OR, Purvis A, Baumgart E, Quicke DLJ (2009) Using taxonomic revision data to estimate the geographic and taxonomic distribution of undescribed species richness in the Braconidae (Hymenoptera: Ichneumonoidea). *Insect Conservation and Diversity* 2: 204–212. doi: 10.1111/j.1752-4598.2009.00057.x
- LaSalle J, Gauld ID (1991) Parasitic Hymenoptera and the biodiversity crisis. *Redia* 74: 315–334.
- Lewis CN, Whitfield JB (1999) Braconid wasp (Hymenoptera: Braconidae) diversity in forest plots under different silvicultural methods. *Environmental Entomology* 28: 986–997.
- Losos JB, Schluter D (2000) Analysis of an evolutionary species–area relationship. *Nature* 408: 847–850. doi: 10.1038/35048558

- Martínez JJ, Ceccarelli FS, Zaldívar-Riverón A (2012) Two new species of *Pambolus* (Hymenoptera, Braconidae) from Jamaica. *Journal of Hymenoptera Research* 24: 85–93. doi: 10.3897/JHR.24.2300
- Masner L, Garcia RJL (2002) The genera of Diapriinae (Hymenoptera: Diapriidae) in the New World. *Bulletin of the American Museum of Natural History* 268: 1–138. doi: 10.1206/0003-0090(2002)268<0001:TGODHD>2.0.CO;2
- Missa O, Basset Y, Alonso A, Miller SE, Curletti G, De Meyer M, Eardley C, Mansell MW, Wagner T (2009) Monitoring arthropods in a tropical landscape: relative effects of sampling methods and habitat types on trap catches. *Journal of Insect Conservation* 13 (1): 103–118. doi: 10.1007/s10841-007-9130-5
- Noyes JS (1989) A study of five methods of sampling Hymenoptera (Insecta) in a tropical rainforest, with special reference to the Parasitica. *Journal of Natural History* 23: 285–298. doi: 10.1080/00222938900770181
- Ord TJ, Stamps JA, Losos JB (2013) Convergent evolution in the territorial communication of a classic adaptive radiation: Caribbean Anolis lizards. *Animal Behaviour* 85: 1415–1426. doi: 10.1016/j.anbehav.2013.03.037
- Quicke DLJ (1997) *Parasitic Wasps*. Chapman & Hall, London: 1–492.
- van Benthem S, Govers R, Spakman W, Wortel R (2013) Tectonic evolution and mantle structure of the Caribbean. *Journal of Geophysical Research: Solid Earth* 118: 3019–3036. doi: 10.1002/jgrb.50235

Supplementary material I

Collection data

Authors: Fadia S. Ceccarelli, Dwight E. Robinson, Hans Clebsch, Alejandro Zaldívar-Riverón

Data type: Collection details

Explanation note: Table showing the number of individual parasitoid wasps collected during this study in each collecting event.

Copyright notice: This dataset is made available under the Open Database License (<http://opendatacommons.org/licenses/odbl/1.0/>). The Open Database License (ODbL) is a license agreement intended to allow users to freely share, modify, and use this Dataset while maintaining this same freedom for others, provided that the original source and author(s) are credited.

Link: doi: 10.3897/JHR.37.7081.app1

